Polymer-Scaffolded Dynamic Combinatorial Libraries

Clare S. Mahon

A thesis submitted for the degree of

Doctor of Philosophy in Chemistry

School of Chemistry

Newcastle University

August 2014

Abstract of the Dissertation

Polymer-Scaffolded Dynamic Combinatorial Libraries

Clare S. Mahon

Polymer-Scaffolded Dynamic Combinatorial Libraries (PS-DCLs) apply the principles of dynamic combinatorial chemistry to macromolecular systems in an effort to generate synthetic macromolecular species with similar capacity for molecular recognition to antibodies and other proteins. PS-DCLs have been constructed by functionalising polyacrylamide scaffolds containing aldehyde moieties with residues incorporating different functionalities through acylhydrazone linkages, generating a diverse library of polymers which vary in their residual composition. The dynamic nature of the acylhydrazone linkage allows residues to exchange with one another, producing a system of interconverting polymers, with exchange reactions proceeding in aqueous solution at a moderate pH of 4.5. The system operates under thermodynamic control, with its composition determined by the relative stabilities of library members. The addition of macromolecular templates, including synthetic polymers, a bacterial toxin and other proteins, has been shown to induce compositional change within the system, producing a population of polymers of improved affinities towards the template. Enhancements in free energy of binding of up to 8.8 kJ mol^{-1} have been observed. PS-DCLs revert to their initial composition upon removal of the template, demonstrating the thermodynamically-controlled nature of the templating process. Solid supported templates have been employed for the convenient separation of the best-binding fraction of the library from the rest of the system, constituting an important step in the development of the PS-DCL concept. A systematic evaluation of how features of the polymer scaffold, including its molecular weight and functional density of aldehyde units, affect the behaviour of resultant PS-DCLs has been performed, allowing for the confident design of PS-DCLs in a manner which optimises the response of the library towards template addition. The development of more complex PS-DCLs, with an increased number of residues offering additional scope for interaction with templates, may lead to a general route for the discovery of synthetic receptors for proteins and other biologically-important macromolecules.

Acknowledgements

I would like to take this opportunity to express my thanks to all of those who have contributed to the work described in this thesis. My thanks must go firstly to my PhD supervisor, Dr. David Fulton, for his constant guidance and inspiration, and for giving me the opportunity to become a capable scientist. David has encouraged me to continually push the boundaries and achieve my very best, with a confidence in my abilities that I sometimes lacked.

I have been fortunate to have worked alongside some incredibly talented and inspirational scientists during my time at Newcastle. I will be forever grateful to Dr. Ben Murray and Dr. Alex Jackson, who were both so generous with their time and patience. I thank them both for their invaluable assistance, but also for their friendship, and the many happy hours spent together in the lab.

I also wish to thank Dr. Bruce Turnbull at University of Leeds for his generosity with his time, advice and assistance during our collaboration. My thanks also to those members of his group who have contributed to the work described here, particularly Dr. Martin Fascione, Chadamas Sakonsinsiri and Dr. Tom McAllister.

During my time at Newcastle University, I have been blessed with many friendships I will cherish for the rest of my life. I am particularly indebted to Chris McGurk for his affection and support throughout the course of my doctoral studies. I have been privileged to have worked alongside friends rather than coworkers, and am thankful especially to Dr. David Smith, Dr. Scott Watson, Dr. Jonny Pate, Judith Houston, Daniel Whitaker and Michael Bracchi for their companionship and sense of humour throughout. My heartfelt thanks also to my friends Dr. Michael Hunter and Terri Freedman, who have been a constant source of support and amusement during my eight years at Newcastle University.

I have been blessed with an extraordinary family, and will be forever indebted to them for their encouragement and support throughout my education. In particular, I would like to thank my Mum and Anne Marie for always offering sympathy, and my Dad for never offering any! I am thankful to my brother Niall and sister Cara, along with Rhiannon Parsons, Sophie Murray and Emma Fluke, for regularly making me laugh to the point of tears, and reminding me of the world outside my PhD. I am thankful always for the encouragement of my grandparents, and Sean and Cathy, who believed I could achieve anything.

I am truly grateful to have been given the opportunity to continue my university studies and pursue a career in research, and am thankful to the Engineering and Physical Sciences Research Council, who provided my studentship.

Table of Contents

List of Symbols and Abbreviations

µg	Micromolar
µL	Microlitre
AcOH	Acetic acid
AIBN	2,2'-azobis(2-methylpropionitrile)
BSA	Bovine serum albumin
Con A	Concanavalin A
Da	Dalton
DCC	Dynamic combinatorial chemistry
DCL	Dynamic combinatorial library
DDMAT	*S*-1-dodecyl-*S*'-(α,α'-dimethyl-α''-acetic acid)trithiocarbonate
DMA	*N*,*N*-dimethylacrylamide
DMF	Dimethylformamide
DMSO	Dimethylsulphoxide
DNA	Deoxyribonucleic acid
dRI	Differential refractive index
E. coli	*Escherichia coli*
EDTA	Ethylenediaminetetraaceticacid
ESI-MS	Electrospray ionisation mass spectrometry
Et_3N	Triethylamine
EtOAc	Ethyl acetate
FT-IR	Fourier transform infrared spectroscopy
GPC	Gel permeation chromatography
h	Hour
HEPES	4-(2-hydroxyethyl)piperazine-1-ethanesulphonic acid
HRMS	High resolution mass spectrometry
K_a	Association constant
LC-MS	Liquid chromatography mass spectrometry
LCST	Lower critical solution temperature
LTB	*E. coli* heat labile toxin
MeOH	Methanol
mg	Milligram
MHz	Megahertz

MIP	Molecularly imprinted polymer
mL	Millilitre
mM	Millimolar
M_n	Number average molecular weight
M_w	Weight average molecular weight
NH_4OAc	Ammonium acetate
NIPAm	*N*-isopropylacrylamide
NMR	Nuclear magnetic resonance
PDI	Polydispersity index
PNA	Peptide nucleic acid
PS-DCL	Polymer-scaffolded dynamic combinatorial library
RAFT	Reversible addition-fragmentation chain transfer
THF	Tetrahydrofuran
UV-Vis	Ultraviolet-visible
ε	Molar extinction coefficient

Chapter 1.

Strategies for the Development of Synthetic Macromolecular Receptors

This chapter is based upon the following article:

Clare S. Mahon and David A. Fulton, Mimicking Nature with Synthetic Macromolecules Capable of Recognition. *Nature Chem*., 2014, **6**, 665-672

Table of Contents

1.1 Abstract

Through billions of years of evolution, nature has assembled a multitude of polymeric macromolecules capable of exquisite molecular recognition. This functionality is achieved by the precise control of amino acid sequence during the assembly of proteins, producing three-dimensional macromolecules with key residues anchored in the correct positions to interact with their targets. Developing 'wholly-synthetic' macromolecular analogues which mimic this function presents a considerable challenge to chemists, who lack the 'biological machinery' used by nature in the precision-assembly of polymers. In addressing this challenge, familiar chemical concepts, such as combinatorial methods and supramolecular interactions, have been adapted for application in the macromolecular arena. Working from a limited set of residues, synthetic macromolecules have been produced which display surprisingly high binding affinities towards target proteins, even possessing useful in vivo activities. These observations are all the more surprising when one considers the heterogeneity inherent within these synthetic macromolecular receptors, and provoke intriguing questions regarding our assumptions about the design of receptors.

1.2 Introduction

The recognition of one molecule by another is a phenomenon which inspires fascination amongst chemists, and is inarguably crucial to many biological processes. Indeed, proteins capable of molecular recognition span functions as diverse as the transport of oxygen by haemoglobin, the detection of pathogens by our immune system and the control of metabolic pathways by enzyme catalysts of enviable specificities. Such a multitude of functionality is achieved, for the most part, using a palette of just twenty amino acids. Proteins are macromolecular in nature, and typically interact over large areas, but with binding events usually confined to small "hot-spots" on surfaces where interactions are mediated by 'weak' supramolecular interactions between just a few amino acids.[1] The recognition capabilities of proteins are ultimately dictated by the sequences of residues within polypeptide chains which fold with incredible precision to produce complex three dimensional structures which display these crucial residues in key positions to interact with their target. The effects of weak interactions acting in concert, through multivalency,[2-4] can be significant. Nature has, through billions of years of evolution,

optimised the sequences of its proteins to accurately position key functional groups to produce receptors of exquisite function.

The development of synthetic systems capable of comparable functionality within a more reasonable timescale presents a formidable challenge indeed. The potential rewards of developing such synthetic receptors are, however, attractive. Synthetic materials capable of highly specific molecular recognition could deliver low-cost mimics of antibodies for use in diagnostic applications, potentially circumventing the use of expensive monoclonal antibodies as tools for the detection of disease (the growing market for clinical *in vitro* diagnostics was estimated to be worth ~$38 billion in 2010[5]). Additionally, a growing focus in drug discovery is the inhibition of protein-protein interactions,[6, 7] which because of their importance in mediating biological processes, make promising yet incredibly challenging drug targets. Part of the difficulty in targeting such interactions is that our current understanding of macromolecular association processes is still limited, and the development of synthetic models will undoubtedly help to improve matters. The hegemony often invoked in the design of receptors for biological applications is the need for a high level of homogeneity within receptors, and the precise arrangement of functional groups. Considerable effort has been expended in the development of elegant molecular architectures such as dendrimers,[8] which offer precision in the placement of functional groups for efficient molecular recognition. The iterative and challenging nature of their syntheses, however, often prohibits the widespread use of dendritic receptors, prompting the need for a more universal solution.

Progress in terms of developing receptors for such challenging macromolecular targets can, in the majority of cases, be classified into one of three pathways – the molecular imprinting of recognition sites within polymer matrices, the generation of combinatorial libraries of synthetic polymers, and the application of dynamic combinatorial chemistry to macromolecular systems. Each approach may provide insights which will aid in the further development of macromolecular synthetic receptors, arguably one of the most under developed areas of supramolecular chemistry.

1.3 The molecular imprinting of polymer matrices

The earliest and most well-established strategy for the production of macromolecular receptors has been the development of molecularly imprinted

polymers (MIPs).[9-14] Molecular imprinting (Fig. 1) involves the assembly of judiciously chosen polymerisable building blocks around template molecules, allowing complementary functionalities within both species to align in a favourable orientation. Monomer units are then 'fixed' in place by polymerisation, and the template removed to yield a three dimensional polymer matrix containing cavities of appropriate size, shape and functionality for complexation with the template. The imprinting of a polymer matrix around a template was first reported by Günter Wulff in 1972,[9, 10] and the now very familiar concept has been developed by numerous labs over the last four decades to deliver receptors for a broad spectrum of small and macromolecules,[11] in many cases providing useful receptor species for molecules as diverse as pharmaceuticals, pesticides and sugars. Frequently, MIPs are constructed using vinylic or acrylic monomer units,[12] with the wide range of readily accessible monomers providing scope for a range of supramolecular interactions between monomer units and templates. These monomer units may be cross-linked with relative ease, by the initiation of a simple radical polymerisation reaction. MIPs prepared in this way often provide robust receptor species which may withstand extremes of temperature and pH,[14] as a consequence of the strong covalent cross-links which hold monomer units in place. Because the MIP approach is experimentally so simple, even scientists with minimal chemical training can apply it to make MIPs, particularly for chromatographic or biosensing applications. After imprinting, the polymer matrix can be ground to a powder and the template extracted, giving the researcher useful amounts of MIP to work with.

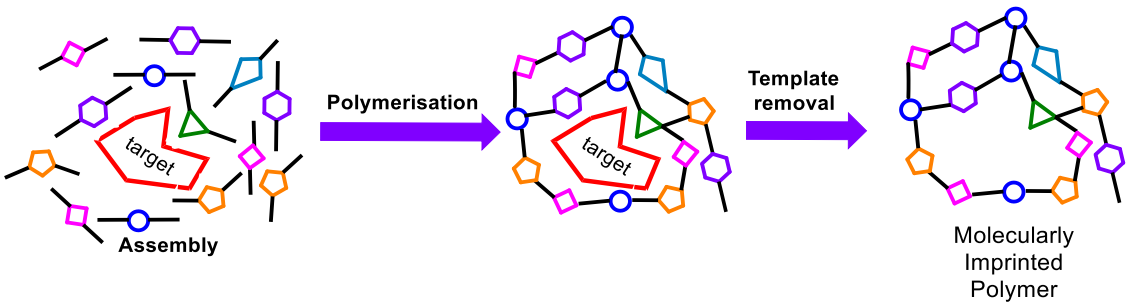

Fig. 1. The molecular imprinting of polymer matrices involves the self assembly of monomer units around a template, allowing functionalities to align in a favourable orientation before polymerisation is initiated, fixing these units in place. Removal of the template yields a polymer matrix containing cavities of appropriate size, shape and functionality for interaction with the template, or similar molecules.

The pinnacle of the molecular imprinting approach is arguably the recent elegant work of Kenneth Shea[15] and co-workers, who have extended the familiar MIP concept from bulk polymers into the nano-regime. Molecularly imprinted polymer

nanoparticles were produced to target melittin, a toxic peptide, and were found to display a high affinity for the target, with an association constant of 10^{11} M^{-1}. Impressively, these nanoparticles neutralised the toxin in a living mouse (Fig. 2), demonstrating beautifully the viability of synthetic macromolecular receptors in a practical context.

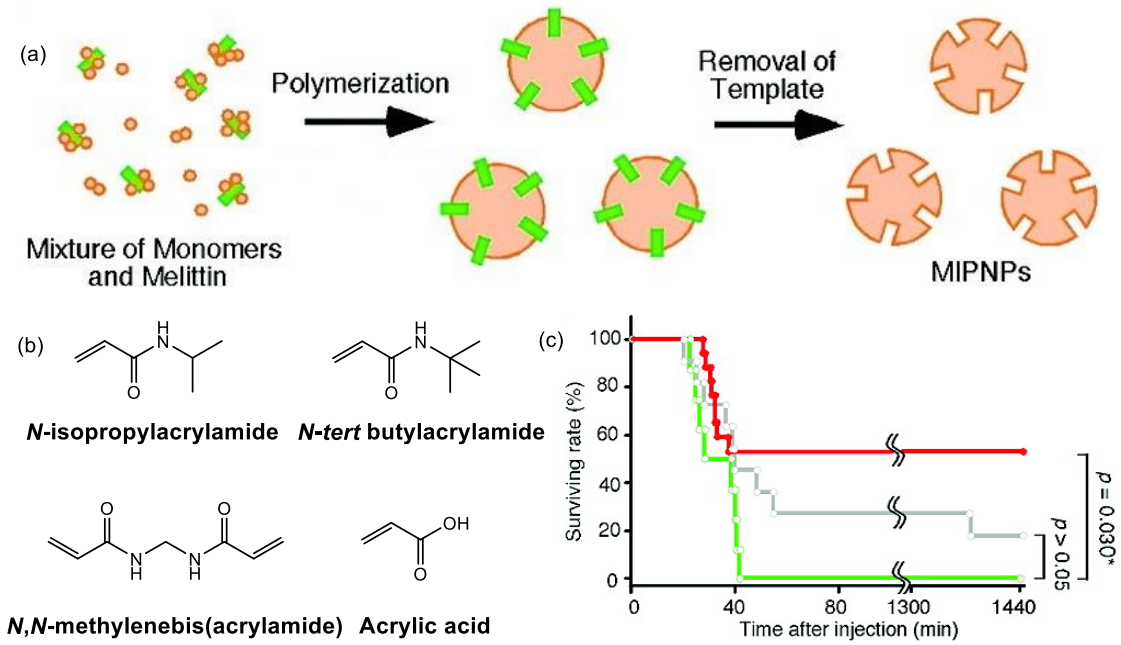

Fig. 2[15] (a) The process of molecularly imprinting polymer nanoparticles with melittin, a toxic peptide. A mixture of monomers (peach circles) is exposed to melittin (green rectangles) before polymerisation is initiated, generating polymer nanoparticles complexed with melittin. Removal of melittin yields nanoparticles displaying cavities of appropriate size, shape and functionalisation to complex the toxin on subsequent exposure. (b) The palette of monomers used to generate molecularly imprinted nanoparticles. (c) Survival rates of mice after injection of a toxic dose of melittin (green); a toxic dose of melittin followed by melittin-imprinted nanoparticles (red) or a toxic dose of melittin followed by nanoparticles of the same monomer composition as those imprinted with melittin, but produced without exposure to melittin. Reprinted (adapted) with permission from Hoshino, Y.; Koide, H.; Urakami, T.; Kanazawa, H.; Kodama, T.; Oku, N.; Shea, K. J., Recognition, Neutralization, and Clearance of Target Peptides in the Bloodstream of Living Mice by Molecularly Imprinted Polymer Nanoparticles: A Plastic Antibody. *J. Am. Chem. Soc.* **2010,** *132* (19), 6644-6645. Copyright 2010 American Chemical Society.

Interestingly, non-imprinted nanoparticles of the same statistical monomer composition did not significantly neutralise melittin *in vivo*, suggesting that the precise placement of functional groups in the recognition site of the nanoparticle is key for successful complexation of the target. It is thought-provoking that a small palette of just three functionalised monomers and a single crosslinking agent could achieve sufficient *in vivo* specificity, an observation which raises the question: do we really need a palette of residues as large as nature's to achieve comparable recognition?

Molecular imprinting, despite its successes, does possess some significant limitations. The use of robust covalent cross-links may produce poorly-permeable matrices which allow only slow mass transfer of target molecules in and out of cavities. Templates used during crosslinking may not always be completely removed from the polymer matrix after polymerisation, and may leach out of cavities over long time periods, causing problems if the MIP is to be used for detection of an analyte. Binding sites within the matrix may not be optimised for successful complexation with the target, and the nature of binding sites is unlikely to be uniform throughout the sample. This inherent heterogeneity could pose an intractable problem that may prevent the widespread application of the technique. One study demonstrated[16] that the recognition characteristics of an MIP are primarily determined by a large number of sites of relatively low affinity for the template, rather than the small number of high affinity sites contained within the material. Ultimately, these limitations arise because the imprinting of binding sites occurs wholly under kinetic control, leaving no scope for their refinement. This crucial restriction often has a detrimental effect on the recognition properties of the resultant MIP,[17] both in terms of affinity for and selection of target molecules. One could argue that only through further refinement of these many low affinity sites can materials which truly rival antibodies be achieved.

1.4 Combinatorial libraries of polymers

Combinatorial chemistry[18] involves the generation of large libraries of compounds and the screening of each compound in turn against a target molecule, in an effort to identify a receptor of high-affinity for further development. Combinatorial chemistry has been embraced by the pharmaceutical industry as a valuable tool in the identification of small-molecule lead compounds.[19] Often libraries constitute several hundred thousand compounds,[20] constructed with the aid of high-throughput robotic techniques.[21]

The combinatorial strategy may be adjusted for application in a macromolecular context (Fig. 3 (a)), and is well-illustrated by the efforts of Schrader and co-workers. Their approach involves the selection from a manageably small palette of monomers possessing various functionalities, of which some are predisposed towards favourable interactions with the target, and generation of a library of random statistical copolymers which may be assessed in terms of their affinities to the

chosen protein. No detailed structural information of the target protein need be known for successful application of this strategy, and choice of monomers can be made based on readily available general information about protein targets such as surface charges and amino acid composition, rather than sequence-specific information.

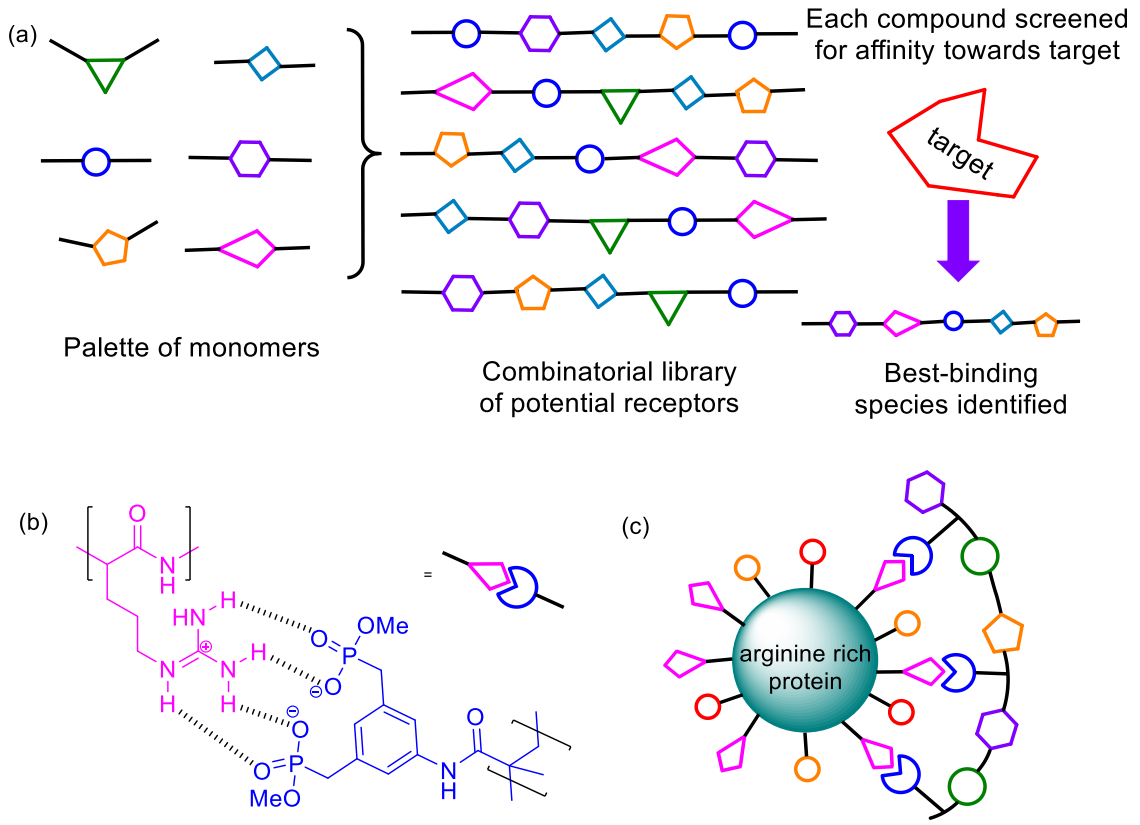

Fig. 3 (a) A combinatorial library of macromolecules may be generated from a palette of monomers with functionalities predicted to interact favourably with the target. Each compound in this library may then be screened for its ability to bind to the target. (b) This bis-phosphonate motif has been identified as capable of recognising arginine residues in organic solution, with weaker interactions observed in water.[22] (b) The multiple incorporation of this recognition unit in polymeric receptors[23] leads to species with high affinities and selectivities for proteins with arginine-rich surface functionalisation.

The key to the success of this particular example lies in the relative importance of arginine in protein-protein interactions,[1] with previous work[22] from the Schrader lab identifying a recognition unit with a high affinity for arginine residues (Fig. 3 (b)), where strong binding affinities were observed in organic solvents but much weaker effects in water. Knowing that the multiple incorporation of this receptor would likely lead to improved binding in aqueous solution, it was incorporated into a series of copolymers (Fig. 3 (c)) which were screened for their affinities to various protein targets.[23] Although this approach may seem somewhat crude, binding interactions of remarkably high affinity were observed, with dissociation constants

on the nanomolar scale determined in some cases. This work also highlights the importance of hydrophobic interactions, with copolymers containing a higher proportion of greasy dodecyl appendages shown to bind most effectively with BSA, a protein known to possess a hydrophobic binding cleft. Later work from the same group also provides some evidence for selectivity in the binding of copolymers to proteins,[24] with one copolymer shown to bind to lysozyme ten times more strongly than cytochrome c, even though these proteins are of similar size and surface charge. Again, this work highlights that useful affinities and selectivities can be accessed using a limited palette of residues, and with significant heterogeneity in macromolecular structure. Schrader suggests that the concept could be improved upon the identification of other receptor units which are selective for each class of amino acid residue.[24]

The reliance of this work on the use of linear copolymer chains raises an interesting question: would cross-linking lead to polymers which are more pre-organised for complexation, and therefore bind more strongly to the target? Schrader envisaged that flexible copolymers would be able to adopt an "induced fit" conformation[24] on protein surfaces and therefore declined to add a crosslinking species. Flexible polymer chains have the advantage of being able to wrap around the target, potentially accessing multiple remote binding sites. This conformational rearrangement could, however, be thought of as a significant entropic barrier to effective binding. Conversely, in a more "pre-organised" cross-linked structure, restriction of conformational freedom could have a detrimental effect on recognition, by preventing the key residues along the polymer chain from accessing binding sites on the target. Given the importance of tertiary structure in proteins, which imparts pre-organisation, one is encouraged to believe that cross-linking will most likely be a beneficial feature for most systems. Indeed, Shea and co-workers have investigated[25] the effect of cross-linking on the complexation of polymer nanoparticles with heparin, a sulphonated polysaccharide, determining that the affinity of the nanoparticle-heparin interaction increases significantly as the level of cross-linking within the nanoparticle is increased from 0% to 10%.

Shea has also utilized[26-28] a combinatorial approach to nanoparticle receptor development, where small libraries of nanoparticles of varying monomer composition are generated and screened for their affinities to a chosen protein.

These 'non-imprinted' nanoparticles have been shown to neutralise melittin *in vivo*, in contrast to the aforementioned work (pages 5-6),[15] where nanoparticles not exposed to melittin were unsuccessful in its *in vivo* complexation. A feature of these combinatorially-generated nanoparticles is their greater variety of monomer functionalities, so these findings may suggest that the need for specificity in orientation of key residues discussed earlier may be circumvented by expanding the palette of monomers in use, and simply relying on multivalency[2-4] to a greater extent.

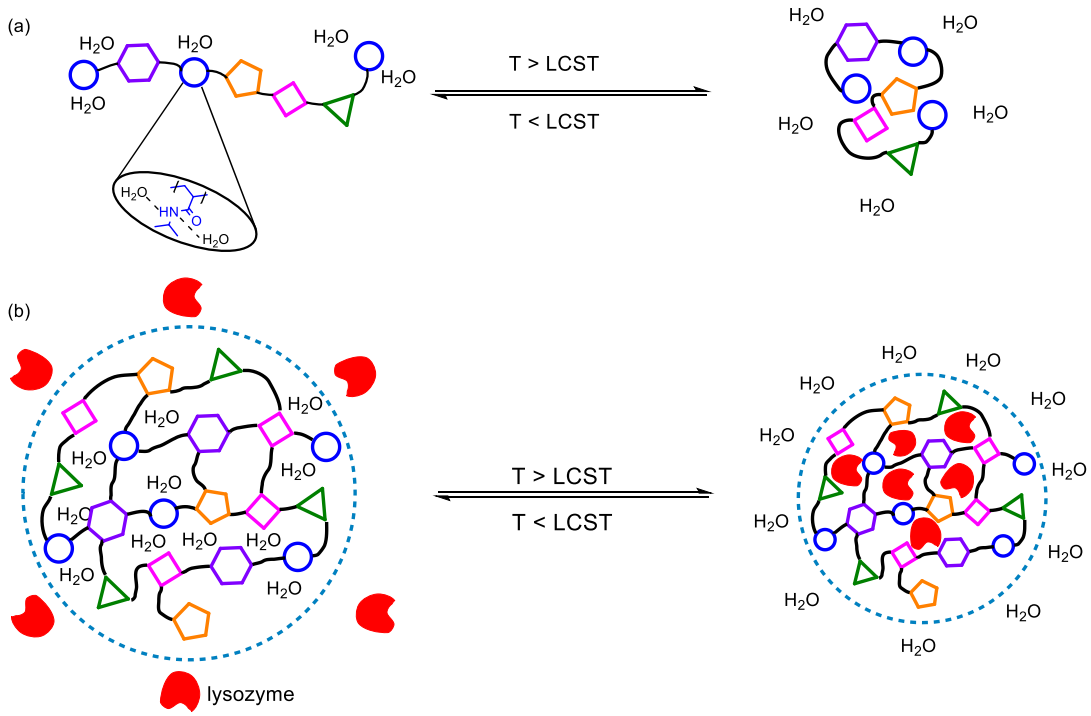

Fig. 4. (a) Polymers containing *N*-isopropylacrylamide (NIPAm) or other thermoresponsive monomer display lower critical solution temperatures (LCSTs), above which they are insoluble in aqueous solution. At temperatures below the LCST, polymer chains are hydrophilic in character and are solvated by water molecules. At the LCST polymer chains are reversibly desolvated, resulting in their precipitation from solution. Upon cooling below the LCST, polymer chains may again be solvated, allowing the polymer to redissolve. (b) Polymer nanoparticles were prepared[29] incorporating NIPAm amongst a palette of monomers proposed to interact favourably with lysozyme, a protein extracted from chicken egg white. Heating a solution of polymer nanoparticles and lysozyme results in the reversible hydrophobic collapse of the nanoparticles, encapsulating lysozyme in their cores. The protein may be released by cooling the solution below the LCST of the nanoparticles.

For many applications of polymeric receptors, it is desirable for them to not only complex their target with high selectivities, but to release it at a later stage. An elegant 'catch-and-release' system targeting lysozyme,[29] where the protein can be reversibly captured and released in response to changes in temperature, has been developed by Shea, utilising the combinatorial approach described previously. In addition to judiciously choosing monomer units so as to afford functionalities with the potential to interact favourably with the highly-negatively charged protein, Shea

exploits the thermoresponsive behaviour of *N*-isopropylacrylamide-containing polymers to generate nanoparticles which bind lysozyme at temperatures below their lower critical solution temperature (LCST, Fig. 4). Temperature increases above the LCST of the nanoparticles induces release of lysozyme in a fully reversible process, neatly isolating this single component from the complex mix of proteins found in chicken egg whites.

It is encouraging to note that macromolecular receptors of impressively high affinity, and even demonstrable *in vivo* activity, may be generated through application of simple combinatorial principles, with reasonably small palettes of residues. The need to synthesise and screen each compound individually against the target still remains labour-intensive and may prohibit rapid receptor generation. It could also be argued that, ultimately, these systems suffer the same limitations in terms of presenting a viable approach to receptor identification as the molecular imprinting of polymer matrices – there is no mechanism to allow for error correction or adaptation of library members to further enhance binding properties.

1.5 Dynamic combinatorial chemistry

The achievement of effective molecular recognition is a goal which more often than not is achieved through rational design and complex multi-step synthesis. Around two decades ago a fresh approach to the challenge was presented by the development of dynamic combinatorial chemistry (DCC).[30, 31] This concept expands upon the application of traditional combinatorial methods by harnessing reversible chemical processes[32] to generate a combinatorial library in which constituents may structurally interconvert with one another. This system, termed a dynamic combinatorial library (DCL), strives to attain a thermodynamic minimum by favouring the generation of the most energetically stable library members. The equilibrium may be perturbed by addition of a template species which may interact favourably with one or more library members, inducing a compositional shift within the system, which 'recycles' species of low affinity for the template to amplify the concentrations of the better-binding library members (Fig. 5).

This amplification simplifies the identification of the key stabilising species, as the species of highest affinity then constitute a significant proportion of the library composition. The reversible nature of the chemical processes used provides a

mechanism for refinement of binding sites, a critical limitation of kinetically-controlled templating processes.

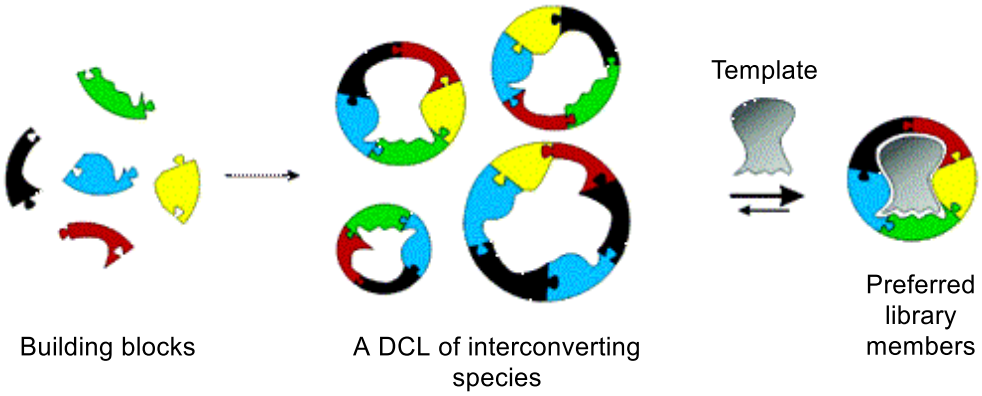

Fig. 5[30] Schematic representation of the use of a DCL for the discovery of a receptor for a template. Building blocks are combined and allowed to self-assemble into a mixture of interconverting species. Addition of a template molecule induces compositional change, amplifying the concentration of library members which best interact with the template. Reprinted (adapted) with permission from Corbett, P. T.; Leclaire, J.; Vial, L.; West, K. R.; Wietor, J.-L.; Sanders, J. K. M.; Otto, S., Dynamic Combinatorial Chemistry, *Chem. Rev.*, **2006**, *106* (9), 3652-3711. Copyright 2006 American Chemical Society.

1.5.1 Dynamic combinatorial libraries of macrocycles

Dynamic combinatorial chemistry has predominantly been used to generate macrocyclic receptors[33-47] for small molecules or ions, with impressive amplifications of favoured species observed in a number of cases. In these systems, building blocks are designed to display complementary functional groups at either end of the molecule to allow for cyclisation to generate a number of macrocycles simultaneously. Upon addition of the template, equilibrium shifts so as to amplify the concentration of macrocycles with cavities that best complex the template, using unfavoured species as feedstock for the generation of these receptors.

One example of such a DCL, constructed by Sanders and co-workers,[46] is illustrated (Scheme 1). Cyclisation of building block **1**, which displays an acylhydrazide unit in addition to a masked aldehyde group, in the presence of an acid catalyst generates a DCL of macrocycles which at equilibrium, consists mainly of dimeric (88%) and trimeric (11%) macrocycles. The authors have suggested that π-π interactions between aromatic rings contributes to the increased thermodynamic stability of the dimer. Addition of *N*-methyl quinuclidinium iodide initiates compositional change which amplifies the concentration of the trimer (56%) at the expense of the dimer (41%). Acetylcholine chloride has also been shown to exert a templating effect on

the DCL, leading to a more pronounced increase in the concentration of the trimer (86%), with the initially preferred dimer now accounting for a small proportion of the library composition (11%).

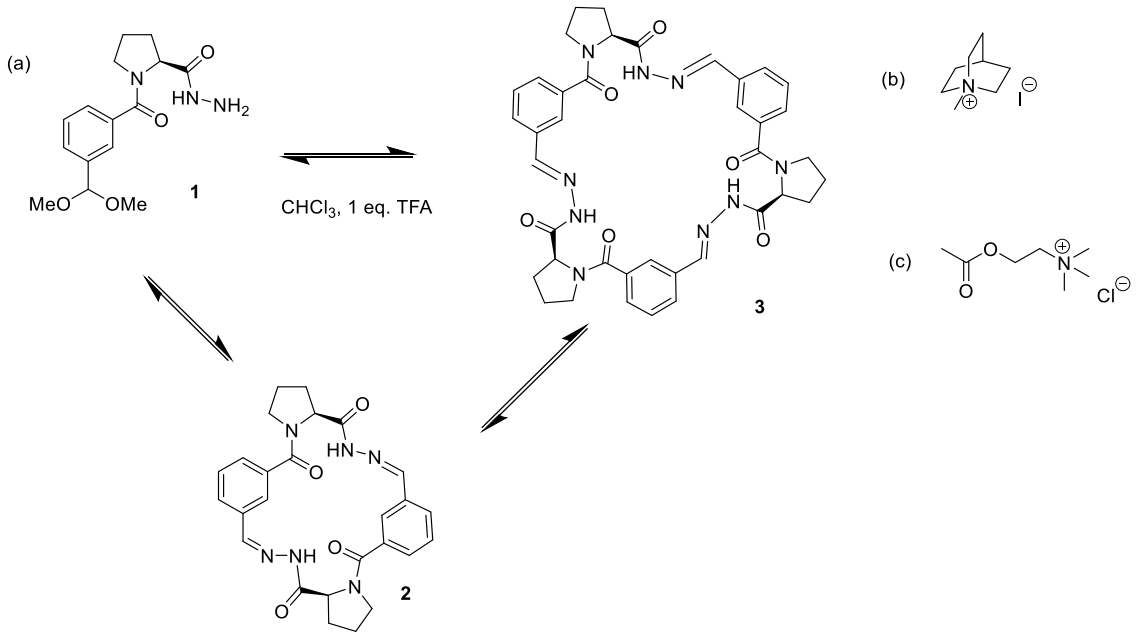

Scheme 1 (a) A DCL of macrocycles[46] generated using building block **1**, in the absence of any other species consists mainly of dimer **2**, with a much smaller amount of trimer **3**. Addition of an ammonium template, *N*-methyl quinuclidinium iodide (b), or acetylcholine chloride (c), induces compositional change which amplifies the concentration of trimer **3**.

Complexation between template molecules and the trimeric macrocycle **3** has been established using ESI-MS and various ^{1}H NMR spectroscopic techniques, suggesting that compositional change is driven by favourable interactions between template molecules and the amplified species.

1.5.2 Exchange chemistry for DCC

If a chemical process is to provide the basis for the construction of a DCL, it must be reversible on a practical timescale,[30] and proceed under mild conditions of temperature and pH, so as not to disrupt interactions between library members and templates. All library members must be completely soluble in the solvent in use,[30] as insoluble library members may act as a thermodynamic trap, thereby skewing library composition towards their production. Additionally, it is preferable that all library members are approximately isoenergetic[30] to avoid initial bias within the library composition which could hinder the process of re-equilibration upon exposure to template. Exchange processes commonly employed for DCL production include dynamic covalent reactions,[32] metal-ligand coordinative processes[48-52] and non-covalent interactions.[53-56] Exchange processes involving non-covalent or metal-

ligand bonding, whilst generally faster to equilibrate, produce comparatively labile species, which may complicate the isolation of library members, and consequently these exchange processes are employed less frequently than reversible covalent exchange processes. A number of dynamic covalent reactions[30, 31] have been utilised successfully in the generation of DCLs, most notably disulphide exchange,[33-38, 57-67] imine exchange[47, 68-86] and hydrazone exchange.[39-46, 87-99] For the purposes of this investigation, we will restrict our discussion to systems based upon acylhydrazone exchange chemistry.

1.5.3 Acylhydrazone exchange

Acylhydrazides present a more reactive alternative to amines in their condensation reactions with aldehyde or ketone carbonyl groups to produce imine-like species. Acylhydrazides react reversibly with aldehydes and ketones (Scheme 2(a)) with equilibria tending to favour formation of the acylhydrazone even in aqueous solution.[100] The acylhydrazone may undergo component exchange upon exposure to another acyhydrazide (Scheme 2 (b)), generating a mixture of interconverting acylhydrazones.

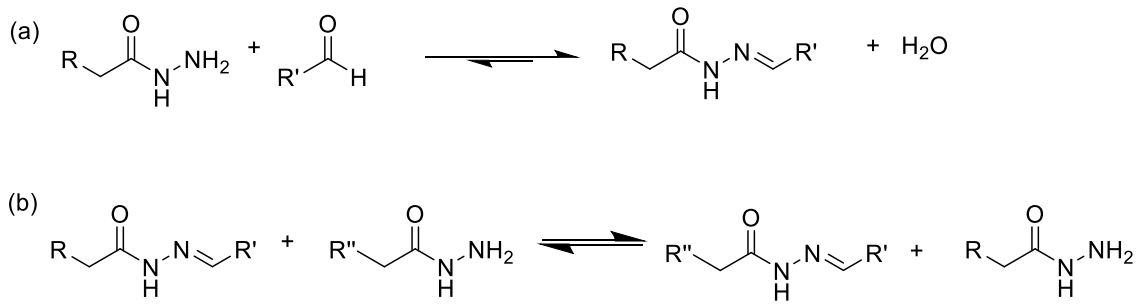

Scheme 2 (a) The formation of an acylhydrazone through condensation of an aldehyde and an acylhydrazide. (b) Exposure of an acylhydrazone to another acylhydrazide generates a mixture of interconverting acylhydrazones.

The increased reactivity of acylhydrazides in comparison to the corresponding amines may be explained by the presence of an electronegative group adjacent to the nucleophilic nitrogen, a phenomenon known as the α-heteroatom effect.[100] Acylhydrazones are stabilised by resonance effects, which slow hydrolysis and exchange reactions considerably compared to the corresponding imines, and therefore acylhydrazones may be considered to be kinetically inert under neutral conditions.[101] Acylhydrazone formation and exchange reactions are typically fastest

in aqueous solution at around pH 4.5,[102] a condition which may be accommodated for within most systems.

For some applications, however, it is desirable to construct DCLs under neutral conditions, particularly if the template is a biomolecule which is unstable under acidic conditions. Lehn and co-workers[84,85] have overcome this limitation by constructing the DCL in an acidic medium and allowing it to equilibrate before increasing the pH to kinetically fix composition and screening libraries against the template. Active members of the library may be identified by a "dynamic deconvolution" strategy, where building blocks are sequentially removed from the library, thus eliminating some species from the DCL, and the effects of overall potency are assessed in terms of binding to the target compound. It could be argued, however, that this method presents a time-consuming, labour-intensive route to potential receptors which offers little advantage to traditional combinatorial methods.

More recently, it has been established that acylhydrazone exchange may be catalysed under neutral conditions by addition of aniline[102] to reaction mixtures. Aniline may catalyse both acylhydrazone formation and exchange reactions through formation of an activated imine intermediate, with rate enhancements of up to 70-fold observed under neutral conditions. It is, however, noteworthy that aniline is added in large excess (100/1000-fold) to these reaction mixtures, a factor which may complicate compositional analysis of DCLs in some cases.

Other researchers have focussed on the structural modification of building blocks in order to accelerate exchange. Nguyen and Huc[88] have reported that hydrazones derived from hydrazines with adjacent electron-withdrawing groups are generated and hydrolysed rapidly in neutral aqueous solutions. Kool and co-workers[103] have since demonstrated that carbonyl compounds with neighbouring acidic or basic groups yield hydrazones at accelerated rates, an effect which has been attributed to intramolecular proton transfer to the leaving group of the tetrahedral intermediate which decomposes to yield the acylhydrazone (Scheme 3).

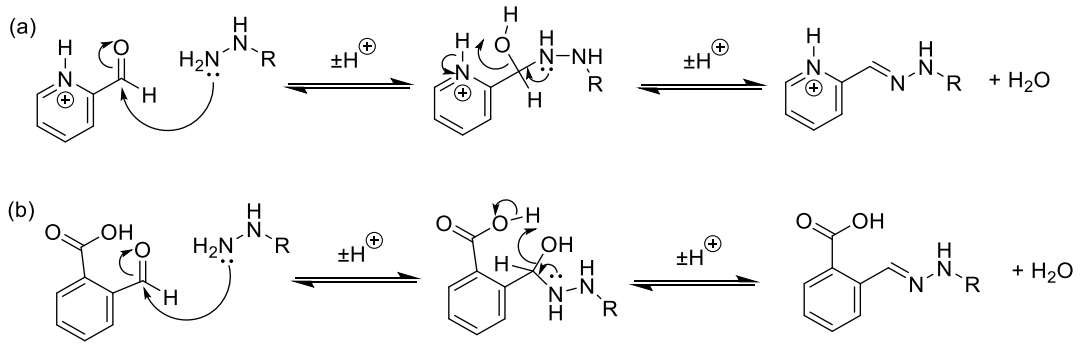

Scheme 3 Proposed mechanism for rate enhancement of acylhydrazone exchange by adjacent basic (a) or acidic (b) groups.[103] Intramolecular protonation of the leaving group accelerates decomposition of the tetrahedral intermediate, which is the rate-determining step of the reaction under neutral conditions.[104]

The approach proposed by Nguyen and Huc,[88] and Kool and co-workers,[103] of modifying structural parameters of reactants in order to accelerate rates of reaction is very appealing, as it avoids increasing the complexity of mixtures by addition of catalysts. Adaptation of structural features of building blocks to afford DCLs which establish and re-equilibrate rapidly under neutral conditions without the addition of an external catalyst may present the most desirable solution for the acceleration of receptor discovery using DCLs.

1.5.4 Design of dynamic combinatorial libraries

Most DCLs reported to date have consisted of a limited number of library members, a factor which allows significant amplifications of effective binding species to be observed. This situation is largely a consequence of researchers' drive to establish proof-of-principle – that the best binding species may be amplified and detected within the DCL. The production of much larger libraries would increase the number of potential receptors available for screening, and will ultimately be required in order for DCC to deliver on its potential as a viable tool for receptor development.[105] As the size of a DCL is increased, however, practical challenges arise in terms of monitoring library composition, which requires the quantitative detection of large numbers of compounds in a complex mixture. In a complex library consisting of many thousands of interconverting compounds, the identification of a single best-binding species may not be feasible, as the concentration of this compound may fall below the limit of detection.

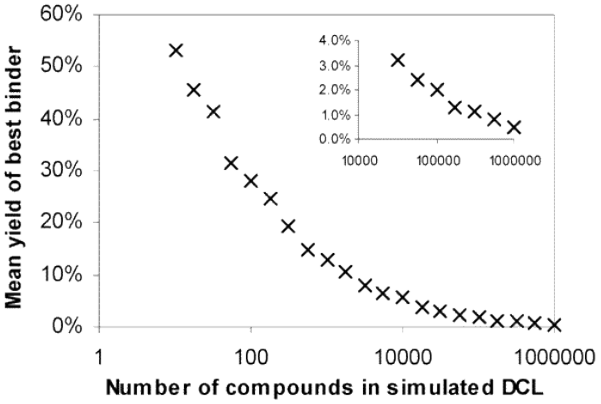

Fig. 6[106] Mean yield of highest affinity binders in a series of computer-simulated DCLs as size is increased. Each point represents an average of 100 simulated libraries. Reprinted (adapted) from Corbett, P. T.; Otto, S.; Sanders, J. K. M., What Are the Limits to the Size of Effective Dynamic Combinatorial Libraries? *Org. Lett.* **2004,** *6* (11), 1825-1827. Copyright 2004 American Chemical Society.

In an effort to determine if this issue presents an intractable challenge to the further development of the DCC approach, researchers have turned to computational modelling to assess the effects of library size on potential amplification of a single species. Sanders and co-workers[106] have developed DCLSim, software which applies a modified version of the COGS algorithm[107] to model equilibrium distributions upon input of equilibrium constants and mass balances, and have modelled DCLs ranging in size from 10 to 10^{16} library members. As the size of the DCL is increased, the mean yield of the best-binding library member decreases (Fig. 6), as building blocks must be distributed over a much larger number of library members. In a DCL of 10,000 compounds, the best-binding species accounts for just 8% of the library composition, illustrating the difficulties of increasing library size. A change in DCL composition of this magnitude may appear small in comparison to the large amplification factors associated with smaller libraries, but such a change would fall within the limit of detection of analytical methods commonly used to monitor DCL composition, such as LC-MS. It may then be possible to prepare a biased library[106] using building blocks known to stabilise the template, in judiciously chosen proportions so as to produce a greater yield of the preferred receptor.

Another study by Otto and Ludlow[108] simulated the response of DCLs composed of up to 16 building blocks and up to a possible 4828 library members, to template addition at a range of concentrations of building blocks and templates. The authors examined the mean affinity, over 100 simulations, of the three species with greatest amplification factor in each DCL. Results indicate that as library size increases, the affinity of these best-binding species also increases, improving the probability of identifying a receptor of very high affinity within the mixture. Encouragingly, the authors observe that, in their experience, a compound which accounts for 1% of the composition of an untemplated library and is amplified by at least a factor of two

upon exposure to template may be detected by LC-MS, suggesting that increasing the size and complexity of DCLs may not pose intractable analytical difficulties.

Another computational study[109] has examined the correlation between binding affinities of library members towards the template and their levels of amplification within the library, thus testing the key premise that addition of a template to a DCL will increase the concentration of the best-binding species. A total of 14,450 DCLs were simulated at a range of different concentrations of building blocks and template, with relationships between amplification factor and binding affinities of library members assessed in terms of the linear correlation constant R^2. At concentrations of building blocks greater than 10 mM, a reasonably strong correlation between binding affinity and amplification factor was demonstrated, with R^2 values of 0.8 ±0.1 obtained when the template is present at less than one-tenth of the total building block concentration. This observation provides a useful rule-of-thumb for researchers designing DCLs, and is a factor which may easily be incorporated into the design of the experiment. Under these conditions of limited template availability, library members must compete to interact with the template, increasing the probability of the best-binding species being most significantly amplified. It is, however, important to note that decreasing the concentration of the template within the DCL will tend to reduce amplification factors, potentially allowing effective binders to remain undetected.

1.6 Systems of interconverting polymers

Whilst the vast majority of research applying dynamic combinatorial principles to the discovery of receptors focusses on small molecule systems, one could imagine that the application of DCC could be expanded successfully to the generation of polymeric receptors. The reversible nature of chemical processes used could provide a mechanism for the refinement and optimisation of binding sites, a critical limitation of kinetically controlled processes such as the molecular imprinting of polymer matrices. Additionally, macromolecular systems provide increased scope for multivalency in interactions with targets, which would be particularly advantageous when the target itself is macromolecular in nature.

1.6.1 Dynamers

One approach to the transfer of the principles of DCC to macromolecular systems is the concept of dynamers,[93, 110] as conceived by Lehn. Dynamers are produced by the

reversible linkage of monomer units to form a constitutionally dynamic polymer capable of exchanging its component residues. One intriguing report within this field is the "self-sensing" behaviour of a dynamer system in response to Zn (II) ions.[74] Addition of Zn (II) to a system of interconverting dynamers containing aromatic and aliphatic imine units (Scheme 4) leads to preferential co-ordination of the more basic aliphatic amine to Zn (II), and consequently dynamers containing increased proportions of the aromatic imine unit are formed. The consequence of this constitutional rearrangement is an increase in the fluorescence of the dynamers, a phenomenon which may be exploited to allow for the sensing of Zn (II) ions. The system presents an example of "reverse templation," where addition of the target compound to a DCL induces compositional change to allow the target species to better interact with the building blocks that make up the library rather than any combination of building blocks.

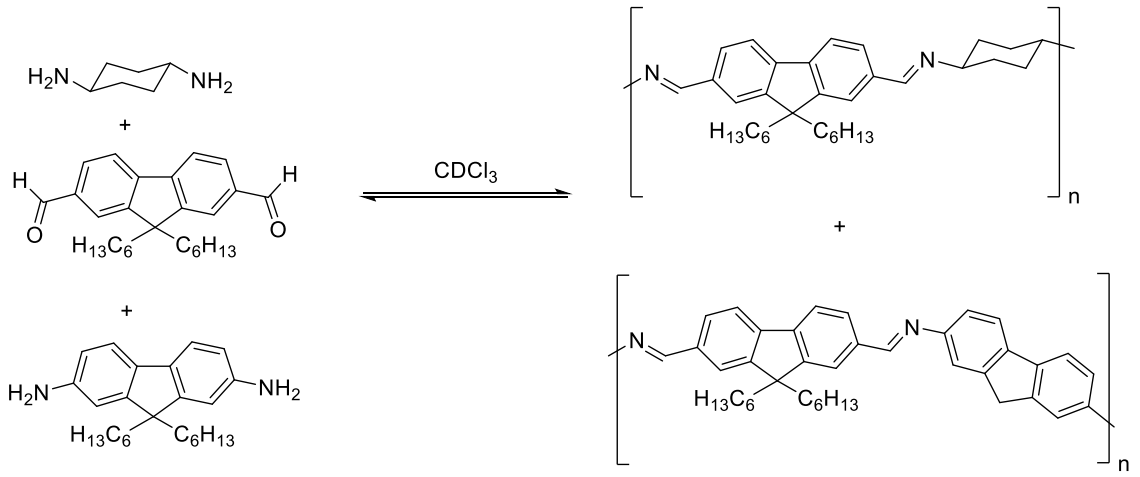

Scheme 4 A "self-sensing" system of dynamers[74] which responds to the addition of Zn (II) by rejecting the aliphatic amine unit, which co-ordinates preferentially to Zn (II). The resulting dynamers contain the aromatic imine unit predominantly, resulting in enhanced fluorescence emission of the system.

Dynamers may present intriguing possibilities in materials chemistry,[111-114] however, the approach may be less well-suited to the generation of synthetic polymers capable of molecular recognition. Condensation polymerisations are likely to give rise to a Flory distribution of library members of varying chain length and monomer composition, in stark contrast to many of the condensation polymers (proteins, nucleic acids) found in nature which are precision-assembled by enzymes to ensure their homogeneities and fidelities.

1.6.2 Sequence-adaptive peptide nucleic acids

Nucleic acids are biomacromolecules whose structure can be viewed as sequences containing four possible types of nucleobases appended onto a poly(phosphodiester) scaffold, raising the intriguing possibility of making 'dynamic' analogues. In a remarkably elegant piece of work,[115] Ghadiri and co-workers reversibly tethered nucleobase analogues onto a peptide scaffold via reversible thioester linkages, generating a 'family' of sequence-adaptive peptide nucleic acids which responded to the addition of a single-stranded DNA template by selecting the complementary nucleobase from solution to maximise favourable base-pairing interactions (Fig. 7).

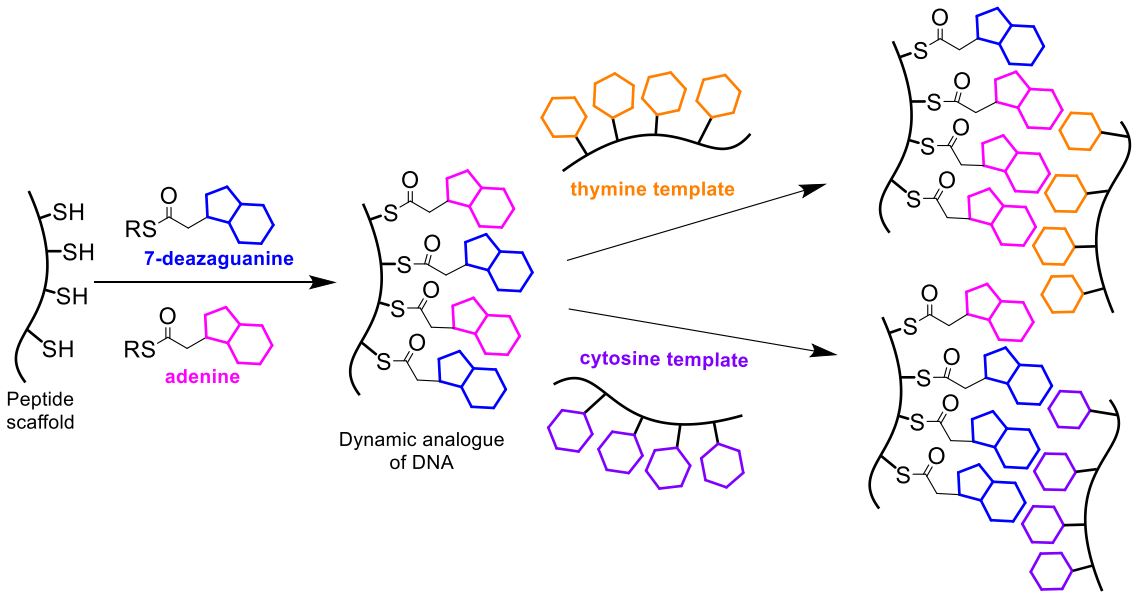

Fig. 7 Sequence-adaptive peptide nucleic acids (PNAs), as reported by Ghadiri.[115] Thioester-functionalised analogues of nucleobases such as 7-deazaguanine and adenine have been reversibly conjugated onto thiol-functionalised peptide scaffolds, through dynamic thioester linkages, producing a dynamic analogue of DNA. When single-stranded oligonucleotide templates are added the system undergoes component exchange mediated by trans-thioesterification, with PNA scaffolds preferentially incorporating the complementary nucleobase.

This response is arguably akin to artificial DNA replication, which is notable as it has largely been thought that nucleotide building blocks do not undergo efficient self-assembly in the presence of a DNA template, in the absence of enzymatic catalysis.[116] This observation may suggest that the construction of the scaffold is a key step in the generation of polymeric receptors for macromolecular species. In systems with pre-formed scaffolds the bulk of the entropic penalty of assembling many residues into a macromolecular construct has already been paid prior to templating, allowing the compositional change associated with templating to proceed efficiently. The use of a fixed-length scaffold also significantly simplifies the product distribution of the

system by limiting chain length, a factor which may help to limit the complexity of the distribution and improve ease of analysis.

1.6.3 Theoretical treatment of macromolecular DCLs

As discussed previously, theoretical studies have shown that as the size and complexity of a DCL is increased, the mean yield of the best-binding library member decreases,[106] possibly resulting in the concentration of strongly binding species falling below the limit of detection. This phenomenon is particularly relevant to mixtures of interconverting polymers, which offer vast scope for diversity by their very nature, and it may not be possible to identify a single best-binding species from such a complex mixture.

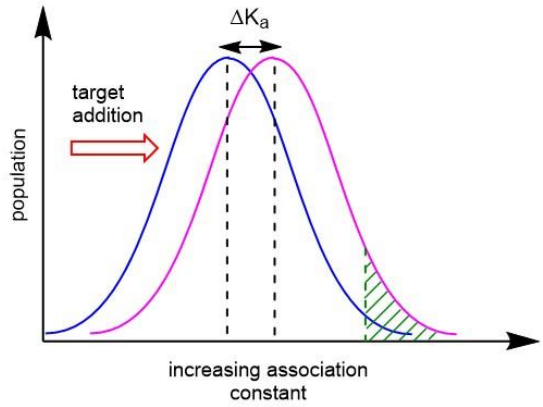

Fig. 8 A population of interconverting polymers may be modelled as normally distributed in terms of logK_a towards a particular target.[117] Addition of the target may shift the entire distribution towards greater association constants for the target, and yield a significant fraction (shaded in green) of receptors of greatly enhanced affinity.

Moore and Zimmerman[117] have constructed an elegant, yet realistic model of populations of interconverting polymers, in an effort to determine if the population may be biased towards production of sequences of higher affinity towards a target molecule. Polymer sequences are modelled as being normally distributed in terms of logK_a towards the target (Fig. 8), an assumption which has been accepted as generally representative of populations where composition is determined by non-covalent interactions.[118] Results indicate that the mean affinity constant for the distribution may be shifted to a limited but measurable degree upon addition of the target but this increase will be limited to around two orders of magnitude. The model does, however, predict that a small fraction of this distribution (~5%) will have a significantly enhanced affinity towards the target, with association constants more than 10^4 times larger than the original mean.

1.6.3 Polymer-scaffolded dynamic combinatorial libraries

Previous work in our laboratory[119] has led to the construction of dynamic combinatorial libraries on polymer scaffolds. A polymer with pendant aldehyde groups may be reversibly functionalised with different residues by means of

acylhydrazone linkages. The dynamic nature of this linkage allows side chain residues to exchange, producing a mixture of interconverting polymers – a Polymer-Scaffolded Dynamic Combinatorial Library (PS-DCL).

In the first example of a PS-DCL,[119] acylhydrazide residues were grafted onto poly(vinylbenzaldehyde) scaffolds through acylhydrazone linkages to generate polymers which were fully functionalised with a single residue (Scheme 5). Upon mixing two of these functionalised polymers in the presence of an acid catalyst, acylhydrazone exchange was shown to occur, generating a library of polymers functionalised with both acylhydrazide residues.

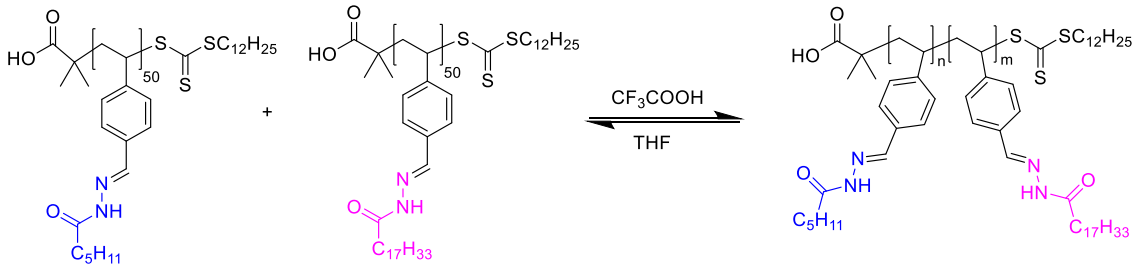

Scheme 5 A PS-DCL consisting of two acylhydrazide building blocks reversibly appended onto poly(vinylbenzaldehyde) scaffolds.[119] Upon mixing two differently functionalised polymers, component exchange was observed, generating a mixture of interconverting polymers.

This observation demonstrates that PS-DCLs possess the capacity for re-equilibration, as has been demonstrated extensively with macrocyclic DCLs. Transferring the principles of DCC to polymer-scaffolded systems may allow for the development of a convenient route to macromolecular receptors, if PS-DCLs can be demonstrated to respond to template addition.

1.7 Conclusions

Whilst the coveted 'artificial antibody' has so far remained outside our grasp, significant progress has been made towards its realisation. Much has been achieved with small combinatorial libraries of polymers and limited palettes of functional monomers. Kinetically-controlled imprinting processes, which may seem crude in comparison to nature's precision assembly of macromolecular architectures, have in some cases yielded synthetic receptors of remarkable specificities, suggesting that perhaps heterogeneity within receptors need not necessarily be avoided.

The ideal route to the generation of synthetic macromolecular receptors would provide the scope for error correction and refinement of binding sites afforded by a thermodynamically-controlled templating process. The development of DCC has

allowed for the production of receptors for a wide range of small-molecule targets, and DCC is now well-established as a route towards receptor discovery. Progress has been made towards the application of DCC in a macromolecular context, potentially presenting a viable route towards the discovery of synthetic polymeric receptors.

1.8 References

1. W. E. Stites, *Chem. Rev.*, 1997, **97**, 1233-1250.
2. M. Mammen, S.-K. Choi and G. M. Whitesides, *Angew. Chem., Int. Ed.*, 1998, **37**, 2754-2794.
3. W. J. Lees, A. Spaltenstein, J. E. Kingery-Wood and G. M. Whitesides, *J. Med. Chem.*, 1994, **37**, 3419-3433.
4. C. W. Cairo, J. E. Gestwicki, M. Kanai and L. L. Kiessling, *J. Am. Chem. Soc.*, 2002, **124**, 1615-1619.
5. S. A. Piletsky, N. W. Turner and P. Laitenberger, *Med. Eng. Phys.*, 2006, **28**, 971-977.
6. H. Yin and A. D. Hamilton, *Angew. Chem. Int. Ed.*, 2005, **44**, 4130-4163.
7. M. R. Arkin and J. A. Wells, *Nature Rev. Drug. Discov.*, 2004, **3**, 301-317.
8. A. Carlmark, C. Hawker, A. Hult and M. Malkoch, *Chem. Soc. Rev.*, 2009, **38**, 352-362.
9. G. Wulff and A. Sarhan, *Angew. Chem. Int. Ed.*, 1972, **11**, 341.
10. G. Wulff, W. Vesper, R. Grobe-Einsler and A. Sarhan, *Makromol. Chem.*, 1977, **178**, 2799-2816.
11. G. Wulff, *Angew. Chem. Int. Ed. Engl.*, 1995, **34**, 1812-1832.
12. K. Haupt and K. Mosbach, *Chem. Rev.*, 2000, **100**, 2495-2504.
13. C. Alexander, H. S. Andersson, L. I. Andersson, R. J. Ansell, N. Kirsch, I. A. Nicholls, J. O'Mahony and M. J. Whitcombe, *J. Mol. Recognit.*, 2006, **19**, 106-180.
14. L. Ye and K. Mosbach, *Chem. Mater.*, 2008, **20**, 859-868.
15. Y. Hoshino, H. Koide, T. Urakami, H. Kanazawa, T. Kodama, N. Oku and K. J. Shea, *J. Am. Chem. Soc.*, 2010, **132**, 6644-6645.
16. K. J. Shea, D. A. Spivak and B. Sellergren, *J. Am. Chem. Soc.*, 1993, **115**, 3368-3369.
17. R. J. Umpleby II, S. C. Baxter, A. M. Rampey, G. T. Rushton, Y. Chen and K. D. Shimizu, *J. Chromatog. B*, 2004, **804**, 141-149.
18. G. Jung, *Combinatorial Chemistry*, Wiley-VCH, Cambridge, 1999.
19. T. Kshirsagar, *High-Throughput Lead Optimization in Drug Discovery*, Taylor & Francis 2008.
20. P. G. Alluri, M. M. Reddy, K. Bachhawat-Sikder, H. J. Olivos and T. Kodadek, *J. Am. Chem. Soc.*, 2003, **125**, 13995-14004.
21. T. Kodadek, M. M. Reddy, H. J. Olivos, K. Bachhawat-Sikder and P. G. Alluri, *Acc. Chem. Res.*, 2004, **37**, 711-718.
22. S. Rensing, M. Arendt, A. Springer, T. Grawe and T. Schrader, *J. Org. Chem.*, 2001, **66**, 5814-5821.
23. C. Renner, J. Piehler and T. Schrader, *J. Am. Chem. Soc.*, 2005, **128**, 620-628.
24. S. J. Koch, C. Renner, X. Xie and T. Schrader, *Angew. Chem. Int. Ed.*, 2006, **45**, 6352-6355.

25. Z. Zeng, J. Patel, S.-H. Lee, M. McCallum, A. Tyagi, M. Yan and K. J. Shea, *J. Am. Chem. Soc.*, 2012, **134**, 2681-2690.
26. Y. Hoshino, H. Koide, K. Furuya, W. W. Haberaecker, S.-H. Lee, T. Kodama, H. Kanazawa, N. Oku and K. J. Shea, *Proc. Natl Acad. Sci. USA*, 2012, **109**, 33-38.
27. S.-H. Lee, Y. Hoshino, A. Randall, Z. Zeng, P. Baldi, R.-a. Doong and K. J. Shea, *J. Am. Chem. Soc.*, 2012, **134**, 15765-15772.
28. Y. Yonamine, Y. Hoshino and K. J. Shea, *Biomacromolecules*, 2012, **13**, 2952-2957.
29. K. Yoshimatsu, B. K. Lesel, Y. Yonamine, J. M. Beierle, Y. Hoshino and K. J. Shea, *Angew. Chem. Int. Ed.*, 2012, **51**, 2405-2408.
30. P. T. Corbett, J. Leclaire, L. Vial, K. R. West, J.-L. Wietor, J. K. M. Sanders and S. Otto, *Chem. Rev.*, 2006, **106**, 3652-3711.
31. J. N. H. Reek and S. Otto, *Dynamic Combinatorial Chemistry*, Wiley-VCH, 2010.
32. S. J. Rowan, S. J. Cantrill, G. R. L. Cousins, J. K. M. Sanders and J. F. Stoddart, *Angew. Chem. Int. Ed.* , 2002, **41**, 898-952.
33. H. Y. Au-Yeung, F. B. L. Cougnon, S. Otto, G. D. Pantos and J. K. M. Sanders, *Chem. Sci.*, 2010, **1**, 567-574.
34. J. M. A. Carnall, C. A. Waudby, A. M. Belenguer, M. C. A. Stuart, J. J. P. Peyralans and S. Otto, *Science*, 2010, **327**, 1502-1506.
35. P. T. Corbett, L. H. Tong, J. K. M. Sanders and S. Otto, *J. Am. Chem. Soc.*, 2005, **127**, 8902-8903.
36. A. L. Kieran, A. D. Bond, A. M. Belenguer and J. K. M. Sanders, *Chem. Commun.*, 2003, 2674-2675.
37. S. Otto, R. L. E. Furlan and J. K. M. Sanders, *Science*, 2002, **297**, 590-593.
38. B. Brisig, J. K. M. Sanders and S. Otto, *Angew. Chem. Int. Ed.*, 2003, **42**, 1270-1273.
39. S. R. Beeren and J. K. M. Sanders, *Chem. Sci.*, 2011, **2**, 1560-1567.
40. R. T. S. Lam, A. Belenguer, S. L. Roberts, C. Naumann, T. Jarrosson, S. Otto and J. K. M. Sanders, *Science*, 2005, **308**, 667-669.
41. R. L. E. Furlan, Y.-F. Ng, S. Otto and J. K. M. Sanders, *J. Am. Chem. Soc.*, 2001, **123**, 8876-8877.
42. G. R. L. Cousins, S.-A. Poulsen and J. K. M. Sanders, *Chem. Commun.*, 1999, 1575-1576.
43. S. L. Roberts, R. L. E. Furlan, S. Otto and J. K. M. Sanders, *Org. Biomol. Chem.*, 2003, **1**, 1625-1633.
44. R. L. E. Furlan, G. R. L. Cousins and J. K. M. Sanders, *Chem. Commun.*, 2000, 1761-1762.
45. J. M. Klein, V. Saggiomo, L. Reck, M. McPartlin, G. D. Pantos, U. Luning and J. K. M. Sanders, *Chem. Commun.*, 2011, **47**, 3371-3373.
46. G. R. L. Cousins, R. L. E. Furlan, Y. F. Ng, J. E. Redman and J. K. M. Sanders, *Angew. Chem. Int. Ed.*, 2001, **40**, 423-428.
47. A. Gonzalez-Alvarez, I. Alfonso and V. Gotor, *Chem. Commun.*, 2006, 2224-2226.
48. B. Hasenknopf, J.-M. Lehn, B. O. Kneisel, G. Baum and D. Fenske, *Angew. Chem., Int. Ed. Engl.*, 1996, **35**, 1838-1840.
49. V. Goral, M. I. Nelen, A. V. Eliseev and J.-M. Lehn, *Proc. Natl. Acad. Sci.*, 2001, **98**, 1347-1352.
50. E. C. Constable, C. E. Housecroft, T. Kulke, C. Lazzarini, E. R. Schofield and Y. Zimmermann, *J. Chem. Soc., Dalton Trans.*, 2001, 2864-2871.
51. M. A. Case and G. L. McLendon, *J. Am. Chem. Soc.*, 2000, **122**, 8089-8090.

52. H. J. Cooper, M. A. Case, G. L. McLendon and A. G. Marshall, *J. Am. Chem. Soc.*, 2003, **125**, 5331-5339.
53. M. Crego Calama, P. Timmerman, D. N. Reinhoudt, M. Crego Calama, R. Hulst, P. Timmerman, R. Fokkens and N. M. M. Nibbering, *Chem. Commun.*, 1998, 1021-1022.
54. F. Cardullo, M. C. Calama, B. H. M. Snellink-Ruel, J. L. Weidmann, A. Bielejewska, R. Fokkens, N. M. M. Nibbering, P. Timmerman and D. N. Reinhoudt, *Chem. Commun.*, 2000, 367-368.
55. P. Timmerman, R. H. Vreekamp, R. Hulst, W. Verboom, D. N. Reinhoudt, K. Rissanen, K. A. Udachin and J. Ripmeester, *Chem. Eur. J.*, 1997, **3**, 1823-1832.
56. M. C. Calama, P. Timmerman and D. N. Reinhoudt, *Angew. Chem., Int. Ed.*, 2000, **39**, 755-758.
57. H. Hioki and W. C. Still, *J. Org. Chem.*, 1998, **63**, 904-905.
58. K. C. Nicolaou, R. Hughes, S. Y. Cho, N. Winssinger, C. Smethurst, H. Labischinski and R. Endermann, *Angew. Chem., Int. Ed.*, 2000, **39**, 3823-3828.
59. K. C. Nicolaou, R. Hughes, S. Y. Cho, N. Winssinger, H. Labischinski and R. Endermann, *Chem. Eur. J.*, 2001, **7**, 3824-3843.
60. J. Leclaire, L. Vial, S. Otto and J. K. M. Sanders, *Chem. Commun.*, 2005, 1959-1961.
61. A. T. ten Cate, P. Y. W. Dankers, R. P. Sijbesma and E. W. Meijer, *J. Org. Chem.*, 2005, **70**, 5799-5803.
62. S. Otto and S. Kubik, *J. Am. Chem. Soc.*, 2003, **125**, 7804-7805.
63. K. R. West, K. D. Bake and S. Otto, *Org. Lett.*, 2005, **7**, 2615-2618.
64. L. Vial, J. K. M. Sanders and S. Otto, *New J. Chem.*, 2005, **29**, 1001-1003.
65. T. Hotchkiss, H. B. Kramer, K. J. Doores, D. P. Gamblin, N. J. Oldham and B. G. Davis, *Chem. Commun.*, 2005, 4264-4266.
66. B. R. McNaughton and B. L. Miller, *Org. Lett.*, 2006, **8**, 1803-1806.
67. M. Royo, M. À. Contreras, E. Giralt, F. Albericio and M. Pons, *J. Am. Chem. Soc.*, 1998, **120**, 6639-6650.
68. J. T. Goodwin and D. G. Lynn, *J. Am. Chem. Soc.*, 1992, **114**, 9197-9198.
69. I. Huc and J.-M. Lehn, *Proc. Natl. Acad. Sci.*, 1997, **94**, 2106-2110.
70. Bryan Klekota, Mark H. Hammond and B. L. Miller, *Tetrahedron Lett.*, 1997, **38**, 8639–8642.
71. M. Hochgürtel, R. Biesinger, H. Kroth, D. Piecha, M. W. Hofmann, S. Krause, O. Schaaf, C. Nicolau and A. V. Eliseev, *J. Med. Chem.*, 2003, **46**, 356-358.
72. S. J. Rowan and J. F. Stoddart, *Org. Lett.*, 1999, **1**, 1913-1916.
73. J. R. Nitschke and J.-M. Lehn, *Proc. Natl. Acad. Sci.*, 2003, **100**, 11970-11974.
74. N. Giuseppone and J.-M. Lehn, *J. Am. Chem. Soc.*, 2004, **126**, 11448-11449.
75. D. M. Epstein, S. Choudhary, M. R. Churchill, K. M. Keil, A. V. Eliseev and J. R. Morrow, *Inorg. Chem.*, 2001, **40**, 1591-1596.
76. J. R. Nitschke, *Angew. Chem., Int. Ed.*, 2004, **43**, 3073-3075.
77. N. Giuseppone, J.-L. Schmitt, E. Schwartz and J.-M. Lehn, *J. Am. Chem. Soc.*, 2005, **127**, 5528-5539.
78. K. Oh, K.-S. Jeong and J. S. Moore, *Nature*, 2001, **414**, 889-893.
79. D. Zhao and J. S. Moore, *J. Am. Chem. Soc.*, 2002, **124**, 9996-9997.
80. D. Zhao and J. S. Moore, *Macromolecules*, 2003, **36**, 2712-2720.
81. M. Hochgürtel, H. Kroth, D. Piecha, M. W. Hofmann, C. Nicolau, S. Krause, O. Schaaf, G. Sonnenmoser and A. V. Eliseev, *Proc. Natl. Acad. Sci.*, 2002, **99**, 3382-3387.
82. O. Storm and U. Lüning, *Chem. Eur. J.*, 2002, **8**, 793-798.

83. S. Gerber-Lemaire, F. Popowycz, E. Rodríguez-García, A. T. C. Asenjo, I. Robina and P. Vogel, *ChemBioChem*, 2002, **3**, 466-470.
84. A. Bugaut, J.-J. Toulmé and B. Rayner, *Angew. Chem., Int. Ed.*, 2004, **43**, 3144-3147.
85. Bryan Klekota and B. L. Miller, *Tetrahedron*, 1999, **55**, 11687–11697.
86. T. Nishinaga, A. Tanatani, K. Oh and J. S. Moore, *J. Am. Chem. Soc.*, 2002, **124**, 5934-5935.
87. D. Rideout, *Science*, 1986, **233**, 561-563.
88. Nguyen and R. Ivan Huc, *Chem. Commun.*, 2003, 942-943.
89. R. L. E. Furlan, Y.-F. Ng, G. R. L. Cousins, J. E. Redman and J. K. M. Sanders, *Tetrahedron*, 2002, **58**, 771-778.
90. S. L. Roberts, R. L. E. Furlan, G. R. L. Cousins and J. K. M. Sanders, *Chem. Commun.*, 2002, 938-939.
91. T. Bunyapaiboonsri, O. Ramström, S. Lohmann, J.-M. Lehn, L. Peng and M. Goeldner, *ChemBioChem*, 2001, **2**, 438-444.
92. T. Bunyapaiboonsri, H. Ramström, O. Ramström, J. Haiech and J.-M. Lehn, *J. Med. Chem.*, 2003, **46**, 5803-5811.
93. W. G. Skene and J.-M. P. Lehn, *Proc. Natl Acad. Sci. USA*, 2004, **101**, 8270-8275.
94. T. Ono, T. Nobori and J.-M. Lehn, *Chem. Commun.*, 2005, 1522-1524.
95. E. Kolomiets and J.-M. Lehn, *Chem. Commun.*, 2005, 1519-1521.
96. V. Berl, I. Huc, J.-M. Lehn, A. DeCian and J. Fischer, *Eur. J. Org. Chem.*, 1999, **1999**, 3089-3094.
97. M. S. Congreve, D. J. Davis, L. Devine, C. Granata, M. O'Reilly, P. G. Wyatt and H. Jhoti, *Angew. Chem., Int. Ed.*, 2003, **42**, 4479-4482.
98. S. Zameo, B. Vauzeilles and J.-M. Beau, *Angew. Chem., Int. Ed.*, 2005, **44**, 965-969.
99. K. Oh, K.-S. Jeong and J. S. Moore, *J. Org. Chem.*, 2003, **68**, 8397-8403.
100. E. G. Sander and W. P. Jencks, *J. Am. Chem. Soc.*, 1968, **90**, 6154-6162.
101. Francis A. Carey and R. J. Sundberg, *Advanced Organic Chemistry Part A: Structure and Mechanisms*, Fifth edn., Springer, 2007.
102. A. Dirksen, S. Dirksen, T. M. Hackeng and P. E. Dawson, *J. Am. Chem. Soc.*, 2006, **128**, 15602-15603.
103. E. T. Kool, D.-H. Park and P. Crisalli, *J. Am. Chem. Soc.*, 2013, **135**, 17663-17666.
104. W. P. Jencks, *J. Am. Chem. Soc.*, 1959, **81**, 475-481.
105. S. Ladame, *Org. Biomol. Chem.*, 2008, **6**, 219-226.
106. P. T. Corbett, S. Otto and J. K. M. Sanders, *Org. Lett.*, 2004, **6**, 1825-1827.
107. D. D. Perrin and I. G. Sayce, *Talanta*, 1967, **14**, 833-842.
108. R. F. Ludlow and S. Otto, *J. Am. Chem. Soc.*, 2010, **132**, 5984-5986.
109. P. T. Corbett, J. K. M. Sanders and S. Otto, *J. Am. Chem. Soc.*, 2005, **127**, 9390-9392.
110. J. Lehn, *Aust. J. Chem.*, 2010, **63**, 611-623.
111. B. Levrand, Y. Ruff, J.-M. Lehn and A. Herrmann, *Chem. Commun.*, 2006, 2965-2967.
112. T. Ono, S. Fujii, T. Nobori and J.-M. Lehn, *Chem. Commun.*, 2007, 4360-4362.
113. Y. Ruff and J.-M. Lehn, *Angew. Chem. Int. Ed.*, 2008, **47**, 3556-3559.
114. J. F. Folmer-Andersen and J.-M. Lehn, *J. Am. Chem. Soc.*, 2011, **133**, 10966-10973.
115. Y. Ura, J. M. Beierle, L. J. Leman, L. E. Orgel and M. R. Ghadiri, *Science*, 2009, **325**, 73-77.

116. M. P. Robertson and G. F. Joyce, *Cold Spring Harb. Perspect. Biol.*, 2012, **4**, a003608.
117. J. S. Moore and N. W. Zimmerman, *Org. Lett.*, 2000, **2**, 915-918.
118. K. A. Connors, *Chem. Rev.*, 1997, **97**, 1325-1358.
119. D. A. Fulton, *Org. Lett.*, 2008, **10**, 3291-3294.

Chapter 2.

Templating Polymer-Scaffolded Dynamic Combinatorial Libraries

This chapter is based upon the following article:

Clare S. Mahon, Alexander W. Jackson, Benjamin S. Murray and David A. Fulton, Templating a Polymer-Scaffolded Dynamic Combinatorial Library. *Chem*. *Commun.*, 2011, **47**, 7209-7211

Table of Contents

2.1 Abstract

Polymer-Scaffolded Dynamic Combinatorial Libraries (PS-DCLs) have been prepared in aqueous media by the reversible conjugation of acylhydrazide residues onto an aldehyde-functionalised polymer scaffold. PS-DCLs have been shown to undergo compositional change in response to the addition of macromolecular templates, including proteins, preferentially incorporating residues proposed to interact favourably with the template added.

2.2 Introduction

The design and synthesis of species with the capacity for molecular recognition has long been a goal of modern chemical research, with the efforts of many researchers focussing on the development of receptors for biologically important macromolecules, including antibodies and other proteins. The difficulty faced in the rational design of receptors for such macromolecules with large and relatively featureless areas of interaction has proven to be a major obstacle.[1-3] The traditional approach of synthesising and screening libraries of lead compounds remains labour intensive and time consuming, even with combinatorial methods[4] presenting less demanding routes to structurally diverse libraries of compounds.

Dynamic Combinatorial Chemistry (DCC)[5, 6] has emerged in recent years as a powerful tool for the discovery of receptors, and has proven its worth in the discovery of macrocyclic receptors for small molecules and ions.[7-21] DCC uses reversible reactions to link together building blocks, producing libraries of compounds whose product distributions are under thermodynamic control. The reversible nature of these linkages enables the library members to reconfigure their structures by exchange of their building blocks. Equilibrium perturbations, such as the addition of a template, may induce structural adaptation of the library to amplify the concentrations of library members which interact most favourably with the template. This re-equilibration process consumes poorly-binding library members, using their constituent building blocks to construct favoured library members. The dynamic combinatorial approach combines synthesis and screening processes into a single step, potentially presenting a rapid and cost-effective route to new receptor species.

The Polymer-Scaffolded Dynamic Combinatorial Library (PS-DCL)[22] has been designed to apply the principles of DCC towards the discovery of macromolecular

receptors. PS-DCLs are constructed on synthetic polymer scaffolds, with functionalised residues grafted onto the scaffold through dynamic covalent[23] linkages. The reversible nature of these linkages allows library members to interconvert through the exchange and re-shuffling of side-chain residues. It is hypothesised that PS-DCLs should respond to the addition of a template in the same manner as that demonstrated by other DCLs, by amplifying the concentration of library members which best interact with the template. This thermodynamically-controlled templating process could provide a mechanism for the refinement of binding sites, potentially producing macromolecular receptors of high affinities and selectivities.

Acylhydrazone exchange was proposed to be a suitable dynamic covalent reaction to reversibly conjugate residues onto an appropriately functionalised polymer scaffold in order to generate a PS-DCL. Under acidic conditions, acylhydrazone linkages[24] are generated by the condensation of aldehydes with acylhydrazides, and undergo component exchange within a convenient timescale. In aqueous environments, equilibria lie to the side of products,[25] with the optimum rates for acylhydrazone formation and exchange reactions observed at pH 4.5.[26] Acylhydrazones are more stable in water than the corresponding imines, and may be considered kinetically inert under neutral conditions,[27] providing a convenient method to 'fix' the composition of a PS-DCL.

2.3 Results and Discussion

2.3.1 Preparation of aldehyde-functionalised polymer scaffold

PS-DCLs were constructed upon polyacrylamide scaffolds which contain aromatic aldehyde functionalities on account of the incorporation of the aldehyde-containing monomer **M1**. This monomer was prepared (Scheme 1) by treatment of 4-formylbenzoic acid with trimethylorthoformate in MeOH to afford **1**, which was subjected to aminolysis with 1,2-ethylenediamine and subsequent reaction with acryloyl chloride to yield protected aldehyde **2**. Treatment of **2** with aqueous hydrochloric acid furnished monomer **M1**.

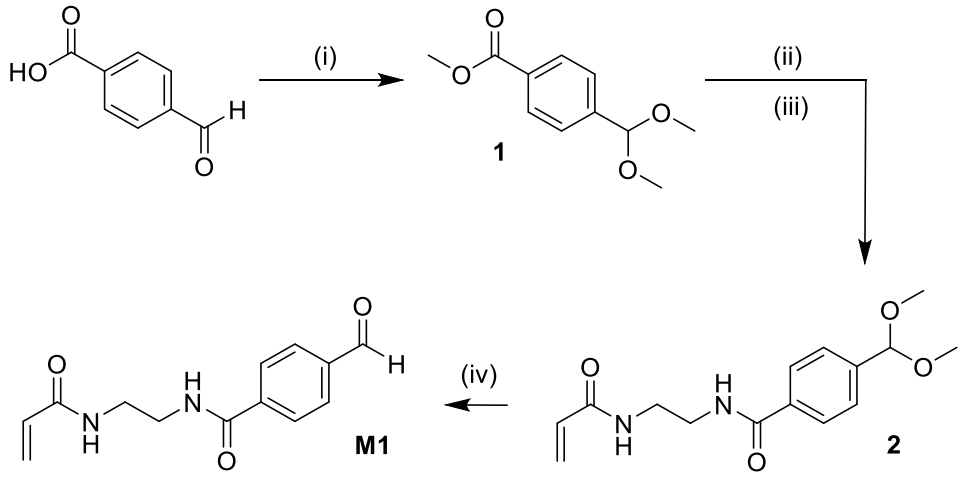

Scheme 1 Preparation of aldehyde-containing monomer **M1**. (i) $CH(OCH_3)_3$, MeOH, H_2SO_4, 80 °C, 48 h. (ii) 1,2-diaminoethane, 130 °C, 24 h. (iii) Acryloyl chloride, Et_3N, CH_2Cl_2, 0 °C, 16 h. (iv) 1 M $HCl_{(aq)}$, 2 h.

Polymer scaffold **P1** was prepared by the RAFT[28] copolymerisation of **M1** with *N*,*N*-dimethylacrylamide (Scheme 2), with incorporation of *N*,*N*-dimethylacrylamide serving to improve the water solubility of the resultant polymer. **P1** was shown by ^{1}H NMR spectroscopy to possess a degree of polymerisation of approximately 85 and display approximately 14 aldehyde functionalities. Analysis by gel permeation chromatography (GPC) confirmed a monomodal distribution of polymer molecular weights with a polydispersity index of 1.2, suggesting that the polymerisation proceeded with a good level of control.

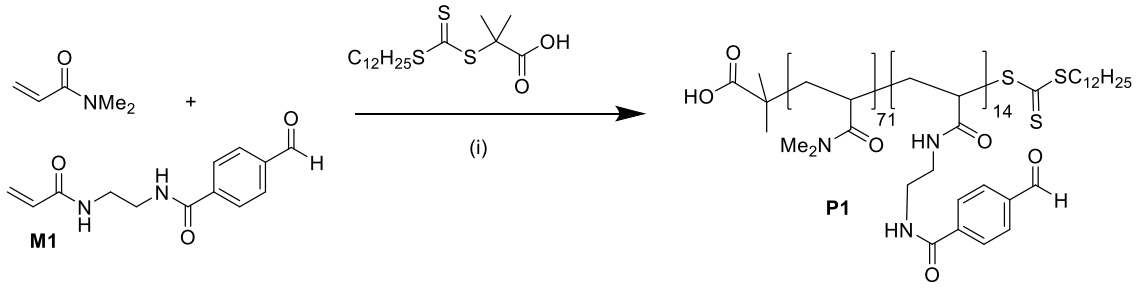

Scheme 2 Synthesis of aldehyde functional copolymer **P1**. (i) Azobis(isobutyronitrile) (AIBN), DMF, 70 °C.

2.3.2 Preparation of acylhydrazide residues

To ensure that the driving force for PS-DCLs to respond to addition of templates is sufficiently strong, we have designed our early systems to harness strong electrostatic interactions as the driving force for templation. Acylhydrazides **R1**-**R3** were identified as presenting the possibility of attractive electrostatic interactions between polymers and macromolecular templates, incorporating positive, neutral and negatively charged units respectively. **R1** is commercially available, and **R2** was prepared (Scheme 3) by a mono-*O*-alkylation of ethylene glycol with bromoacetic acid to yield the intermediate **3**, which was then treated with hydrazine hydrate to

afford **R2**. Residue **R3** was prepared (Scheme 3) by sulphonation of ethyl chloroacetate with aqueous potassium sulphate solution to afford **4**, which was then treated with hydrazine hydrate to furnish **R3**.

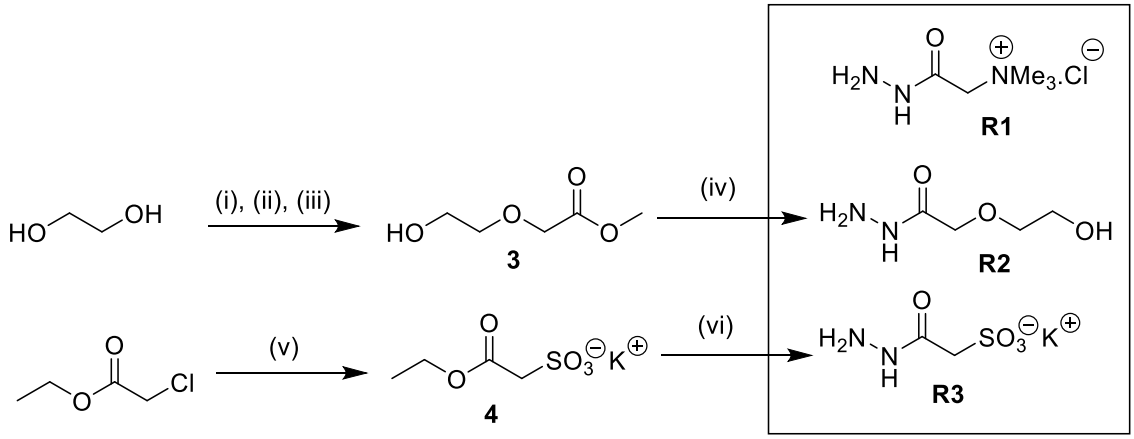

Scheme 3 Acylhydrazide building blocks **R1**-**R3** used for construction of PS-DCLs. (i) Na, RT to 100 °C, 3 h. (ii) 2-bromoacetic acid, 100 °C, 48 h. (iii) H_2SO_4, MeOH, reflux, 12 h. (iv) $NH_2NH_2.H_2O$, reflux, 4 h. (v) K_2SO_3, H_2O, reflux, 7.5 h. (vi) $NH_2NH_2.H_2O$, MeOH, reflux, 16 h.

2.3.3 Generation of PS-DCLs

PS-DCLs were initially generated upon polymer scaffold **P1**, using acylhydrazides **R1** and **R2**. Scaffold **P1** was found to exhibit limited water-solubility, so PS-DCLs were prepared in a two-step process (Scheme 4). Conjugation of **R1** or **R3** onto **P1** through acylhydrazone formation produces a water-soluble polymer, by virtue of display of multiple charged groups. Upon addition of a second acylhydrazide derivative **R2**, the polymers undergo component exchange to produce PS-DCLs which are composed of inter-converting mixtures of polymers adorned with varying amounts of the residues **R1**/**R3** and **R2**. All experiments were performed using 50 mM concentrations of **R1**/**R3** and **R2**, with **P1** present at 2.8 mM concentration in buffered D_2O (NH_4OAc/AcOH pH 4.5).

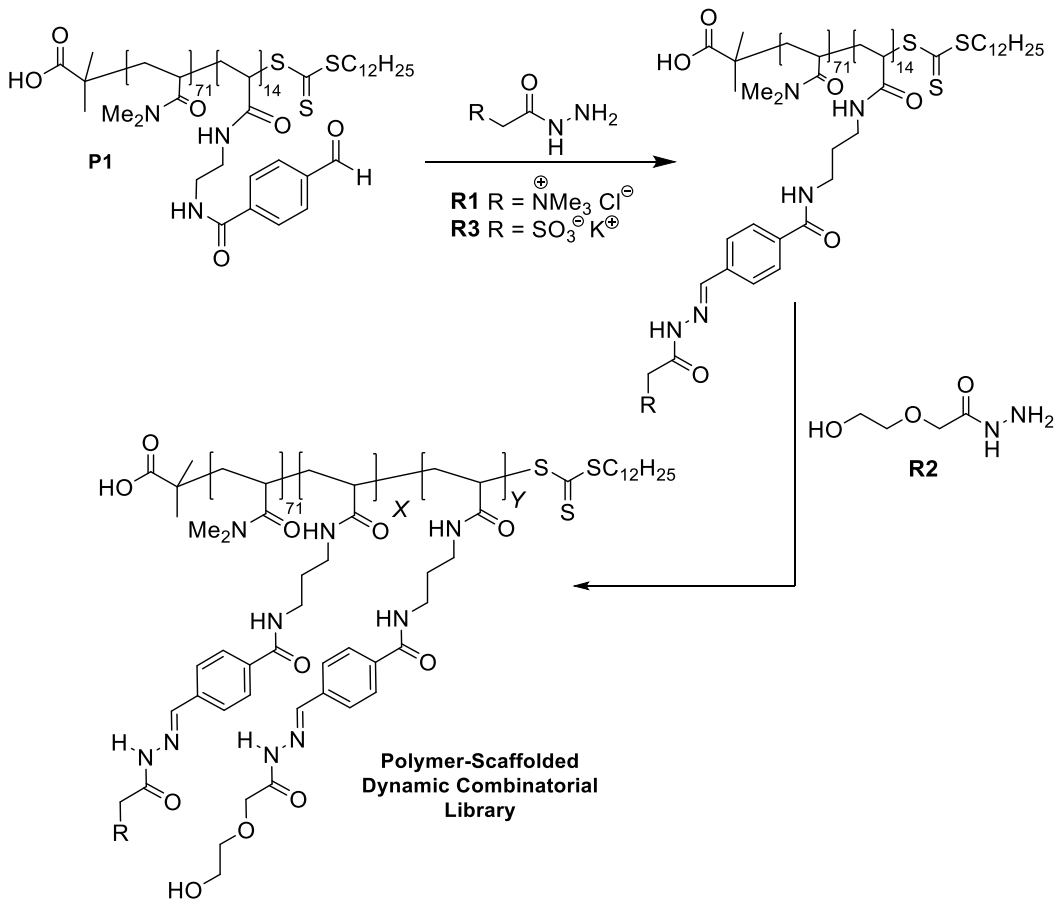

Scheme 4 Preparation of PS-DCLs. Acylhydrazide formation and exchange reactions were performed in buffered D_2O (100 mM NH_4OAc/AcOH, pH 4.5).

In the case of PS-DCLs constructed upon **P1** using acylhydrazides **R1** and **R2**, the residual composition of the polymer scaffold cannot be monitored directly by ^{1}H NMR spectroscopy because the diagnostic signals corresponding to conjugated residues overlap. Instead, the residual composition may be determined indirectly by using ^{1}H NMR spectroscopy to measure the relative concentrations of unconjugated residues **R1** and **R2** in solution, thus allowing the residual composition upon the polymer scaffolds to be ascertained. Equilibrium was reached after 16 h, with ^{1}H NMR spectroscopy revealing both unconjugated acylhydrazides to be present in solution in a 1.0 : 1.0 ratio, implying the residual composition of the polymer scaffolds is also 1.0 : 1.0. No aldehyde signal was observed at 10.0 ppm, indicating that the polymer is fully functionalised with acylhydrazone residues. The PS-DCL composition was monitored over a period of 48 h, with no further deviation from this composition observed. This observation suggests that in the absence of any template, the polymer scaffold displays no particular preference for the incorporation of either residue **R1** or **R2**.

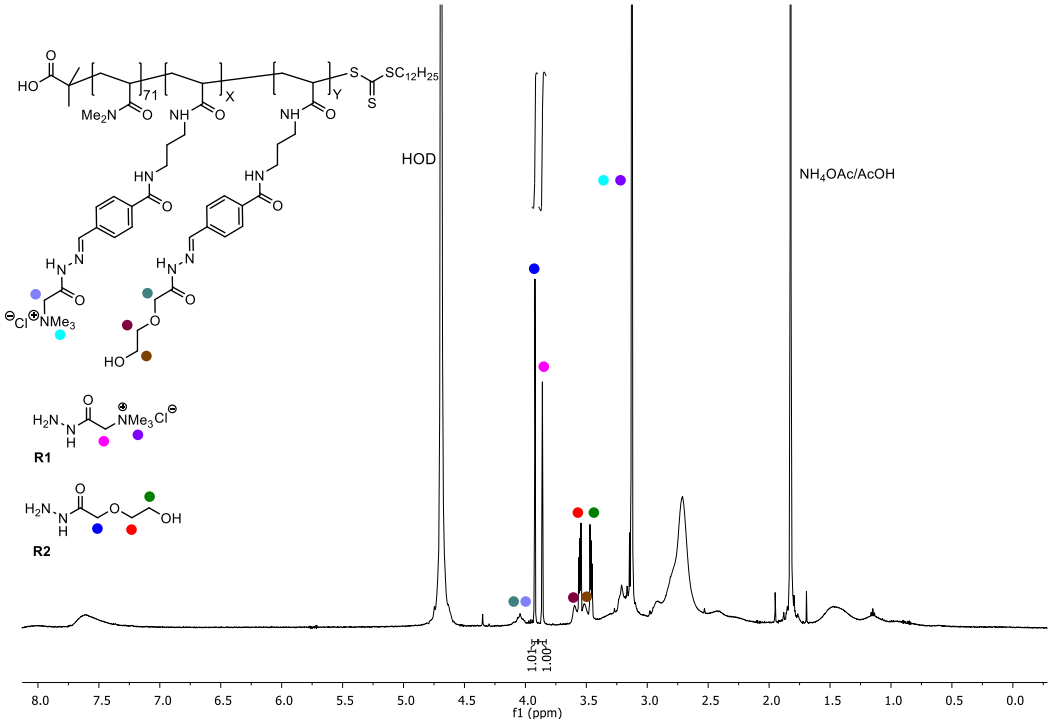

Fig. 1 ^{1}H NMR spectrum (500 MHz, D_2O, pH 4.5) of a PS-DCL constructed on **P1** using acylhydrazides **R1** and **R2**, prior to the addition of template. Integral analysis of the signals corresponding to the methylene units of **R1** (pink circle) and **R2** (blue circle) which are not conjugated onto **P1** reveals that residues are incorporated onto polymer scaffolds in equal proportions.

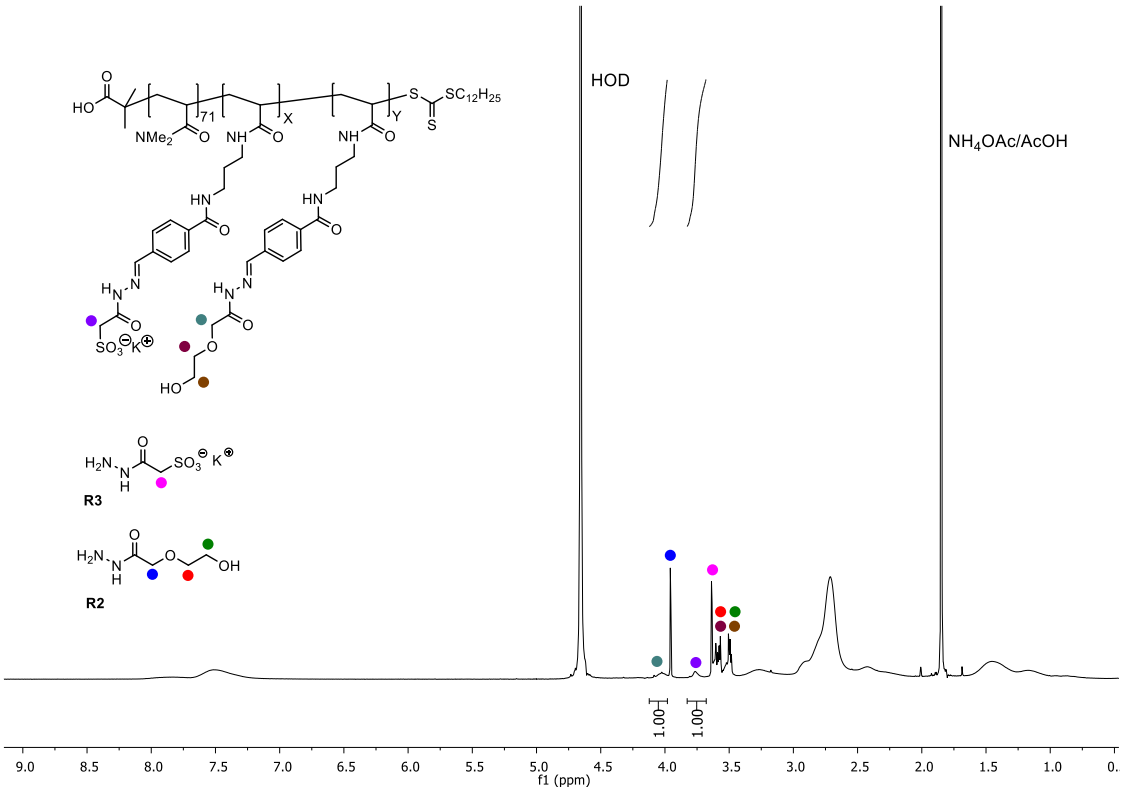

Fig. 2 ^{1}H NMR spectrum (500 MHz, D_2O, pH 4,5) of a PS-DCL constructed on **P1** using acylhydrazides **R3** and **R2**, prior to the addition of template. Integral analysis of the signals corresponding to the methylene units of the acylhydrazide residues **R3** (purple circle) and **R2** (teal circle) which are conjugated onto **P1** reveals that residues are incorporated onto polymer scaffolds in equal proportions.

In the case of PS-DCLs prepared upon **P1** using acylhydrazides **R3** and **R2**, the residual composition of the polymer scaffold may be determined directly using ^{1}H NMR spectroscopy, by integral analysis of the methylene signals of acylhydrazides conjugated onto the polymer scaffold. At equilibrium, residues **R2** and **R3** were conjugated onto the polymer scaffold in equal proportions, again demonstrating that the polymer scaffold displays no preference for the incorporation of a particular acylhydrazide.

2.3.4 Response of PS-DCLs to addition of macromolecular templates

Initial templating experiments were performed using a PS-DCL incorporating **R1** and **R2**. We hypothesised that macromolecular templates with the capacity to engage in multivalent interactions with polymeric receptors would be best suited to our system, so a 70 kDa poly(sodium-4-styrene sulphonate), bovine serum albumin (BSA) and bovine trypsin were identified as potential templates.

Upon addition of poly(sodium-4-styrene sulphonate) (70 kDa), changes in the composition of the PS-DCL as a function of time were monitored by ^{1}H NMR spectroscopy, which revealed an increase in the relative concentration of **R2** compared to **R1** (Fig. 3) of 1.2 : 1.0 from an initial ratio of 1.0 : 1.0. This observation suggests that the PS-DCL has responded to the addition of template to preferentially incorporate **R1**, rejecting **R2**. This templating effect is likely to be a consequence of favourable ion-ion interactions between the template and library members primarily functionalised with **R1**.

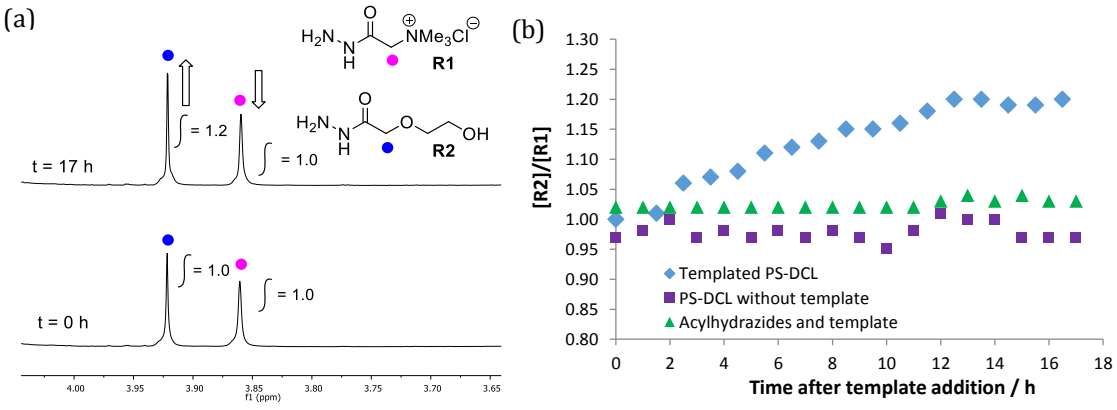

Fig. 3 (a) ^{1}H NMR spectroscopic analysis (500 MHz, D_2O, pH 4.5) of PS-DCL before (*t = 0 h*) and after (*t = 17 h*) addition of poly(sodium-4-styrene sulphonate) highlighting the changes in intensity of the diagnostic signals of **R1** and **R2** 17 h after the addition of poly(sodium-4-styrene sulphonate). (b) Effect of addition of poly(sodium-4-styrene sulphonate) to a PS-DCL constructed on scaffold **P1** using acylhydrazide **R1** and **R2** as a function of time (blue diamonds). There is no observed change in the relative concentrations of **R1** and **R2** in the absence of template (purple squares) or in the absence of polymer (green triangles).

The templating effect of the proteins BSA and bovine trypsin upon the PS-DCL was also investigated. These proteins display isoelectric points of 5.5 and 10 respectively, [29, 30] indicating that the surfaces of these proteins are positively charged under the experimental conditions. Upon addition of BSA or trypsin, ^{1}H NMR spectroscopy revealed an increase in the relative concentration of **R1** compared to **R2** of 1.0 : 0.8 from an initial ratio of 1.0 : 1.0 (Fig. 4). This observation suggests that PS-DCLs have re-equilibrated to incorporate a greater proportion of **R2** onto polymer scaffolds at the expense of **R1**. We propose that this templating effect is a consequence of favourable ion-dipole interactions between the positively charged protein and library members primarily functionalised with **R2**.

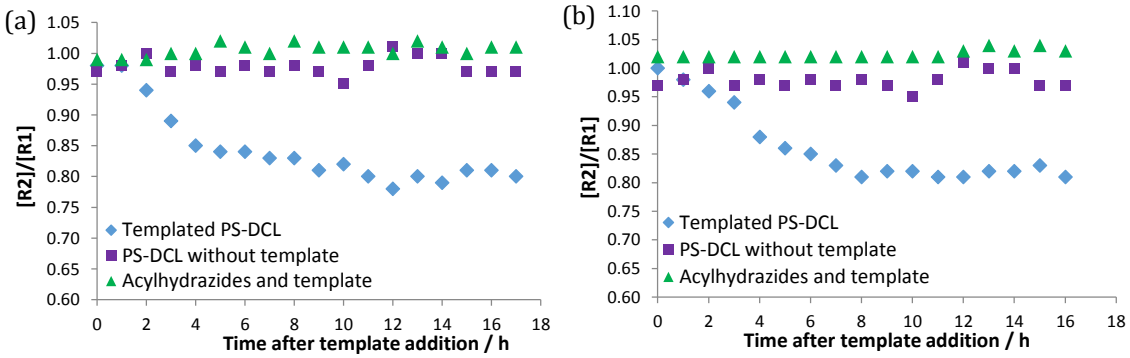

Fig. 4 Effect of addition of (a) BSA and (b) bovine trypsin to PS-DCLs upon relative concentration of unconjugated **R1** and **R2** as a function of time (blue diamonds). There is no observed change in the relative concentrations of **R1** and **R2** in the absence of template (purple squares) or in the absence of polymer (green triangles).

When no macromolecular templates were added to PS-DCLs, libraries maintained a 1.0 : 1.0 composition of **R1** and **R2** over a 17 h period, as determined by ^{1}H NMR spectroscopy. Templates were also added to 50 mM solutions of **R1** and **R2** in the absence of a polymer scaffold. No changes in chemical shift or signal broadening were observed, suggesting that there are no significant interactions between templates and residues **R1**/**R2**. These observations suggest that the re-equilibration processes observed are a consequence of interactions between polymeric library members and templates.

In order to further investigate the behaviour of PS-DCLs upon template addition, a library prepared using **R3** and **R2** was subjected to templation using poly(sodium-4-styrene sulphonate). ^{1}H NMR spectroscopy revealed (Fig. 5) a decrease in the proportion of **R3** conjugated to the polymer scaffold relative to **R2** of 0.8 : 1.0 from

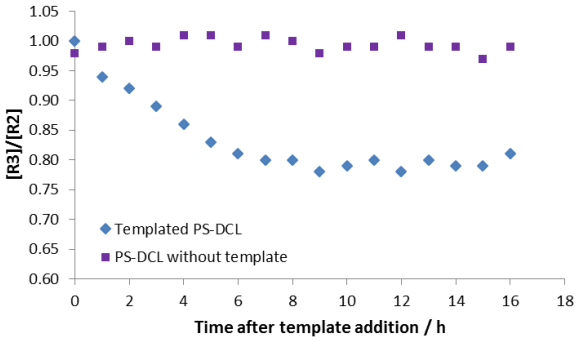

Fig. 5 Effect of addition of poly(sodium-4-styrene sulphonate) to a PS-DCL upon the relative proportions of **R2** and **R3** on the polymer scaffold as a function of time (blue diamonds). There is no observed change in the relative concentrations of **R2** and **R3** in the absence of template (purple squares).

an initial ratio of 1.0 : 1.0. This templating effect may arise in avoidance of unfavourable ion-ion interactions between the template and library members functionalised with **R3**. No change in residual composition was observed over the same timescale for a PS-DCL to which no template had been added. When poly(sodium-4-styrene sulphonate) was added to a solution of acylhydrazides **R2** and **R3**, no signal broadening or changes in chemical shift were observed, again suggesting that re-equilibration of the PS-DCL in response to template addition is a consequence of interactions between the template and acylhydrazone functionalised polymers.

Taken together, these observations demonstrate that PS-DCLs possess the same capacity for re-equilibration upon addition of a template that has been extensively demonstrated using macrocyclic DCLs, and suggest that the library response to template addition is a consequence of interactions between the template and polymeric receptors.

2.4 Conclusions

PS-DCLs have been prepared in aqueous solution by the reversible conjugation of different acylhydrazide residues onto an aldehyde-functionalised polymer scaffold. Library members within the PS-DCL may interconvert through acylhydrazone exchange, and the residual composition of polymer scaffolds may be monitored using ^{1}H NMR spectroscopy. PS-DCLs have been shown to adapt their composition in response to the addition of macromolecular templates, including synthetic polymers and proteins. Whilst the nature of interactions between the constituents of PS-DCLs and templates is yet to be fully elucidated, it is proposed that the observed templating effect is a consequence of multivalent interactions between functionalised polymer scaffolds and macromolecular templates. Upon addition of template, polymer scaffolds have been shown to preferentially incorporate the residue predicted to interact most favourably with the template, supporting this hypothesis.

2.5 Experimental Details

All chemicals, including Girard's reagent T (**R1**) were purchased from Sigma-Aldrich or Alfa Aesar and were used as received without further purification. *N,N*-Dimethylacrylamide was purified by vacuum distillation at 60 ˚C. ^{1}H and ^{13}C NMR spectra of synthesised compounds were recorded on a Bruker Avance 300 spectrometer at 300 MHz and 75 MHz respectively, or on a JEOL ECS-400 spectrometer at 400 MHz and 100 MHz, with the residual solvent signal as an internal standard. FTIR spectroscopy was performed on a Varian 800 FTIR instrument (Varian Inc.). High-resolution mass spectrometry was performed on a Waters LCT premier mass spectrometer (Waters Inc.). Gel permeation chromatography (GPC) was conducted on a Varian ProStar instrument (Varian Inc.) equipped with a Varian 325 UV-Vis dual wavelength detector (254 nm), a Dawn Heleos II multi-angle laser light scattering detector (Wyatt Technology Corp.), a Viscotek 3580 differential RI detector, and a pair of PL gel 5 μm Mixed D 300 × 7.5 mm columns with guard column (Polymer Laboratories Inc.) in series. Near monodisperse methyl methacrylate standards (Agilent Technologies) were used for calibration. Data collection was performed with Galaxie software (Varian Inc.) and chromatograms analyzed with the Cirrus software (Varian Inc.) and Astra software (Wyatt Technology Corp.). ^{1}H NMR spectra of PS-DCLs were measured using a JEOL Lambda spectrometer (^{1}H at 500 MHz), and analysed using MestReNova.

Methyl 4-(dimethoxymethyl)benzoate[31] (**1**)

A solution of 4-carboxybenzaldehyde (15.4 g, 102.6 mmol), trimethylorthoformate (32.7 g, 307.8 mmol) and H_2SO_4 (8 drops) in MeOH (100 mL) was heated under reflux for 48 h. The reaction mixture was transferred to a separating funnel with saturated $NaHCO_{3(aq)}$ (100 mL) and the aqueous layer was extracted with CH_2Cl_2 (3 × 150 mL). The organic extracts were combined and dried over Na_2SO_4, filtered and evaporated to dryness to afford a crude liquid which was purified by vacuum distillation to afford the title product as a clear liquid (19.8 g, 92%). ^{1}H NMR (300 MHz, $CDCl_3$): δ 3.30 (s, 6H, $CH(OC\mathit{H_3})_2$), 3.89 (s, 3H, $OC\mathit{H_3}$), 5.42 (s, 1H, $C\mathit{H}(OCH_3)_2$), 7.51 (d, 2H, Ar, *J*= 8.1 Hz), 8.02 (d, 2H, Ar, *J*= 8.1 Hz). ^{13}C NMR (75 MHz, $CDCl_3$): δ 52.2, 53.0, 103.0, 127.1, 129.8, 130.8, 143.8, 167.1.

N-Ethylacrylamide-2-(4-(dimethoxymethyl)benzamide)[32] (**2**)

A solution of methyl 4-(dimethoxymethyl)benzoate **1** (6.0 g, 28.5 mmol) in 1,2-diaminoethane (100 mL) was heated under reflux for 24 h then evaporated to dryness. The viscous yellow oil obtained was dissolved in CH_2Cl_2 (100 mL) and Et_3N (5.7 g, 56.3 mmol) added. The solution was cooled to 0 ˚C in an ice bath. Acryloyl chloride (2.6 g, 28.5 mmol) in CH_2Cl_2 (50 mL) was added dropwise over 30 min. The reaction was stirred overnight at room temperature then transferred to a separating funnel with saturated $NaHCO_{3(aq)}$ (150 mL). The aqueous layer was extracted with CH_2Cl_2 (2 × 150 mL). The organic extracts were combined and dried over Na_2SO_4, filtered and evaporated to dryness to afford a crude solid which was purified by column chromatography [SiO_2, EtOAc-Et_3N (95:5)] to afford the title product as a white solid (3.3 g, 40 %). ^{1}H NMR (300 MHz, $CDCl_3$): δ 3.28 (s, 6H, CH(OC*H*$_3$)$_2$), 3.52 (m, 4H, (C*H*$_2$)$_2$), 5.37 (s, 1H, C*H*(OCH$_3$)$_2$), 5.58 (dd, 1H, *J*= 9.6 Hz), 6.14 (dd, 1H, *J*= 17.1 Hz), 6.23 (dd, 1H, *J*= 17.1 Hz), 7.37 (s, 1H, N*H*), 7.45 (d, 2H, Ar, *J*= 8.1 Hz), 7.79 (d, 2H, Ar, *J*= 8.1 Hz), 7.84 (s, 1H, N*H*). ^{13}C NMR (75 MHz, $CDCl_3$): δ 41.3, 53.1, 103.1, 127.3, 128.2, 130.0, 131.3, 134.6, 142.1, 167.5, 168.6. FT-IR (wavenumber, cm^{-1}): 3290 (N–H), 3096 (C–H, alkene), 2947 (C–H, alkyl), 1634 (C=O), 1593 (C=O), 1448 (C=C, aromatic), 1413 (C=C, aromatic). HRMS (ES$^+$) $C_{15}H_{21}N_2O_4$: Theoretical: 293.1501. Actual: 293.1503.

N-Ethylacrylamide-2-(4-formylbenzamide) (**M1**)

A solution of *N*-ethylacrylamide-2-(4-(dimethoxymethyl)benzamide) **2** (1.4 g, 4.8 mmol) in 1M $HCl_{(aq)}$ (20 mL) was stirred at room temperature for 2 h then neutralized with saturated $NaHCO_{3(aq)}$ (100 mL). The aqueous layer was extracted with EtOAc (3 × 150 mL). The organic extracts were combined and dried over $MgSO_4$, filtered and evaporated to dryness to afford the title product as a white solid (0.99g, 84 %). ^{1}H NMR (300 MHz, DMSO-d$_6$): δ 3.72 (m, 4H, (C*H*$_2$)$_2$), 5.59 (dd, 1H, *J*= 9.6 Hz), 6.09 (dd, 1H, *J*= 17.1 Hz), 6.23 (dd, 1H, *J*= 17.1 Hz), 7.99 (d, 2H, Ar, *J*= 8.4 Hz), 8.03 (d, 2H, Ar, *J*= 8.4 Hz), 8.23 (s, 1H, N*H*), 8.79 (s, 1H, N*H*), 10.07 (s, 1H, C*H*O). ^{13}C NMR (75 MHz, DMSO-d$_6$): δ 38.7, 125.2, 128.3, 129.6, 132.3, 138.2, 140.1, 165.5, 166.1, 193.0. FT-IR (wavenumber, cm^{-1}): 3264 (N–H), 3091 (C–H, alkene), 2943 (C–H, alkyl), 1699 (C=O, aldehyde), 1627 (C=O, amide), 1549 (C=O, amide), 1447 (C=C, aromatic), 1414 (C=C, aromatic). HRMS (ES$^+$) $C_{13}H_{15}N_2O_3$: Theoretical: 247.1083. Actual: 247.1085.

Methyl 2-(2-hydroxyethoxy)acetate (**3**)

Sodium (4.6 g, 200 mmol) was added in small pieces to ethylene glycol (50 mL, 897 mmol) at room temperature under N_2, then stirred until a homogenous liquid was obtained. The yellow liquid was heated to 100 ˚C for 3 h followed by the addition of bromoacetic acid (13.9 g, 100 mmol) to yield immediately a dark orange-coloured mixture. The reaction was heated at 100 ˚C for a further 48 h followed by removal of excess ethylene glycol by vacuum distillation. The remaining residue was suspended in HCl (37%, 60 mL) then filtered and the filtrate dried under reduced pressure to afford a viscous brown oil. The oil was dissolved in MeOH (100 mL) and then H_2SO_4 (5 mL) was added and the resulting solution was heated at reflux for 12 h then cooled to room temperature and neutralised by the dropwise addition of sat. $NaHCO_3$ solution until effervescence ceased. The solution was concentrated to a volume of 50 mL under reduced pressure, diluted by the addition of CH_2Cl_2 (100 mL) then extracted with brine (100 mL). The brine was backwashed with CH_2Cl_2 (3 x 50 mL) and the combined organic solutions were dried under reduced pressure to afford the crude product as a brown oil which was further purified by column chromatography on silica (100% CH_2Cl_2) to yield the desired product as a white solid (1.22 g, 9.1 mmol, 9 %); R_F = 0.27 (CH_2Cl_2:MeOH 10:1.5, silica); ^{1}H NMR ($CDCl_3$, 400 MHz): δ 4.08 (s, 2H, -C=OC*H*$_2$O-), 3.69 (m, 5H, C*H*$_3$O- and –C*H*$_2$-CH$_2$-), 3.59 (m, 2H, -CH$_2$-C*H*$_2$-), 3.32 (s br, 1H, -OH); ^{13}C NMR ($CDCl_3$, 100 MHz): δ 171.4 (C=O), 73.2, 68.3, 61.5, 51.9 (CH_3); HRMS (CI+) $C_5H_{14}NO_4$ $[M + NH_4]^+$: Theoretical: 152.0917. Actual: 157.0918; m.p. 56-58°C

2-(2-Hydroxyethoxy)acetohydrazide (**R2**)

A solution of hydrazine monohydrate (0.6 mL, 13.6 mmol) and methyl 2-(2-hydroxyethoxy)acetate (1.22 g, 9.1 mmol) in MeOH (50 mL) was heated under reflux for 4 h then dried under reduced pressure to afford a crystalline white solid. The solid was suspended in CH_2Cl_2 (50 mL), sonicated for 20 min then filtered. This process was repeated twice at which point the solid was judged pure by TLC analysis to yield the desired product as a crystalline white solid (0.683 g, 5.1 mmol, 56 %); R_F = 0.13 (CH_2Cl_2:MeOH 10:1.5, silica); ^{1}H NMR (DMSO-*d*$_6$, 300 MHz): δ 9.01 (s br, 1H, N*H*), 4.80 (t, 1H, *J*= 6.0 Hz, O*H*), 4.26 (s br, 2H, N*H*$_2$), 3.89 (s, 2H, -C=OC*H*$_2$O-), 3.50-3.44 (m, 4H, –C*H*$_2$-C*H*$_2$-); ^{13}C NMR (DMSO-*d*$_6$, 100 MHz): δ 168.3 (C=O), 72.9,

69.4, 60.1 ; HRMS (ES^+) $C_4H_{10}N_2O_3Na$: Theoretical: 157.0589. Actual :157.0596; m.p. 74-77 °C.

Potassium ethyl sulphoacetate (**4**)[33]

Ethyl chloroacetate (5.00 g, 4.08 mmol) and potassium sulphite (6.46 g, 4.08 mmol) were combined in H_2O (40 mL) and heated under reflux for 7.5 h, then left to stir at room temperature for 16 h. The solution was evaporated to dryness, yielding a white powder. Recrystallisation from hot 70:30 EtOH:H_2O yielded the title compound as a white solid (5.39 g, 64%). ^1H NMR (300 MHz, D_2O): δ 1.18 (t, 3H, *J*= 6 Hz, CH_2CH_3), 3.86 (s, 2H, $^-O_3SCH_2$), 4.14 (q, 2H, *J*= 6 Hz). ^{13}C NMR (100 MHz, D_2O): δ 166.93 (C=O), 62.93 ($^-O_3SCH_2$), 56.10 (CH_2CH_3), 13.42 (CH_2CH_3). Melting point: 209-211°C.

Sulphoacetylhydrazide (**R3**)

Hydrazine hydrate (3.52 mL, 72.7 mmol) was added to a stirred solution of ethyl sulphoacetate **6** (1.00 g, 4.85 mmol) in H_2O (20 mL). The reaction mixture was left to stir at room temperature for 16 h, then evaporated to dryness, yielding a colourless oil (4.02 g). The oil was cooled in an ice-bath, and MeOH was added dropwise to yield the title product as a white precipitate which was isolated by filtration (0.54 g, 58%). ^1H NMR (300 MHz, D_2O): δ 3.10 (s, $^-O_3SCH_2$). ^{13}C NMR (100 MHz, D_2O): δ 165.57 (C=O). 55.43 ($^-O_3SCH_2$). HRMS(ES^-) $C_2H_5N_2O_4S$: Actual: 153.0660. Theoretical: 152.9970.

Aldehyde-Functionalised Copolymer (**P1**)

S-1-Dodecyl-*S'*-(α,α-dimethyl-α''-acetic acid)trithiocarbonate[34] (DDMAT) (1 eq, 34.2 mg, 0.094 mmol) and AIBN (0.2 eq, 3.08 mg, 19 μmol) were added to a small schlenk tube. *N,N*-Dimethylacrylamide (DMA) (80 eq, 0.745 g, 7.52 mmol) and *N*-ethylacrylamide-2-(4-formylbenzamide) (**M1**, 20 eq, 0.463 g, 1.88 mmol) were then added followed by DMF (3 mL). The reaction mixture was degassed through five freeze-pump-thaw cycles before the vessel was backfilled with N_2, purged with N_2, and allowed to warm to room temperature. The reaction mixture was then placed in an oil bath at 70 ˚C, and the polymerization was quenched after 22 h. The reaction mixture was dissolved in a minimal amount of THF-acetone and added dropwise to a large excess of ice-cold diethyl ether. The polymer precipitate was then isolated by filtration and the precipitation was repeated before drying under high vacuum.

Polymer **P1** was obtained as a pale yellow solid (1.05 g). ^{1}H NMR (300 MHz, $CDCl_3$): 1.4 – 1.8 (br, CHC*H*$_2$, polymer backbone), 2.2 – 2.7 (br, C*H*CH_2, polymer backbone), 2.88 (br, N(C*H*$_3$)$_2$), 3.4 – 3.6 (br, (C*H*$_2$)$_2$), 7.88 (br, Ar), 8.07 (br, Ar), 8.59 (br, N*H*), 10.04 (br, Ar). The composition of **P1** can be determined by comparing the integration of the aldehyde protons of **M1** with the integration of the N(C*H*$_3$)$_2$ protons of DMA, showing the monomer composition to be 5 : 1 DMA : **M1**. The monomer composition was not identical to the feed ratio of 4 : 1 DMA : **M1**, most likely as a consequence of the difference in reactivity of the two monomers.

polymer	chain transfer agent	monomers	initiator	solvent	time / h	temp / °C	M_n[a] / g mol^{-1}	M_n[b] / g mol^{-1}	M_w[b] / g mol^{-1}	PDI[b] (M_w/M_n)
P1	DDMAT (1 eq)	DMA (80 eq) **M1** (20 eq)	AIBN (0.2 eq)	DMF	22	70	10,850	18,500	21,600	1.17

Table 1 Characterisation of copolymer **P1**. [a] As determined by ^{1}H NMR spectroscopy. [b] As determined by gel permeation chromatography in DMF (0.6 mL/ min) calibrated against near monodisperse methyl methacrylate standards. AIBN: azobis(isobutyronitrile), DMF: dimethylformamide, DMA: *N*,*N*-dimethylacrylamide, DDMAT: *S*-1-dodecyl-*S*'-(α,α-dimethyl-α''-acetic acid)trithiocarbonate.

General procedure for preparation of PS-DCLs

Polymer **P1** (15.9 mg, 1.5 x 10^{-5} mol) was combined with **R1** (4.2 mg, 2.5 x 10^{-5} mol) or **R3** (4.8 mg, 2.5 x 10^{-5} mol) in 100 mM NH_4OAc/AcOH deuterated buffer (pH 4.5, 0.5 mL) and sonicated until a clear solution was obtained. **R2** (3.4 mg, 2.5 x 10^{-5} mol) was added to the reaction mixture, which was left overnight to equilibrate. Equilibration to a 1.0 : 1.0 ratio of **R1** and **R2**, or **R2** and **R3**, was confirmed by ^{1}H NMR spectroscopic analysis prior to template addition.

2.6 References

1. H. Yin and A. D. Hamilton, *Angew. Chem. Int. Ed.*, 2005, **44**, 4130-4163.
2. W. E. Stites, *Chem. Rev.*, 1997, **97**, 1233-1250.
3. M. R. Arkin and J. A. Wells, *Nature Rev. Drug. Discov.*, 2004, **3**, 301-317.
4. G. Jung, *Combinatorial Chemistry*, Wiley-VCH, Cambridge, 1999.
5. P. T. Corbett, J. Leclaire, L. Vial, K. R. West, J.-L. Wietor, J. K. M. Sanders and S. Otto, *Chem. Rev.*, 2006, **106**, 3652-3711.
6. J. N. H. Reek and S. Otto, *Dynamic Combinatorial Chemistry*, Wiley-VCH, 2010.
7. A. Gonzalez-Alvarez, I. Alfonso and V. Gotor, *Chem. Commun.*, 2006, 2224-2226.
8. G. R. L. Cousins, R. L. E. Furlan, Y. F. Ng, J. E. Redman and J. K. M. Sanders, *Angew. Chem. Int. Ed.*, 2001, **40**, 423-428.
9. J. M. Klein, V. Saggiomo, L. Reck, M. McPartlin, G. D. Pantos, U. Luning and J. K. M. Sanders, *Chem. Commun.*, 2011, **47**, 3371-3373.

10. R. L. E. Furlan, G. R. L. Cousins and J. K. M. Sanders, *Chem. Commun.*, 2000, 1761-1762.
11. S. L. Roberts, R. L. E. Furlan, S. Otto and J. K. M. Sanders, *Org. Biomol. Chem.*, 2003, **1**, 1625-1633.
12. H. Y. Au-Yeung, F. B. L. Cougnon, S. Otto, G. D. Pantos and J. K. M. Sanders, *Chem. Sci.*, 2010, **1**, 567-574.
13. J. M. A. Carnall, C. A. Waudby, A. M. Belenguer, M. C. A. Stuart, J. J. P. Peyralans and S. Otto, *Science*, 2010, **327**, 1502-1506.
14. P. T. Corbett, L. H. Tong, J. K. M. Sanders and S. Otto, *J. Am. Chem. Soc.*, 2005, **127**, 8902-8903.
15. A. L. Kieran, A. D. Bond, A. M. Belenguer and J. K. M. Sanders, *Chem. Commun.*, 2003, 2674-2675.
16. S. Otto, R. L. E. Furlan and J. K. M. Sanders, *Science*, 2002, **297**, 590-593.
17. B. Brisig, J. K. M. Sanders and S. Otto, *Angew. Chem. Int. Ed.*, 2003, **42**, 1270-1273.
18. S. R. Beeren and J. K. M. Sanders, *Chem. Sci.*, 2011, **2**, 1560-1567.
19. R. T. S. Lam, A. Belenguer, S. L. Roberts, C. Naumann, T. Jarrosson, S. Otto and J. K. M. Sanders, *Science*, 2005, **308**, 667-669.
20. R. L. E. Furlan, Y.-F. Ng, S. Otto and J. K. M. Sanders, *J. Am. Chem. Soc.*, 2001, **123**, 8876-8877.
21. G. R. L. Cousins, S.-A. Poulsen and J. K. M. Sanders, *Chem. Commun.*, 1999, 1575-1576.
22. D. A. Fulton, *Org. Lett.*, 2008, **10**, 3291-3294.
23. S. J. Rowan, S. J. Cantrill, G. R. L. Cousins, J. K. M. Sanders and J. F. Stoddart, *Angew. Chem. Int. Ed.* , 2002, **41**, 898-952.
24. S. Patai, ed., *The Chemistry of the Carbon-Nitrogen Double Bond*, Interscience, London, 1968.
25. E. G. Sander and W. P. Jencks, *J. Am. Chem. Soc.*, 1968, **90**, 6154-6162.
26. A. Dirksen, S. Dirksen, T. M. Hackeng and P. E. Dawson, *J. Am. Chem. Soc.*, 2006, **128**, 15602-15603.
27. Francis A. Carey and R. J. Sundberg, *Advanced Organic Chemistry Part A: Structure and Mechanisms*, Fifth edn., Springer, 2007.
28. G. Moad, E. Rizzardo and S. H. Thang, *Aust. J. Chem.*, 2005, **58**, 379-410.
29. T. Clackson and J. A. Wells, *Science*, 1995, **267**, 383-386.
30. K. A. Walsh, in *Meth. Enzymol.*, ed. L. L. Gertrude E. Perlmann, Academic Press, 1970, vol. 19, pp. 41-63.
31. I. T. Crosby, G. A. Pietersz and J. A. Ripper, *Aust. J. Chem.*, 2008, **61**, 138-143.
32. A. W. Jackson and D. A. Fulton, *Chem. Commun.*, 2011, **47**, 6807-6809.
33. *United States Pat.*, 4,041,162, 1977.
34. J. T. Lai, D. Filla and R. Shea, *Macromolecules*, 2002, **35**, 6754-6756.

Chapter 3.

Investigating Templating within Polymer-Scaffolded Dynamic Combinatorial Libraries

This chapter is based upon the following article:

Clare S. Mahon, Alexander W. Jackson, Benjamin S. Murray and David A. Fulton, Investigating Templating within Polymer-Scaffolded Dynamic Combinatorial Libraries. *Polym*. *Chem.*, 2013, **4**, 368-377

Table of Contents

3.1 Abstract

Polymer-Scaffolded Dynamic Combinatorial Libraries (PS-DCLs) have previously been shown to adapt their composition in response to the addition of macromolecular templates. A systematic evaluation of how properties of the polymer scaffold, including molecular weight and density of aldehyde functionalities, affect the behaviour of resultant PS-DCLs has been performed. Increasing the molecular weight of the polymer scaffold has been shown to induce a linear decrease in the amplification of the preferred residue upon template addition. A linear relationship between the molar weight percentage of the aldehyde-functionalised monomer and the extent of amplification of the preferred residue upon template addition has also been demonstrated.

3.2 Introduction

It has previously been established[1] that PS-DCLs may adapt their composition in response to the addition of macromolecular templates by preferentially incorporating residues proposed to interact favourably with the template onto polymer scaffolds. In order to optimise the design of PS-DCLs so that practically useful quantities of favoured polymers may be generated, it is necessary to gain a deeper understanding of the behaviour of these systems. It was therefore decided to study the process of compositional adjustment in response to template addition in greater detail.

Theoretical work[2] on macrocyclic DCLs has demonstrated that as library size is increased, the mean yield of the best-binding library member decreases, potentially presenting difficulties in the identification and isolation of favoured species. PS-DCLs, by their nature, present vastly complex mixtures, as the probability of polymer chains having precisely the same sequence is low.[*] We wished to investigate how properties of the polymer scaffold may be adjusted so as to optimise the response of the PS-DCL to template addition. DCLs have been constructed on polymer scaffolds generated by RAFT[3] copolymerisation of an aldehyde-containing monomer and *N*,*N*-dimethylacrylamide, which serves to improve the water-solubility of resultant polymers. RAFT is a living radical polymerisation which

[*] If we consider a PS-DCL constructed on a polymer scaffold displaying 14 aldehyde functionalities, and just two acylhydrazide residues, the library contains a possible 16,384 members (2^{14}). This simple treatment ignores additional complexity arising from the random copolymeric nature of the polymer scaffold.

allows for the generation of polymers of controlled chain length and low polydispersity, allowing for a series of polymer scaffolds of varying molecular weight to be accessed readily. In addition, the comonomer composition of polymer scaffold may be conveniently controlled during polymerisation, allowing a thorough investigation of the effects of altering structural parameters of the polymer scaffold on library response to template addition to be undertaken,

Another theoretical study,[4] which examined the relationship between the binding affinity of library members towards a particular template and their amplification within macrocyclic DCLs, demonstrated that reducing the amount of template relative to the amounts of building blocks within the library improves this correlation. The effects of varying template concentration upon PS-DCL response to template addition must also be investigated to establish if the same rationale may be applied to polymer-scaffolded systems.

3.3 Results and Discussion

3.3.1 Varying the molecular weight of the polymer scaffold

In order to investigate the effects of increasing the molecular weight of the polymer scaffold upon the behaviour of resultant PS-DCLs when exposed to macromolecular templates, a series of polymers was prepared through RAFT[3] polymerisation (Scheme 1). Polymer scaffolds **P1**-**P6** incorporated *N*,*N*-dimethylacrylamide and the aldehyde-functionalised monomer **M1** in a 5:1 ratio, consistent with previous work,[1] but with varying molecular weights (Table 1).

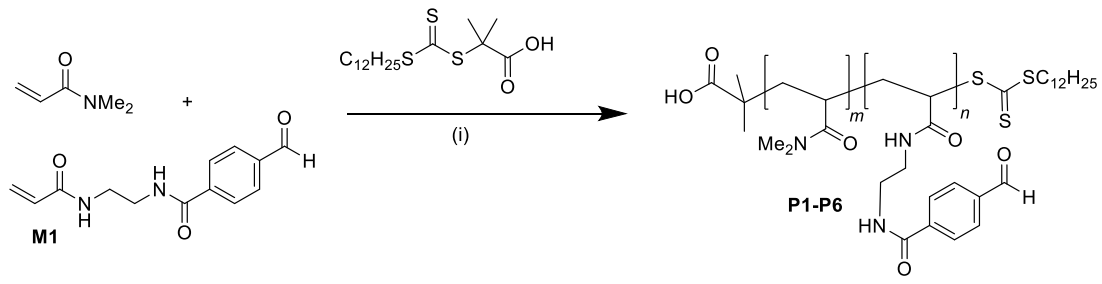

Scheme 1 Synthesis of aldehyde functional copolymers **P1-P6**. (i) Azobis(isobutyronitrile) (AIBN), DMF, 70 °C.

Polymers **P1**-**P6** display low polydispersity indices (Table 1), indicating that the polymerisation reactions were controlled. Unfortunately, polymer scaffolds of higher molecular weight (>50 kDa) could not be synthesised with acceptable polydispersity indices by RAFT polymerisation.

Polymer	**DDMAT** / eq.	**AIBN** / eq.	**DMA** / eq.	**M1** / eq.	n[a]	m[a]	n : m[a]	M_n[a] / gmol^{-1}	M_n[b] / gmol^{-1}	M_w[b] / gmol^{-1}	PDI[b] (M_w/M_n)
P1	1	0.2	80	20	14	71	1:5	11,400	14,300	18,300	1.28
P2	1	0.2	80	20	25	124	1:5	19,300	28,100	34,000	1.21
P3	1	0.2	160	40	28	154	1:5	23,000	25,600	32,000	1.25
P4	1	0.2	240	60	45	244	1:5	34,800	49,200	66,600	1.35
P5	1	0.2	320	80	54	269	1:5	41,300	59,700	75,700	1.33
P6	1	0.2	40	10	9	47	1:5	7,400	6,200	7,200	1.16

Table 1 Characterisation of copolymers **P1-P6**. [a] As determined by ^{1}H NMR spectroscopy [b] As determined by gel permeation chromatography in DMF + 1 g L^{-1} LiBr (0.6 mL/ min) calibrated against near monodisperse methyl methacrylate standards. AIBN: azobis(isobutyronitrile), DMA: *N*,*N*'-dimethylacrylamide, DDMAT: *S*-1-dodecyl-*S*'-(α,α-dimethyl-α''-acetic acid)trithiocarbonate.

A series of PS-DCLs were generated by reaction of scaffolds **P1-P6** with acylhydrazide residues **R1** and **R2**, as described previously[1] (Scheme 2).

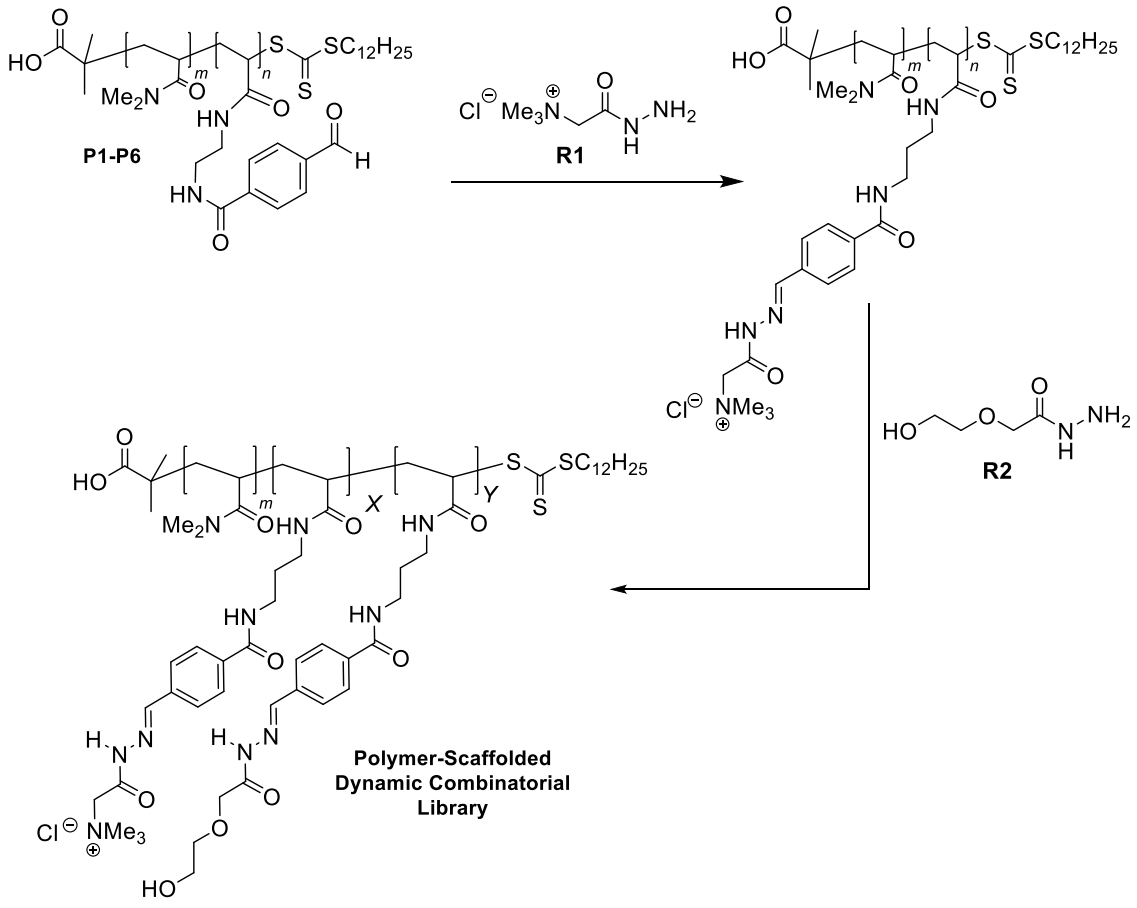

Scheme 2 Preparation of PS-DCLs upon polymer scaffolds **P1**-**P6** using acylhydrazides **R1** and **R2**. Acylhydrazide formation and exchange reactions were performed in buffered D_2O (100 mM NH_4OAc/AcOH, pH 4.5).

The residual composition of each PS-DCL was determined to be 1.0 : 1.0 by ^{1}H NMR spectroscopy prior to addition of templates. The templates selected for this investigation were poly(sodium-4-styrenesulphonate) (70 kDa) and bovine serum albumin (BSA), presenting net positively and negatively charged templates under experimental conditions. The response of each PS-DCL upon addition of these templates was monitored over a 16 h period by ^{1}H NMR spectroscopic analysis of

the relative concentrations of unconjugated acylhydrazides **R1** and **R2** in solution. Experiments were performed so that each PS-DCL contained the same effective concentration of aldehyde units and identical concentrations of **R1** and **R2**.

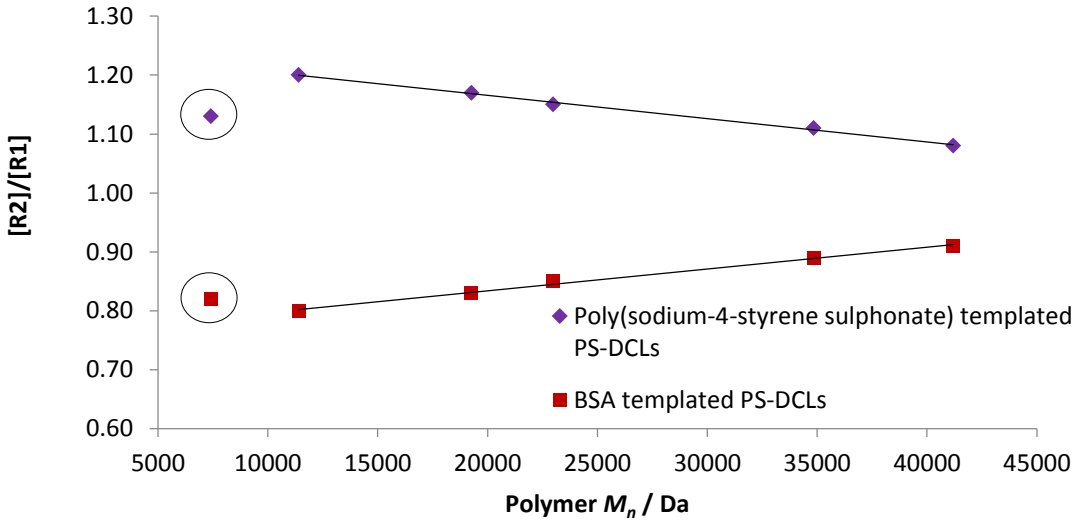

Fig. 1 The effect of increasing the polymer scaffold molecular weight upon the final composition of the PS-DCL after templating with poly(sodium-4-styrene sulphonate) (70 kDa) and BSA. M_n values were determined by ^{1}H NMR spectroscopy.

Each PS-DCL was shown to respond to template addition in the expected manner,[1] by amplifying the concentration of the preferred acylhydrazide upon the polymer scaffold in a manner which may be rationalised in terms of favourable multivalent ion-ion or ion-dipole interactions between library members and macromolecular templates. As the molecular weight of the polymer scaffold was increased (**P2**-**P5**), however, the extent of amplification of the preferred residue decreased linearly (Fig. 1), as judged by the final library composition. This observation may appear counterintuitive, as polymer scaffolds of increasing molecular weight possess greater numbers of aldehyde functionalities and may therefore be expected to undergo greater degrees of component exchange upon exposure to templates.

This observation can be rationalised. In solution, polymer scaffolds may be expected to adopt a globular conformation, with some acylhydrazide residues adorning the surface and others 'buried' inside the globule. The hydrophobic nature of **M1** is proposed to confer hydrophobicity onto the polymer scaffolds, so it is appropriate in this case to model polymers as globules rather than the usually presumed 'random-coil' conformation. The globular conformation may be approximated as a sphere in solution (Fig. 2). As the molecular weight of the polymer scaffold is increased, the radius of the resultant sphere would be expected to increase. For a sphere of radius r, surface area A and volume V, we may define:

$A = 4\pi r^2$ $\qquad$ $V = \frac{4}{3}\pi r^3$

The rates of change of A and V with respect to r may then be obtained:

(1) $\frac{dA}{dr} = 8\pi r$ $\qquad$ (2) $\frac{dV}{dr} = 4\pi r^2$

Combining (1) and (2) elucidates the linear relationship between the rates of change of surface area and volume:

$$\frac{dV}{dA} = \frac{r}{2}$$

Thus for values of r>2, it is predicted that the volume of the sphere will increase at a greater rate than surface area when r is increased, with a linear relationship demonstrated between the two rates of change.

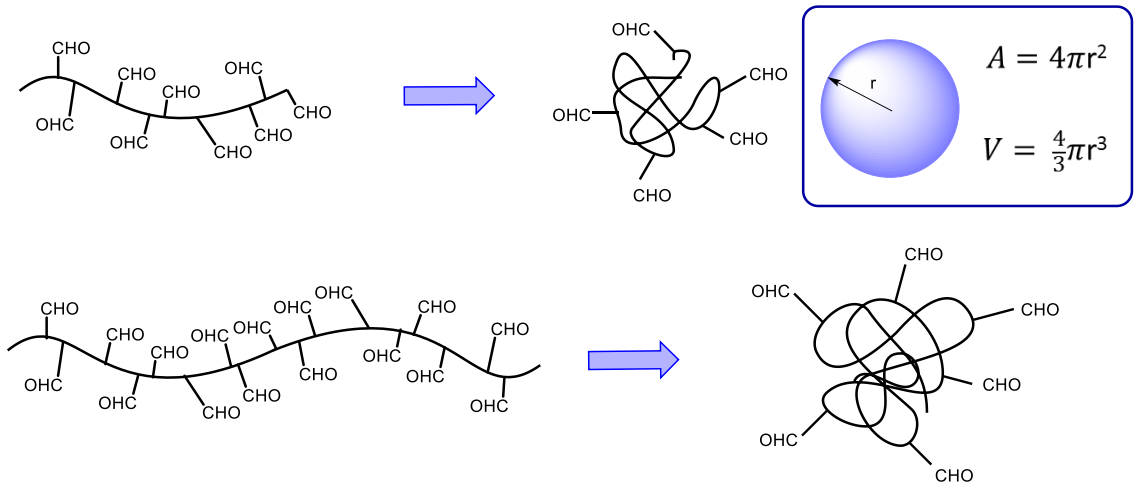

Fig. 2 Surface area : volume relationships of polymer globules. As the length of the polymer scaffold is increased, fewer reactive groups are displayed on the surface of the globule, with a greater number 'buried' inside. The polymer globules may be approximately modelled as spheres, with surface area and volume dependant on the radius of the globule.

It is therefore proposed that as the length of the polymer scaffold increases, and the surface area : volume relationship of the resultant polymer globule in solution decreases linearly, a relatively smaller number of acylhydrazide residues are exposed to the template, with the majority contained inside the globule, providing less scope for change in overall residual composition.

PS-DCLs constructed on the shorter scaffold **P6** (M_n 7.4 kDa) did not incorporate the preferred residue upon template addition to the same extent as **P1** (M_n 11. 4 kDa), deviating from the linear trend observed with the rest of the series (Fig. 1, circled

points). It is proposed that in solution the shorter scaffold **P6** does not form a spherical globule of sufficient radius for the surface area : volume relationship identified to apply.

3.3.2 Varying the functional density of aldehyde groups on polymer scaffolds

The effect of varying the density of aldehyde functionalities on polymer scaffold on the response of resultant PS-DCLs upon exposure to template was also investigated. A series of polymers was prepared (Table 2) which contained varying proportions of **M1** and *N*,*N*-dimethylacrylamide, each with a degree of polymerisation of approximately 85 (**P1**, **P7**-**P9**; 1:5, 1:7, 1:3, 1:20). The low polydispersity indices displayed by these polymers suggest that polymerisation reactions were controlled.

Polymer	**DDMAT** / eq.	**AIBN** / eq.	**DMA** / eq.	**M1** / eq.	n[a]	m[a]	n : m[a]	M_n[a] / gmol^{-1}	M_n[b] / gmol^{-1}	M_w[b] / gmol^{-1}	PDI[b] (M_w/M_n)
P1	1	0.2	80	20	14	71	1:5	11,400	14,300	18,300	1.28
P7	1	0.2	90	10	10	74	1:7	10,500	12,500	18,300	1.28
P8	1	0.2	93	7	6	77	1:13	9,550	14,100	17,600	1.25
P9	1	0.2	95	5	4	81	1:20	9,450	11,300	18,800	1.22

Table 2 Characterisation of copolymers **P1**,**P7**-**P6**. [a] As determined by ^{1}H NMR spectroscopy [b] As determined by gel permeation chromatography in DMF + 1 g L^{-1} LiBr (0.6 mL/ min) calibrated against near monodisperse methyl methacrylate standards. AIBN: azobis(isobutyronitrile), DMA: *N*,*N*'-dimethylacrylamide, DDMAT: *S*-1-dodecyl-*S'*-(α,α-dimethyl-α''-acetic acid)trithiocarbonate.

A series of PS-DCLs were generated upon scaffolds **P1**,**P7**-**P9** by reaction with acylhydrazides **R1** and **R2**, as described previously (Scheme 2). ^{1}H NMR spectroscopy was used to confirm that the residual composition of each PS-DCL was 1.0 : 1.0 prior to addition of either poly(sodium-4-styrenesulphonate) (70 kDa) or BSA as a template. Experiments were performed to ensure that each PS-DCL contained the same effective concentration of aldehyde functionalities and identical concentrations of acylhydrazides **R1** and **R2**. The residual composition of each PS-DCL was monitored over a 17 h period using ^{1}H NMR spectroscopy, with each PS-DCL responding to template addition in the expected manner by amplifying the proportion of the preferred residue on the polymer scaffold.

The results of these experiments show (Fig. 3) that as the molar weight percentage of the aldehyde functionalised monomer **M1** is increased, the amplification of the preferred residue upon the polymer scaffold upon templation increases linearly. Polymers **P1**,**P7**-**P9** may be expected to form similar sized globules in aqueous solution as their degrees of polymerisation are essentially identical at

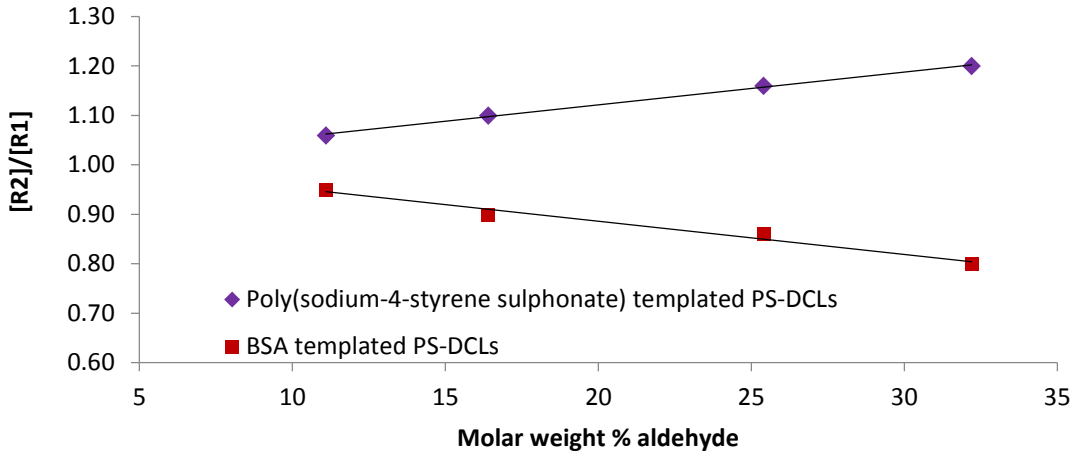

Fig. 3 Effect of increasing the molar weight percentage of aldehyde functionalities on the polymer scaffold upon the final composition of the PS-DCL after templating with poly(sodium-4-styrene sulphonate) (70 kDa) and BSA..

approximately 85. As the molar weight percentage of monomer **M1** is increased, the surface of the globule may be expected to display a greater proportion of acylhydrazide residues, and therefore offer greater scope for component exchange upon exposure to template. Polymers containing a greater molar weight percentage of **M1** do not display sufficient water solubility to allow for the construction of PS-DCLs, and therefore a wider range of parameters may not be investigated.

3.3.3 Varying the concentration of template added to PS-DCLs

In addition to investigating how parameters of the polymer scaffold affect the PS-DCL response to template addition, an exploration of the effects of varying the amount of template added to PS-DCLs was also conducted. Preliminary experiments suggested that addition of poly(sodium-4-styrene sulphonate) or BSA to PS-DCLs did not induce a change in the composition of the PS-DCL at template concentrations below 5.0 mg mL^{-1}, so a series of experiments was performed where the amount of each template added to PS-DCLs was systematically increased (Fig. 4).

Poly(sodium-4-styrene sulphonate) and BSA templates were added to PS-DCLs constructed on scaffold **P7** (10.3 kDa), with ^{1}H NMR spectroscopy used to determine the composition of the system after 24 h. Amplification of the preferred residue upon exposure to template was found to increase within the 15-20 mg mL^{-1} range of template concentrations. The maximum response of PS-DCLs towards both templates is observed at 20 mg mL^{-1}, an observation proposed to be as a consequence of similarity in M_n values for the two templates. At template concentrations above 20 mg mL^{-1} the template species appear to be associating with acylhydrazide residues which are not conjugated to the polymer scaffold, as changes

in the chemical shifts of ^{1}H NMR signals corresponding to these residues are observed.

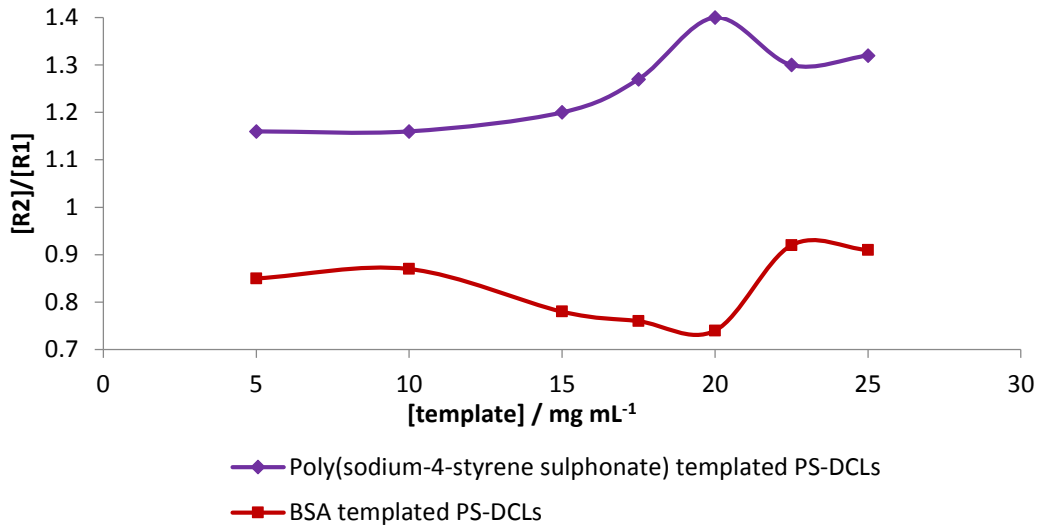

Fig. 4 Effect of varying the concentration of poly(sodium-4-styrene sulphonate) (70 kDa) and BSA templates upon the response of PS-DCLs to addition of template. The composition of the PS-DCL was determined using ^{1}H NMR spectroscopic analysis 24 h after addition of template. Lines are shown to guide the eye, and are not lines of best fit.

It is proposed that as the concentration of the template is increased, the stoichiometry of binding interactions between the template and functionalised polymers changes, allowing a greater proportion of library members to interact with the template and thus adapt their composition. At lower concentrations of template, the surface of the template may be effectively saturated with bound polymers as library members compete with one another to interact with the template. Polymer scaffolds are positively charged, so binding of one or more polymers to a template may actually inhibit the subsequent binding of other polymers. As the concentration of the template is increased, the stoichiometry of binding interactions between polymers and templates may change, so as to allow a greater proportion of polymers within the library to interact with the template.

It is interesting to note that the trends observed with each template appear to mirror one another. This 'mirror-image' behaviour is also observed when the properties of the polymer scaffold, such as chain length and functional density of aldehyde units, are altered. The templating process is proposed to be driven by electrostatic interactions between polymeric library members and templates, so is likely to proceed through similar processes with both charged templates. The 'mirror-image' behaviour observed potentially arises because these templates are similar in size but of opposite overall surface charges.

3.4 Conclusions

PS-DCLs have previously been shown to adapt their composition in response to the addition of macromolecular templates, by preferentially incorporating the residue proposed to interact most favourably with the template added. In this study, the factors which affect the magnitude of this compositional change have been investigated. The effect of increasing the molecular weight of the polymer scaffold upon the behaviour of PS-DCLs in response to addition of templates has been explored, and it is proposed that greater amplification of the preferred residue upon the polymer scaffold is observed when the surface area:volume ratio of the polymer globule is increased. The effect of altering the co-monomer composition of polymer scaffolds on the response of resultant PS-DCLs has also been investigated and it has been observed that as the molar weight percentage of the aldehyde functionalised monomer is increased, the extent of amplification of the preferred residue upon exposure to template increases linearly.

Our experiments involving increasing the amount of template added to PS-DCLs have produced thought-provoking and somewhat unexpected results, with optimum amplification of the preferred residue observed at template concentrations of 20 mg mL^{-1}. At higher template concentrations, templates have been shown to interact with acylhydrazide residues in solution, in addition to members of the PS-DCL.

The results of our investigations into the factors affecting templation will allow for the confident design of more complex PS-DCLs, and for the optimisation of their design in a way that will allow for the isolation of useful quantities of polymeric receptors. An investigation into the nature of binding interactions between template species and library members, particularly the elucidation of association constants and binding stoichiometries, is needed in order to further our understanding of templating processes within PS-DCLs. These interactions are explored in detail in the following chapter.

3.5 Experimental Details

All chemicals, including Girard's reagent T (**R1**) were purchased from Sigma-Aldrich or Alfa Aesar and were used as received without further purification. *N,N*-Dimethylacrylamide was purified by vacuum distillation at 60 °C. ^{1}H and ^{13}C NMR spectra of synthesised compounds were recorded on a Bruker Avance 300

spectrometer at 300 MHz and 75 MHz respectively, or on a JEOL ECS-400 spectrometer at 400 MHz and 100 MHz, with the residual solvent signal as an internal standard. FTIR spectroscopy was performed on a Varian 800 FTIR instrument (Varian Inc.). High-resolution mass spectrometry was performed on a Waters LCT premier mass spectrometer (Waters Inc.). Gel permeation chromatography (GPC) was conducted on a Varian ProStar instrument (Varian Inc.) equipped with a Varian 325 UV-Vis dual wavelength detector (254 nm), a Dawn Heleos II multi-angle laser light scattering detector (Wyatt Technology Corp.), a Viscotek 3580 differential RI detector, and a pair of PL gel 5 μm Mixed D 300 × 7.5 mm columns with guard column (Polymer Laboratories Inc.) in series. Near monodisperse methyl methacrylate standards (Agilent Technologies) were used for calibration. Data collection was performed with Galaxie software (Varian Inc.) and chromatograms analyzed with the Cirrus software (Varian Inc.) and Astra software (Wyatt Technology Corp.). ^{1}H NMR spectra of PS-DCLs were measured using a JEOL Lambda spectrometer (^{1}H at 500 MHz), and analysed using MestReNova.

Aldehyde-functionalised copolymers (**P1**-**P9**)

S-1-Dodecyl-*S'*-(α,α-dimethyl-α''-acetic acid)trithiocarbonate[5] (DDMAT) (1 eq.) and AIBN (0.2 eq) were added to a small schlenk tube. *N*,*N*-dimethylacrylamide and *N*-ethylacrylamide-2-(4-formylbenzamide) (**M1**) were then added followed by DMF (3 mL). The reaction mixture was degassed through five freeze-pump-thaw cycles before the vessel was backfilled with N_2, purged with N_2, and allowed to warm to room temperature. The reaction mixture was then placed in an oil bath at 70 ˚C, and the polymerisation was quenched after 22 h by rapid cooling in $N_{2(l)}$ followed by exposure to air. The reaction mixture was dissolved in a minimal amount of THF-acetone (1:1) and added dropwise to a large excess of ice-cold diethyl ether. The polymer precipitate was then isolated by filtration and redissolved in THF-acetone. The precipitation was repeated before drying under high vacuum. Polymers **P1**-**P9** were obtained as pale yellow solids. (^{1}H NMR (300 MHz, $CDCl_3$): 1.40 – 1.80 (br, CHC*H*$_2$, polymer backbone), 2.20 – 2.70 (br, C*H*CH$_2$, polymer backbone), 2.88 (br, N(C*H*$_3$)$_2$), 3.40 – 3.60 (br, (C*H*$_2$)$_2$), 7.88 (br, Ar), 8.07 (br, Ar), 8.59 (br, N*H*), 10.04 (br, Ar). The composition of polymers **P1**-**P9** can be determined by comparing the integration of the aldehyde protons of **M1** with the integration of the N(C*H*$_3$)$_2$ protons of DMA. The monomer compositions of **P1**-**P9** were not identical to the feed

ratios of DMA : **M1**, most likely as a consequence of the difference in reactivity of the two monomers.

General procedure for the preparation of PS-DCLs

PS-DCLs were prepared so as to contain 2.05 x 10^{-5} mol aldehyde functionalities, with the amount of polymer added adjusted according to the expression:

$$\text{mass polymer} = \frac{2.05 \times 10^{-5} \times M_n}{n}$$

where M_n is the polymer mass as determined by ^{1}H NMR spectroscopy and *n* is the number of aldehyde functionalities of the polymer. The contribution of the aldehyde co-monomer **M1** has been calculated and expressed as a percentage according to the following expression:

$$\text{molar weight percentage } \mathbf{M1} = \frac{n \times M_r^{CHO}}{M_n} \times 100\%$$

where *n* is the number of aldehyde functionalities displayed upon the polymer scaffold, M_r^{CHO} is the molecular mass of **M1** and M_n is the molecular mass of the polymer scaffold as determined by ^{1}H NMR spectroscopy.

Polymer (**P1**-**P9**) was combined with Girard's reagent T (**R1**) (4.2 mg, 2.5 x 10^{-5} mol) in 0.1 M NH_4OAc/AcOH deuterated buffer (pH 4.5, 0.5 mL) and sonicated until a clear solution was obtained. 2-(2-Hydroxyethoxy)acetohydrazide (**R2**) (3.4 mg, 2.5 x 10^{-5} mol) was added to the reaction mixture, which was left overnight to equilibrate. Equilibration to a 1.0:1.0 ratio of **R1** and **R2** was confirmed by ^{1}H NMR spectroscopic analysis prior to template addition, as described previously.[1] Compositional analysis of PS-DCLs constructed on **P1**-**P9** and exposed to templates may be found in Appendix A.

3.6 References

1. C. S. Mahon, A. W. Jackson, B. S. Murray and D. A. Fulton, *Chem. Commun.*, 2011, **47**, 7209-7211.
2. P. T. Corbett, S. Otto and J. K. M. Sanders, *Org. Lett.*, 2004, **6**, 1825-1827.
3. G. Moad, E. Rizzardo and S. H. Thang, *Aust. J. Chem.*, 2005, **58**, 379-410.
4. P. T. Corbett, J. K. M. Sanders and S. Otto, *J. Am. Chem. Soc.*, 2005, **127**, 9390-9392.
5. J. T. Lai, D. Filla and R. Shea, *Macromolecules*, 2002, **35**, 6754-6756.

Chapter 4.

Polymer-Scaffolded Dynamic Combinatorial Libraries as a Route to the Generation of Macromolecular Receptors

This chapter is based upon the following article:

Clare S. Mahon and David A. Fulton, Templation-Induced Re-Equilibration in Polymer-Scaffolded Dynamic Combinatorial Libraries Leads to Enhancements in Binding Affinities*. Chem*. *Sci.*, 2013, **4**, 3661-3666

Table of Contents

4.1 Abstract

The addition of macromolecular templates to Polymer-Scaffolded Dynamic Combinatorial Libraries (PS-DCLs) constructed by the reversible conjugation of acylhydrazides onto aldehyde-functionalised polymer scaffolds has been shown to generate a population of polymers with measurably enhanced binding affinities towards templates, as determined by a fluorescence-based method. The templating process, which harnesses electrostatic interactions between library members and templates, has been shown to be reversible, with PS-DCLs returning to their initial composition upon removal of the template. Solid-supported templates have been employed for the convenient isolation of the best-binding fraction of the library, providing polymeric receptors of improved affinity to the template.

4.2 Introduction

The Polymer-Scaffolded Dynamic Combinatorial Library (PS-DCL)[1] concept (Fig. 1) has been reported, whereby aldehyde-containing polymer scaffolds have been functionalised with various acylhydrazide residues through dynamic covalent acylhydrazone linkages. These systems have also shown to adapt their composition in response to the addition of templating species[2] including synthetic polymers and proteins. The polymeric nature of PS-DCLs makes them ideally suited to templation using macromolecular species, where large areas of interaction may be involved in recognition.[3, 4] It has been proposed that polymer scaffolds preferentially incorporate those residues which best interact with the template through favourable multivalent interactions,[5] a hypothesis which is supported by observation but is yet to be categorically proven.

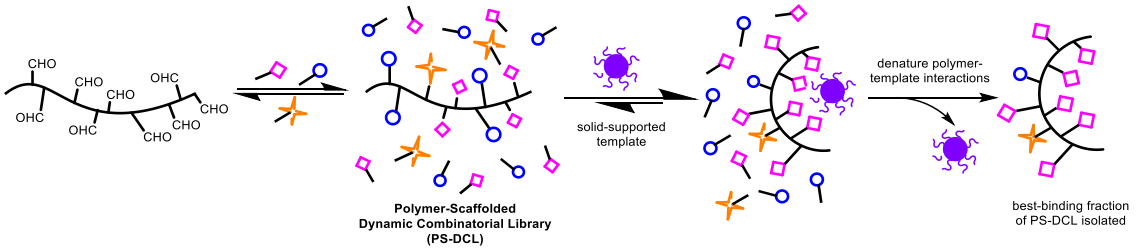

Fig. 1 A dynamic combinatorial library may be generated by the reversible conjugation of various acylhydrazide residues onto an aldehyde-functionalised polymer scaffold. Addition of a template induces compositional exchange, with polymer scaffolds preferentially incorporating residues proposed to interact most favourably with the template. The use of a solid-supported template may allow for the isolation of the best-binding fraction of the library.

PS-DCLs present vastly diverse systems, as the combination of a polymer scaffold and only a few different acylhydrazides may yield a myriad of different sequences.

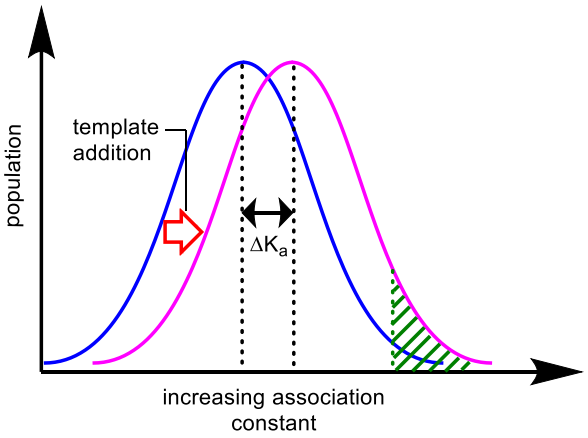

Fig. 2 PS-DCLs may be modelled as a distribution of species which displays variation in the abilities of library members to interact with a template (blue distribution). Addition of a template to a PS-DCL is proposed to shift the entire distribution of binding constants towards greater affinity (pink distribution), with a significant fraction of the new population displaying greatly enhanced affinity for the template (shaded area).

A PS-DCL may be thought to exist as a distribution or 'population' of species, which displays variation in the abilities of library members to interact with a given template. Building on this reasoning, Moore and Zimmerman[6] have conceived an elegant model describing the recognition behaviour of dynamic copolymer sequences in which the binding affinities of the population are normally distributed in log*K*. Addition of a target compound which interacts to varying extents with the copolymer sequences shifts the distribution towards better binding sequences. Moore and Zimmerman have concluded that target addition may shift the mean of the distribution to a limited but measurable degree, and that a significant fraction of sequences within the new population may display greatly enhanced binding constants. Separation of this fraction of the population would, in principle, allow for the isolation of copolymer sequences which display a high affinity for the target. For many applications one could envisage that the precise structure of a receptor need not be known, or be required to be uniform within the sample. Indeed, Molecularly Imprinted Polymers (MIPs)[7-9] have demonstrated promise in the recognition of a wide range of molecules, even succeeding in *in vivo* peptide recognition[10] without the structures of their binding sites being elucidated. The PS-DCL approact may yield macromolecular receptors with improved recognition capacity for their targets, with a thermodynamically-controlled templating process providing scope for the refinement of binding sites, an error-correction mechanism absent from kinetically controlled processes such as the molecular imprinting of polymer matrices.

In this chapter the binding interactions of polymeric library members with macromolecular templates will be quantified and it will be demonstrated that templating PS-DCLs may serve to generate polymers of enhanced affinities towards the template. The use of solid-supported templates for the isolation of the best-

binding fraction of the PS-DCL will also be explored, providing a convenient route to the generation of macromolecular receptors.

4.3 Results and Discussion

4.3.1 Design and construction of PS-DCLs and 'static' libraries

These PS-DCLs have been designed to explore molecular recognition primarily through electrostatic interactions, in order to ensure sufficient thermodynamic driving force for compositional change. Focussing on electrostatic interactions offers the potential for relatively high-affinity multivalent interactions between library members and charged macromolecular templates (Scheme 1 (a)). These interactions may, however, be of low specificity, particularly in comparison to the precise recognition motifs exhibited by antibodies and other natural systems. PS-DCLs have been constructed (Scheme 1(b)) on aldehyde functionalised polymer scaffolds **P1** and **P2** through reaction with acylhydrazide species **R1**-**R3** (Scheme 1(c)).

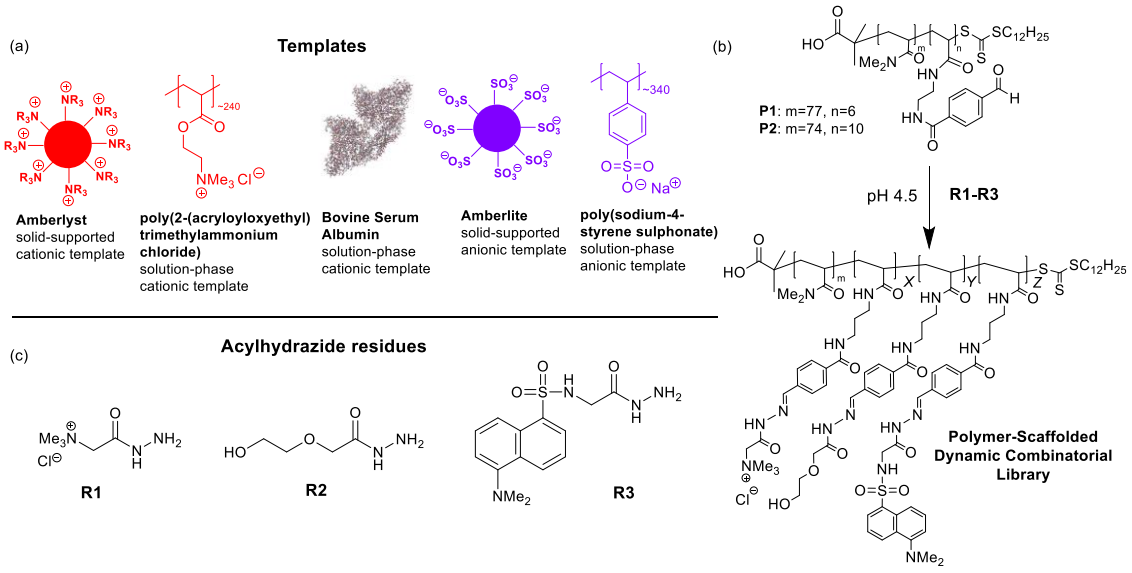

Scheme 1 (a) Solid-supported and solution phase templates used within PS-DCLs. (b) Generation of PS-DCLs using **R1**-**R3** and aldehyde-functionalised polymer scaffolds **P1** and **P2**. (c) Acylhydrazide residues used to construct PS-DCLs.

Acylhydrazides **R1** and **R2** have been selected to promote multivalent ion-dipole interactions between polymeric library members and templates, while **R3** provides a fluorescent label to aid in the determination of association constants and is not anticipated to participate in binding interactions between polymers and templates. Acylhydrazide **R3** was synthesised (Scheme 2) by the reaction of dansyl chloride

with glycine methyl ester hydrochloride to yield the intermediate **1**, and subsequent hydrolysis of the methyl ester functionality to afford **R3**.

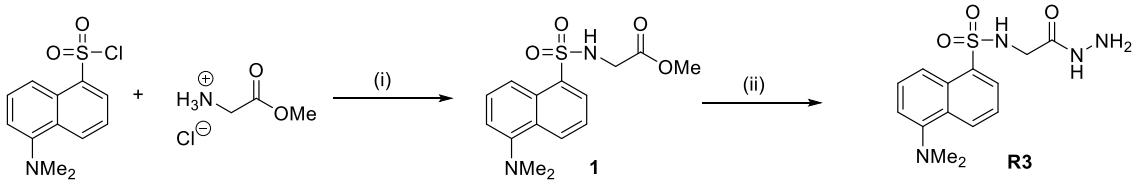

Scheme 2 Synthesis of 5-(dimethylamino)-*N*-(2-hydrazinyl-2-oxoethyl)naphthalene-2-sulphonamide (**R3**): (i) Et_3N, CH_2Cl_2, RT, 24 h. (ii) $NH_2NH_2.2H_2O$, MeOH, RT, 18 h.

The residual composition of PS-DCLs may be monitored[2, 5] indirectly using ^1H NMR spectroscopy, with integral analysis of resonances corresponding to the methylene protons of **R1** and **R2** used to determine the relative concentration of these residues in solution, allowing the relative proportion of these residues on polymer scaffolds to be determined.

4.3.2 Establishing binding affinities of polymer scaffolds at various residual compositions

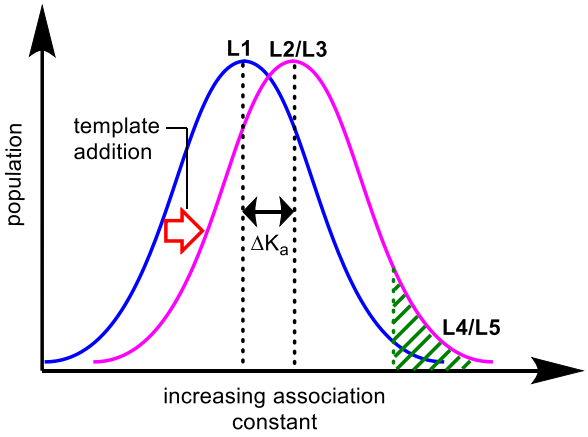

Fig. 3 'Static' libraries may be constructed at various points along proposed population distributions for templated and untemplated PS-DCLs, in order to establish relative binding affinities of polymers of such compositions.

It is hypothesised that templated populations of polymers display higher binding affinities for the template than untemplated populations. Controlling the relative amounts of acylhydrazides **R1**, **R2** and **R3** allows for the preparation of PS-DCLs at various average compositions which are analogous to 'templated' and 'untemplated' libraries, allowing various points along the proposed population distributions to be modelled (Fig. 3). The composition of the PS-DCL may then be fixed by reduction of dynamic acylhydrazone linkages to allow for determination of affinity constants by fluorescence titration. It should be noted that these 'static' libraries have not been exposed to templates, and will therefore lack any sequence-specific information acquired during the templating process.

Static libraries **L1**-**L5** were constructed on scaffold **P1**, with compositions analogous to an untemplated PS-DCL (**L1**), a PS-DCL which has been template with

poly(sodium-4-styrene sulphonate) (**L2**), and a PS-DCL which has been templated with a cationic template such as BSA (**L3**) (Table 1, Fig. 1 (a)). Libraries **L4** and **L5** were also generated with compositions which most likely represent the strongly binding outliers of the templated populations *i.e.* functionalised solely with the preferred acylhydrazide and the fluorescent label **R3**. ^{1}H NMR Spectroscopic analysis confirmed the desired residual compositions of **L1**-**L5**, which were subsequently reduced using $NaCNBH_3$ to prevent unwanted residual exchange during titration experiments. Polymers **L1**-**L5** were isolated by dialysis and titrated against the relevant templates (Table 1, Fig. 4(a)). Binding stoichiometries were determined by Job's method[11, 12] (Fig. 4(b)) to be between 1.0 and 1.3 for each static library investigated and whilst they are not identical, they are sufficiently close to reflect similar modes of binding and thus allow for direct comparison of K_a values.

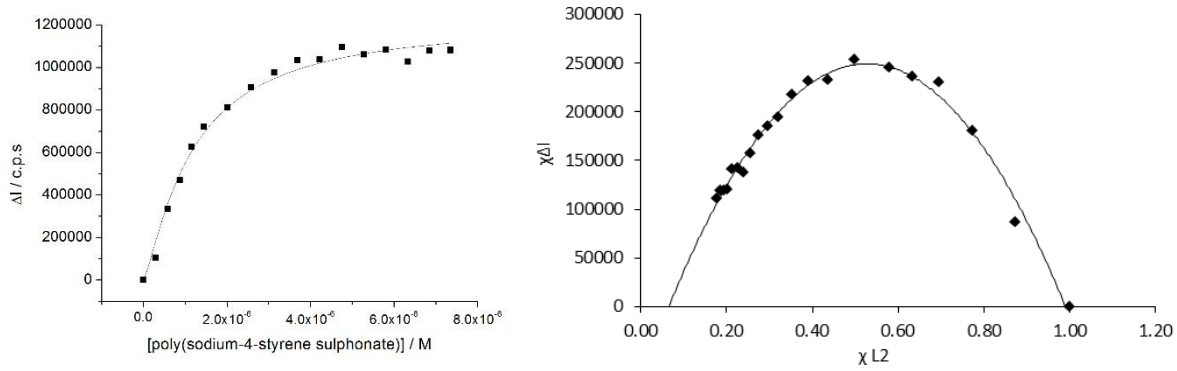

Fig. 4 (a) Representative binding isotherm for the association of 'static' library **L2** with poly(sodium-4-styrene sulphonate). (b) Representative Job plot for 'static' library **L2** and poly(sodium-4-styrene sulphonate).

Library	Average Composition **R1**:**R2**:**R3**	Template	K_a / M^{-1}	*n* (polymer: template)
L1	1.0 : 1.0 : 0.2	Poly(sodium-4-styrene sulphonate)	$7.04 \times 10^5 \pm 9.88 \times 10^4$	1.0
L1	1.0 : 1.0 : 0.2	BSA	$9.01 \times 10^4 \pm 7.93 \times 10^3$	1.3
L1	1.0 : 1.0 : 0.2	Poly(2-(acryloyloxyethyl) trimethylammonium chloride)	$6.12 \times 10^5 \pm 8.84 \times 10^4$	1.0
L2	1.2 : 1.0 : 0.2	Poly(sodium-4-styrene sulphonate)	$9.35 \times 10^5 \pm 9.07 \times 10^4$	1.1
L3	1.0 : 0.8: 0.2	BSA	$1.10 \times 10^5 \pm 1.50 \times 10^4$	1.0
L3	1.0 : 0.8: 0.2	Poly(2-(acryloyloxyethyl) trimethylammonium chloride)	$1.04 \times 10^6 \pm 2.30 \times 10^5$	1.3
L4	1.0 : 0 : 0.2	Poly(sodium-4-styrene sulphonate)	$1.67 \times 10^6 \pm 1.25 \times 10^5$	1.3
L5	0 : 1.0 : 0.2	BSA	$7.75 \times 10^4 \pm 9.16 \times 10^3$	1.0
L5	0 : 1.0 : 0.2	Poly(2-(acryloyloxyethyl) trimethylammonium chloride)	$6.51 \times 10^5 \pm 1.25 \times 10^5$	1.0

Table 1 Association constants K_a and binding stoichiometries *n* for interactions between polymers from libraries **L1**-**L5** and templates, as determined by fluorescence titration methods and Job plot analysis.

Static libraries with compositions analogous to templated PS-DCLs (**L2** and **L3**) were found to have greater binding affinities for the relevant templates than the untemplated library (**L1**), suggesting that the compositional change induced by template addition does lead to an increase in binding affinities between polymers within the library and templates. Library **L4**, which being decorated almost exclusively with cationic residues is arguably representative of strongly binding outliers within a templated population of polymers, demonstrates a greater affinity for poly(sodium-4-styrene sulphonate) than **L2**, supporting the hypothesis that those species at the upper end of the distribution are likely to be of the greatest interest.

Interestingly, the population of polymers functionalised solely with the fluorescent acylhydrazide **R3** and the ethylene glycol derivative **R2** (**L5**) demonstrate lower K_a values with the templates BSA and poly(2-(acryloyloxyethyl)trimethyl ammonium chloride) than populations with templated compositions (**L3**), and even the untemplated composition (**L1**) in the case of BSA. This observation is surprising, as it was expected that incorporation of the positively charged **R1** onto polymer scaffolds would weaken the binding of those polymers with positively charged templates. It is, however, conceivable that the surfaces of these templates may display regions of higher electron density which may interact favourably with **R1**, and therefore the composition of the 'ideal binder' from the PS-DCL may require some incorporation of this residue.

Investigation of the recognition characteristics of these 'static' libraries has provided important insights, with observations largely in line with those predicted by Zimmerman and Moore.[6] The study of PS-DCLs under dynamic conditions would allow for investigation of the effects of template-induced compositional change upon the binding affinities of polymers within the population, and may provide more useful information.

4.3.3 Isolating the best binding fraction of the PS-DCL

The use of solid-supported templates was investigated as a potential route towards the isolation of the best-binding fractions of polymers within PS-DCLs. Solid-supported templates have previously been used successfully to induce compositional exchange within macrocyclic DCLs.[13, 14] In particular, commercially available ion-exchange resins such as the quaternary ammonium-functionalised

Amberlyst and the sulphonate-functionalised Amberlite, were identified as potential templates, as these species present solid-supported analogues of charged macromolecular solution phase templates. It was proposed that those library members which interact most strongly with the template would become bound to its surface, and this 'best-binding' fraction of the system could therefore easily be isolated from the rest of the library, thus presenting a simple and convenient route to the isolation of polymeric receptors for solid-supported species of interest.

PS-DCLs were constructed upon scaffold **P1**, incorporating acylhydrazides **R1**, **R2** and **R3** (Scheme 1(b)). In the absence of a template the system was shown using ^{1}H NMR spectroscopy to contain equal relative concentrations of **R1** and **R2** in solution, indicating that these residues are incorporated onto polymer scaffolds in equal amounts. Solid supported templates Amberlyst and Amberlite were added, and after 24 h, ^{1}H NMR spectroscopic analysis revealed compositional change within both systems: a decrease in the concentration of **R2** relative to **R1** of 0.8:1.0 in the PS-DCL templated by Amberlyst, and an increase in the concentration of **R2** relative to **R1** of 1.2:1.0 in the library templated by Amberlite. In both cases, polymer scaffolds have preferentially incorporated the acylhydrazide predicted to interact through favourable electrostatic interactions with the template added. Solid supported templates were then removed from the PS-DCLs and washed with a denaturant solution (5.0 M guanidinium chloride, 0.5 M NaCl in D_2O in the case of Amberlite, or MeOH-d_4 in the case of Amberlyst[13]) to disrupt interactions between templates and any polymers bound to their surfaces. These washings were shown by ^{1}H NMR spectroscopy to contain polymeric species, which were reduced using $NaCNBH_3$ to prevent further compositional exchange upon exposure to templates, and purified by dialysis. These polymers were titrated against poly(sodium-4-styrene sulphonate) or poly(2-(acryloyloxyethyl) trimethylammonium chloride), which may be considered as solution-phase analogues of Amberlyst and Amberlite.

Library	Average Composition **R1**:**R2**:**R3**	Template	K_a / M^{-1}	n (polymer: template)
L6	unknown	Poly(sodium-4-styrene sulphonate)	$1.30 \times 10^6 \pm 1.36 \times 10^5$	1.4
L7	unknown	Poly(2-(acryloyloxyethyl) trimethylammonium chloride)	$1.17 \times 10^6 \pm 1.98 \times 10^5$	1.2

Table 2 Association constants K_a and binding stoichiometries n for interactions between polymers from libraries **L6**-**L7** and templates, as determined by fluorescence titration.

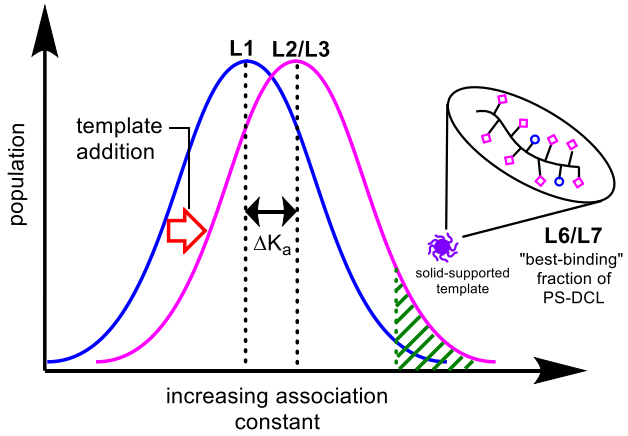

Fig. 5 Addition of a template to a PS-DCL is proposed to induce compositional change which shifts the distribution of polymers towards greater binding affinities. Those species of greatest binding affinity are proposed to be bound to the surface of the solid-supported template (**L6**/**L7**), and these polymers may better represent the best-binding fraction of the library than the proposed ideal receptors **L4**/**L5**.

Polymers isolated from Amberlite (**L6**, Fig. 5, Table 2) displayed a K_a of 1.30 x 10^6 M^{-1} upon binding to poly(sodium-4-styrene sulphonate), indicating that they interact more favourably with the template than polymers within **L2** (9. 35 x 10^5 M^{-1}, Table 1), the polymer library generated with the same average composition as a PS-DCL which has been templated with poly(sodium-4-styrene sulphonate). Similarly, polymers isolated from Amberlyst (**L7**, Fig. 5, Table 2) exhibited a K_a of 1.17 x 10^6 M^{-1} with poly(2-acryloyloxyethyl) trimethylammonium chloride, indicating that they interact more favourably with the template than polymers within **L3** (1.04 x 10^6 M^{-1}, Table 1). These results suggest that a significant proportion of the PS-DCL binds more strongly to the template than polymers with 'library-average' composition, validating the PS-DCL concept as a route to the discovery of receptors of enhanced affinity towards a target compound and supporting Zimmerman and Moore's model[6] of equilibrium shifting within mixtures of interconverting polymers.

The enhancement in binding affinities demonstrated here may appear to be small, however, it must be remembered that the compositions of **L6** and **L7** are unknown, and that these isolated polymers are thought to represent the most strongly binding ~10% of the library, a fraction of the population which may also be expected to display variation in binding affinities. This distribution of polymers is in contrast to those polymers within **L4** and **L5**, which may be presumed to be more uniform in their residual composition.

4.3.4 Demonstrating the reversibility of templating processes within PS-DCLs

Templation of PS-DCLs is proposed to operate wholly under thermodynamic control, with the reversible nature of acylhydrazone linkages allowing for adjustment of composition upon exposure to a template. The system is proposed to strive for a thermodynamic minimum, with compositional exchange serving to

generate a population of polymers which interact more favourably with the template. Continuing this reasoning it was proposed that removal of the template from a PS-DCL would induce a further re-equilibration process which would restore the library to its initial, untemplated composition. Establishing the reversible nature of templation would validate the hypothesis that PS-DCLs operate under true thermodynamic control.

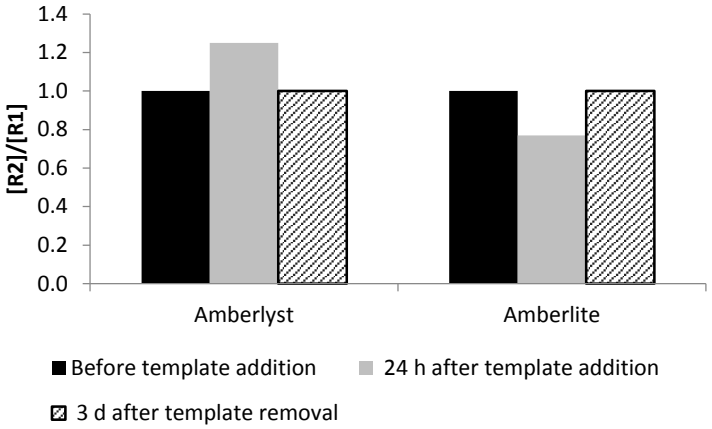

Fig. 6 The composition of PS-DCLs as determined by ^{1}H NMR spectroscopy prior to template addition, after template-induced re-equilibration and after template removal-induced re-equilibration.

In order to investigate this hypothesis, solid supported templates Amberlyst and Amberlite were added to PS-DCLs generated by functionalisation of the scaffold **P2**, which contains approximately 10 aldehyde moieties and displays an overall degree of polymerisation of 84, with acylhydrazide residues **R1** and **R2**. After 24 h, ^{1}H NMR spectroscopy revealed the expected compositional change within both systems (Fig. 6): a decrease in the concentration in the concentration of **R1** relative to **R2** on polymer scaffolds of 0.8:1.0 in the PS-DCL templated by Amberlyst, and an increase in the concentration of **R1** relative to **R2** on polymer scaffolds of 1.3:1.0 in the library templated with Amberlite. Solid supported templates were removed from PS-DCLs and washed with a denaturant solution (5.0 M guanidinium chloride, 0.5 M NaCl in D_2O in the case of Amberlite, or MeOH-d_4 in the case of Amberlyst[13]) to remove strongly-binding library members from the surfaces of the templates. Washings were combined with the rest of the PS-DCL and after 3 days ^{1}H NMR spectroscopy revealed acylhydrazides **R1** and **R2** to be present in both systems in equal concentrations (Fig. 6), demonstrating that PS-DCLs have returned to their original composition.

These observations suggest that the compositional change within PS-DCLs induced by addition of templates is indeed a thermodynamically-controlled process. The dynamic nature of this process would therefore provide the scope for error-correction or sequence optimisation lacking in the production of polymeric receptors by kinetically-controlled processes such as molecular imprinting.

4.4 Conclusions

The results presented in this chapter validate the hypothesis that compositional change within PS-DCLs upon template addition delivers a library of polymers with higher binding affinities for a chosen template than the corresponding untemplated library. The use of solid-supported templates has enabled the convenient isolation of the best binding fraction of PS-DCLs, separating those library members of highest binding affinities for the template from the bulk of the system. The method has been demonstrated using commercially available ion-exchange resins as templates, yet numerous chemical techniques may allow for the attachment of virtually any template of interest onto a solid support,[15] thus widening the scope of the concept to previously unexplored areas.

The re-equilibration of templated PS-DCLs to their initial, untemplated compositions upon removal of the template has been observed, confirming that compositional exchange within PS-DCLs is a consequence of a thermodynamically-controlled templating process elicited by supramolecular interactions between library members and templates.

These important advances to our understanding of PS-DCLs serve to underline the validity of the concept as a route to the generation of receptors for macromolecular species, and pave the way for the design of more complex systems, incorporating greater numbers of side-chain residues, with a view to improving the recognition capabilities of the resultant polymers.

4.5 Experimental Details

All chemicals, including Girard's reagent T (**R1**) were purchased from Sigma-Aldrich or Alfa Aesar and were used as received without further purification. *N,N*-Dimethylacrylamide was purified by vacuum distillation at 60 ˚C. ^{1}H and ^{13}C NMR spectra of synthesised compounds were recorded on a Bruker Avance 300 spectrometer at 300 MHz and 75 MHz respectively, or on a JEOL ECS-400 spectrometer at 400 MHz and 100 MHz, with the residual solvent signal as an internal standard. High-resolution mass spectrometry was performed on a Waters LCT premier mass spectrometer (Waters Inc.). Gel permeation chromatography (GPC) was conducted on a Varian ProStar instrument (Varian Inc.) equipped with a Varian 325 UV-Vis dual wavelength detector (254 nm), a Dawn Heleos II multi-angle laser light scattering detector (Wyatt Technology Corp.), a Viscotek 3580 differential

RI detector, and a pair of PL gel 5 μm Mixed D 300 × 7.5 mm columns with guard column (Polymer Laboratories Inc.) in series. Near monodisperse methyl methacrylate standards (Agilent Technologies) were used for calibration. Data collection was performed with Galaxie software (Varian Inc.) and chromatograms analyzed with Cirrus software (Varian Inc.) and Astra software (Wyatt Technology Corp.). Fluorescence spectroscopy was carried out on a Fluoromax instrument, with corrected spectra used for all analysis.

^{1}H NMR spectra of PS-DCLs were measured using a JEOL Lambda spectrometer (^{1}H at 500 MHz) or on a JEOL ECS-400 spectrometer (^{1}H at 400 MHz), and analysed using MestreNova. PS-DCLs were prepared so as to contain 50.0 mM concentrations of acylhydrazides **R1** and **R2**, with **R3** present in 14.9 mM concentration, and an appropriate amount of **P1**-**P2** so that the total concentration of aldehyde units in solution was 41.0 mM. Equilibration to a 1.0:1.0 ratio of **R1** to **R2** in solution was confirmed by ^{1}H NMR spectroscopic analysis prior to addition of templates. Solid supported templates Amberlyst and Amberlite were added to PS-DCLs at concentrations of 20 mg mL^{-1}.

Aldehyde-Functionalized Copolymers (**P1**-**P2**):

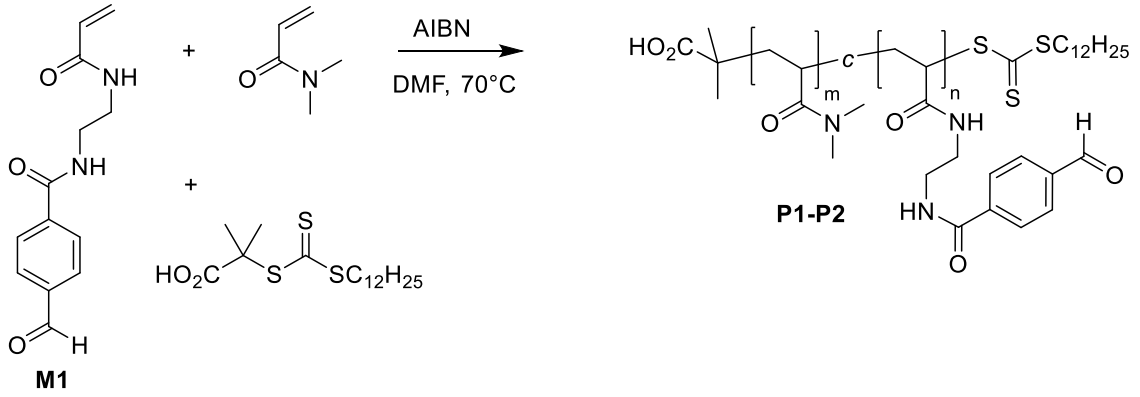

Scheme 3 Synthesis of aldehyde-functionalised copolymers **P1**-**P2**.

S-1-Dodecyl-*S'*-(α,α-dimethyl-α''-acetic acid)trithiocarbonate[16] (DDMAT) (1 eq, 34.2 mg, 0.094 mmol) and AIBN (0.2 eq, 3.08 mg, 19 μmol) were added to a small schlenk tube. *N,N*-Dimethylacrylamide (DMA) and *N*-ethylacrylamide-2-(4-formylbenzamide) (**M1**) were then added followed by DMF (3 mL). The reaction mixture was degassed by five freeze-pump-thaw cycles before the vessel was backfilled with N_2, purged with N_2, and allowed to warm to room temperature. The reaction mixture was then placed in an oil bath at 70 ˚C, and the polymerisation was quenched after 22 h. The reaction mixture was dissolved in a minimal amount of

THF-acetone and added dropwise to a large excess of ice-cold diethyl ether. The polymer was then isolated by filtration and the precipitation was repeated before drying under high vacuum. Polymers **P1-P2** were obtained as pale yellow solids. ^{1}H NMR (300 MHz, $CDCl_3$): 1.40 – 1.80 (br, CHC*H*$_2$, polymer backbone), 2.20 – 2.70 (br, C*H*CH_2, polymer backbone), 2.88 (br, N(C*H*$_3$)$_2$), 3.40 – 3.60 (br, (C*H*$_2$)$_2$), 7.88 (br, Ar), 8.07 (br, Ar), 8.59 (br, N*H*), 10.04 (br, Ar). The composition of **P1**-**P2** can be determined by comparing the integration of the aldehyde protons of **M1** with the integration of the N(C*H*$_3$)$_2$ protons of DMA. The monomer compositions were not determined to identical to the feed ratio of DMA:**M1**, most likely as a consequence of the difference in reactivity of the two monomers.

Polymer	**DDMAT** / eq.	**AIBN** / eq.	**DMA** / eq.	**M1** / eq.	n[a]	m[a]	n : m[a]	M_n[a] / g mol^{-1}	M_n[b] / g mol^{-1}	M_w[b] / g mol^{-1}	PDI[b] (M_w/M_n)
P1	1	0.2	93	7	6	77	1:13	9,550	14,100	17,600	1.25
P2	1	0.2	90	10	10	74	1:7	10,500	12,500	18,300	1.28

Table 3 Characterisation of copolymers **P1-P2**. [a] As determined by ^{1}H NMR spectroscopy [b] As determined by gel permeation chromatography in DMF + 1 g L^{-1} LiBr (0.6 mL/ min) calibrated against near monodisperse poly(methyl methacrylate) standards. AIBN: azobis(isobutyronitrile), DMA: *N*,*N*-dimethylacrylamide, DDMAT: *S*-1-dodecyl-*S'*-(α,α-dimethyl-α''-acetic acid)trithiocarbonate.

Methyl 2-(5-(dimethylamino)naphthalene-1-sulphonamido)acetate (**1**)

Glycine methyl ester hydrochloride (0.85 g, 6.7 mmol) was dissolved in CH_2Cl_2 (100 mL). Triethylamine (1.8 mL, 7.4 mmol) was added followed by dansyl chloride (2.0 g, 7.4 mmol) and the mixture was left to stir under N_2 at room temperature for 24 h, when the reaction was judged to be complete by TLC analysis. The reaction mixture was then washed with $AcOH_{(aq)}$ (1 M, 3 x 100 mL), $NaHCO_{3(aq)}$ (3 x 100 mL) and brine (100 mL). The initial $NaHCO_3$ washings obtained were backwashed with CH_2Cl_2 (100 mL). The combined organic fractions were dried over $MgSO_4$, filtered and evaporated to dryness, yielding a yellow oil which was purified by column chromatography (SiO_2, 7:3 petrol : EtOAc) to afford the title compound as a yellow solid (1. 50 g, 69%). ^{1}H NMR (400 MHz, $CDCl_3$) δ 2.88 (s, 6H, N(C*H*$_3$)$_2$), 3.53 (s, 3H, COC*H*$_3$), 3.72 (d, 2H, C*H*$_2$, *J* = 4.0 Hz), 5.27 (t, 1H, N*H*, *J* = 6.0 Hz), 7.19 (d, 1H, Ar, *J* = 7.6 Hz), 7.51 (t, 1H, Ar, *J* = 8.0 Hz), 7.58 (t, 1H, Ar, *J* = 8.0 Hz), 8.23 (d, 1H, Ar, *J* = 7.2 Hz), 8.30 (d, 1H, Ar, *J* = 8.8 Hz), 8.55 (d, 1 H, Ar, *J* = 8.4 Hz); ^{13}C NMR (100 MHz, $CDCl_3$) δ 44.3, 45.5, 52.6, 115.5, 118.9, 123.2, 129.7, 129.9, 130.0, 130.9, 134.0, 169.2; HRMS (ES+) $C_{15}H_{18}N_2O_4SNa$: Calculated: 345.0885. Actual: 345.0879; m.p. 86-88°C.

5-(Dimethylamino)-N-(2-hydrazinyl-2-oxoethyl)naphthalene-1-sulphonamide (**R3**)

A solution of methyl 2-(5-(dimethylamino)naphthalene-1-sulphonamido)acetate (**1**) (1.28 g, 4.0 mmol) and hydrazine hydrate (1.9 mL, 40 mmol) in methanol (60 mL) was allowed to stir at room temperature for 16 h, when the reaction was judged to be complete by TLC. The reaction mixture was evaporated to dryness, yielding a yellow oil which was purified by column chromatography (SiO_2, 1-3% MeOH/CH_2Cl_2) to afford the title product as a yellow solid (1.27 g, 99%). ^{1}H NMR (400 MHz, $CDCl_3$) δ 2.82 (s, 6H, N(C*H*$_3$)$_2$), 3.53 (s, 2H, C*H*$_2$), 3.95 (s, 2H, NHN*H*$_2$), 6.78 (s, 1H, N*H*NH$_2$), 7.08 (d, 1H, Ar, *J* = 7.2 Hz), 7.43 (m , 2H, Ar), 8.13 (d, 1 H, Ar, *J* = 7.2 Hz), 8.23 (d, 1H, Ar, *J* = 8.8 Hz), 8.47 (d, 1 H, *J* = 8.4 Hz); ^{13}C NMR (100 MHz, $CDCl_3$) δ 45.5, 115.5, 118.6, 123.2, 128.8, 129.5, 129.8, 129.9, 131.0, 133.7, 152.1, 169.0; HRMS (ES+) $C_{14}H_{19}N_4O_3S$ [M+H]: Calculated: 323.1178. Actual: 323.1171; m.p. 74-76°C.

Poly(2-(acryloyloxyethyl)ammonium chloride)

S-1-Dodecyl-*S'*-(α,α-dimethyl-α''-acetic acid)trithiocarbonate[16] (DDMAT) (1.0 eq, 20.0 mg, 54.9 μmol) and AIBN (0.2 eq, 1.8 mg, 11 μmol) were added to a small schlenk tube, followed by 2-(acryloyloxyethyl)ammonium chloride (5.32 g, 22 mmol) and DMF (3 mL). The reaction mixture was degassed five times before the vessel was backfilled with N_2, purged with N_2, and allowed to warm to room temperature. The reaction mixture was then placed in an oil bath at 70 ˚C, and the polymerisation was quenched after 22 h. The reaction mixture was diluted in MeOH and added dropwise to a large excess of Et_2O. The polymer was then isolated by filtration and the precipitation was repeated before the polymer was dialysed against H_2O and lyophilised to yield the title product as a white solid (0.416 g, 8 % conversion). The degree of polymerisation was determined to be approximately 240 using ^{1}H NMR spectroscopic analysis.

General Procedure for Preparation of 'Static' Libraries **L1**-**L5**

L1-**L5** were prepared so as to contain 50.0 mM concentrations of acylhydrazides **R1** and **R2**, with **R3** present in 14.9 mM concentration, and an appropriate amount of **P1**-**P2** so that the total concentration of aldehyde units in solution was 41.0 mM.

Polymer (**P1**-**P2**) was combined with Girard's reagent T (**R1**) in 0.1 M NH_4OAc/AcOH deuterated buffer (pH 4.5, 0.5 mL) and sonicated until a clear

solution was obtained. 2-(2-Hydroxyethoxy)acetohydrazide (**R2**) and 5-(dimethylamino)-N-(2-hydrazinyl-2-oxoethyl)naphthalene-1-sulfonamide (**R3**) were added to the reaction mixture, which was left overnight to equilibrate. Equilibration to the required ratio of **R1** and **R2** was confirmed by ^{1}H NMR spectroscopic analysis prior to reduction. $NaCNBH_3$ (10 eq. per aldehyde functionality) was added to the solution and the reaction mixture was left overnight at room temperature. Reduction was confirmed by ^{1}H NMR spectroscopic analysis prior to dialysis against H_2O and lyophilisation to yield static libraries **L1**-**L5**.

General Procedure for Isolation of Library Members from Solid-supported Templates

Solid supported templates were removed from PS-DCLs by filtration, and washed three times with a suitable denaturant solution. Amberlyst was washed with MeOH-d_4[13] (3 x 0.5 mL), while Amberlite was washed with 5.0 M guanidinium chloride and 0.5 M NaCl in D_2O (3 x 0.5 mL). ^{1}H NMR spectroscopic analysis revealed both sets of washings to contain polymeric species which were purified by dialysis then lyophilised to yield **L6**-**L7**.

General Procedure for Fluorescence Titrations[17]

Solutions of static libraries **L1**-**L5** were prepared at 2.0 μM concentrations in 0.1 M NH_4OAc/AcOH buffer (pH 4.5). Solutions of templates were prepared by dissolving templates in the appropriate polymer solution (100 μM poly(sodium-4-styrene sulphonate), 100 μM poly(2-(acryloyloxyethyl)ammonium chloride), 500 μM BSA) to ensure a constant concentration of polymer throughout the titration. The polymer solution (1700 μL) was placed in a cuvette and the appropriate template solution was added in small aliquots (5-10 μL). The samples were excited at a wavelength of 330 nm and the change in emission intensity at 540 nm or 560 nm was recorded. Control experiments were carried out where a solution of each template (100 μM poly(sodium-4-styrene sulphonate), 100 μM poly(2-(acryloyloxyethyl)ammonium chloride), 500 μM BSA in 0.1 M NH_4OAc/AcOH pH 4.5) was titrated into a solution of the buffer, in the absence of polymer. The change in intensity of fluorescence of the solution as a consequence of template addition was monitored, and these values were subtracted from those obtained during titrations of **L1**-**L5** with templates. Titration curves may be found in Appendix B.

Binding stoichiometries (n) were determined by Job Plot analysis. Dissociation constants were calculated using non-linear regression methods, with data fitted to a modified Hill equation $y = V_{max} \frac{x^n}{K_d{}^n + x^n}$. The binding stoichiometry n was obtained from the relevant Job Plot. This analysis yielded values of n between 1.0 and 1.4 for each static library investigated. While the apparent binding stoichiometries of **L1**-**L7** with templates may not be identical, they are sufficiently similar to reflect comparable modes of binding and thus allow for direct comparison of K_a values.

4.6 References

1. D. A. Fulton, *Org. Lett.*, 2008, **10**, 3291-3294.
2. C. S. Mahon, A. W. Jackson, B. S. Murray and D. A. Fulton, *Chem. Commun.*, 2011, **47**, 7209-7211.
3. W. E. Stites, *Chem. Rev.*, 1997, **97**, 1233-1250.
4. H. Yin and A. D. Hamilton, *Angew. Chem. Int. Ed.*, 2005, **44**, 4130-4163.
5. C. S. Mahon, A. W. Jackson, B. S. Murray and D. A. Fulton, *Polym. Chem.*, 2013, **4**, 368-377.
6. J. S. Moore and N. W. Zimmerman, *Org. Lett.*, 2000, **2**, 915-918.
7. G. Wulff, W. Vesper, R. Grobe-Einsler and A. Sarhan, *Makromol. Chem.*, 1977, **178**, 2799-2816.
8. G. Wulff, *Angew. Chem. Int. Ed. Engl.*, 1995, **34**, 1812-1832.
9. L. Ye and K. Mosbach, *Chem. Mater.*, 2008, **20**, 859-868.
10. Y. Hoshino, H. Koide, T. Urakami, H. Kanazawa, T. Kodama, N. Oku and K. J. Shea, *J. Am. Chem. Soc.*, 2010, **132**, 6644-6645.
11. P. Job, *Ann. Chim.*, 1928, **9**, 113-203.
12. J. S. Renny, L. L. Tomasevich, E. H. Tallmadge and D. B. Collum, *Angew. Chem. Int. Ed.*, 2013, **52**, 11998-12013.
13. S. L. Roberts, R. L. E. Furlan, G. R. L. Cousins and J. K. M. Sanders, *Chem. Commun.*, 2002, 938-939.
14. P. Besenius, P. A. G. Cormack, R. F. Ludlow, S. Otto and D. C. Sherrington, *Chem. Commun.*, 2008, 2809-2811.
15. F. Guillier, D. Orain and M. Bradley, *Chem. Rev.*, 2000, **100**, 2091-2158.
16. J. T. Lai, D. Filla and R. Shea, *Macromolecules*, 2002, **35**, 6754-6756.
17. C. Renner, J. Piehler and T. Schrader, *J. Am. Chem. Soc.*, 2005, **128**, 620-628.

Chapter 5.

Carbohydrate-Functionalised Polymer-Scaffolded Dynamic Combinatorial Libraries

Table of Contents

5.1 Abstract

Carbohydrate-functionalised Polymer-Scaffolded Dynamic Combinatorial Libraries (PS-DCLs) have been prepared in aqueous solution by the reversible conjugation of carbohydrates with acylhydrazide functionalities in their aglycans on to an aldehyde-functionalised polymer scaffold. PS-DCLs have been shown to undergo compositional change in response to the addition of lectin templates, with polymer scaffolds preferentially incorporating the carbohydrate which binds to the lectin added. This compositional change has been shown to generate polymers of significantly enhanced affinity for the lectin added, with enhancements in free energy of binding in the range of 5.2 – 8.8 kJ mol^{-1} observed.

5.2 Introduction

Polymer-Scaffolded Dynamic Combinatorial Libraries (PS-DCLs) have been demonstrated to present a viable route towards the generation of macromolecular receptors.[1-3] Introduction of a template to a PS-DCL induces compositional shift, with polymer scaffolds preferentially incorporating residues which interact favourably with the template and rejecting those which do not. This compositional shift has been shown[3] to produce polymers of measurably enhanced affinities towards the template. The dynamic nature of the templating process offers scope for error correction within library members, a factor which is likely to improve the specificity and uniformity of binding sites within the sample.

The method has been proven to be viable using systems designed to harness multivalent electrostatic interactions between library members and charged macromolecular templates, including synthetic polymers and proteins, in an effort to ensure sufficient thermodynamic driving force for compositional shift. In order to progress the concept to produce polymeric receptors capable of specific macromolecular recognition, protein-carbohydrate interactions were identified as a potential area of exploration.

Lectins are proteins which recognise and bind carbohydrates, often with important biological consequences.[4] Cell surfaces are decorated with glycoprotein 'barcodes' which facilitate cellular recognition[5] (Fig. 1) processes which are frequently implicated in bacterial and viral infection.[6, 7] Some pathogenic bacteria, notably *Vibrio cholerae*, the causative agent of cholera, and *Escherichia coli (E. coli)*, cause disease through the production of toxic lectins which bind to carbohydrates on

cellular surfaces, facilitating entry to cells and initiating a biochemical cascade which results in diarrhoea which may be life-threatening.[8] Compounds which may inhibit these key recognition processes are understandably of considerable interest to chemists and clinicians. In particular, the growing problem of antibiotic resistance may call for an alternative approach to combatting such bacterial disease, where toxins are targeted rather than the pathogens themselves. Additionally, pathogenic cells are often decorated with unique glycan structures, presenting scope for the development of carbohydrate-functionalised synthetic mimics as vaccines against these pathogens.[9]

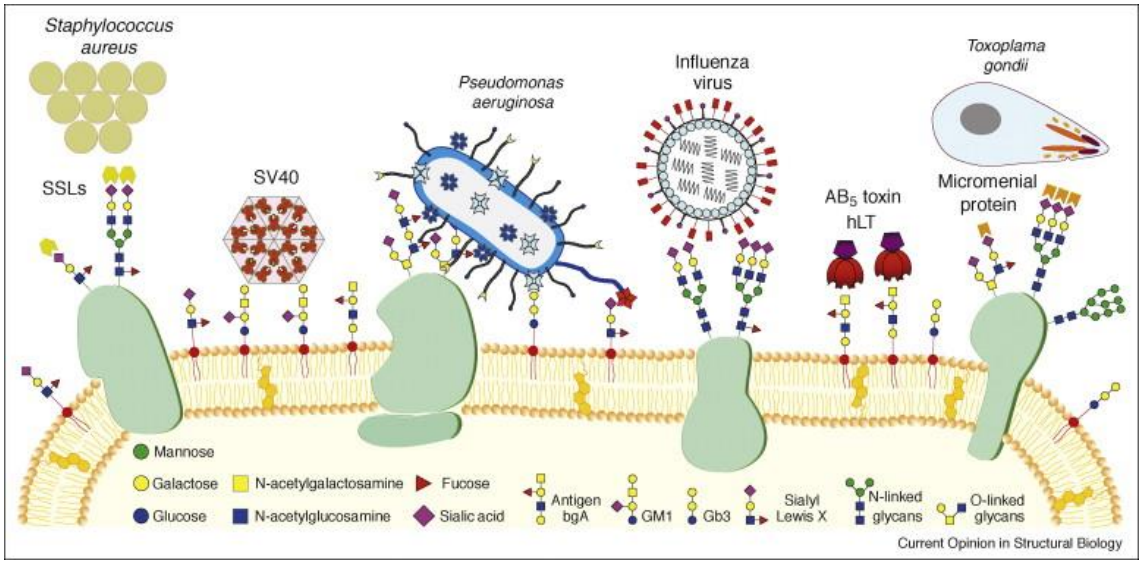

Fig. 1[5] The surfaces of metazoan cells are decorated with oligosaccharides, presenting recognition motifs which may be exploited by pathogens. Reprinted with permission from A. Imberty and A. Varrot, Microbial recognition of human cell surface glycoconjugates, *Curr. Opin. Struct. Biol.*, 2008, **18**, 567-576. Copyright 2008 Elsevier.

The concept of multivalency[4, 10] is key to the recognition of carbohydrates by proteins. Lectins often display multiple identical recognition sites (Fig. 2) which may interact with carbohydrates through low-affinity supramolecular interactions which reinforce one another to facilitate high-affinity binding, with greatly enhanced activities compared to monovalent inhibitors. The attachment of multiple carbohydrates to a molecular scaffold to facilitate their simultaneous binding at multiple sites is therefore a popular approach to inhibitor design, and is perhaps most successfully demonstrated by the success of glyco-dendrimers[11] in inhibiting carbohydrate-protein interactions. Often, such inhibitors constitute elegant yet synthetically-challenging molecular architectures, with their production requiring significant effort on the part of the synthetic chemist. Consequently, the likelihood of mass production of carbohydrate-functionalised dendrimers to provide vaccines or treatments in the vast quantities necessary to impact public health is low.

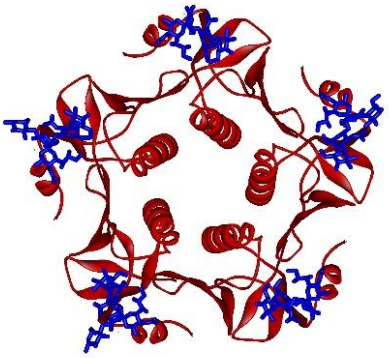

Fig. 2 The recognition unit of the cholera toxin (red) consists of five identical subunits, each bearing a carbohydrate recognition site. Bound carbohydrates are shown in blue.

The use of a system where pre-formed polymer scaffolds could be decorated with the required carbohydrates would enable convenient access to the large molecular architectures offered by dendrimers, without the need for precision synthesis. Living radical polymerisation methods such as RAFT[12] are well-established, allowing control over the length of polymer scaffolds and the density of carbohydrate units. Most importantly, carbohydrate-functionalised PS-DCLs would allow carbohydrates the opportunity to exchange and reshuffle their positions along polymer scaffolds in order to occupy optimum positions for interaction with a lectin template. This adaptive behaviour would present a new approach to the generation of receptors for carbohydrate-binding proteins, and promising initial results investigating the potential of this concept are reported here. The 'static' library approach will be used to explore differences in binding affinities for carbohydrate-functionalised PS-DCLs at varying residual compositions corresponding to templated and untemplated populations of polymers. Templating carbohydrate-functionalised PS-DCLs with lectins will then be shown to yield polymeric receptors of notably enhanced affinities for the template, with enhancements in free energy of binding of up to 8.8 kJ mol^{-1} observed.

5.3 Results and Discussion

5.3.1 Design and construction of PS-DCLs

In contrast to earlier examples,[1-3] these PS-DCLs have been designed to explore specific molecular recognition between two very different lectins and complementary carbohydrates (Fig. 3). Concanavalin A (Con A) is a lectin isolated from *Canavalia ensiformis* (Jack bean), which exists at neutral pH as a tetramer of four identical 26 kDa subunits,[13] each bearing a single mannose recognition site incorporating a penta-coordinated Ca^{2+} ion and a hexa-coordinated Mn^{2+} ion. These mannose-binding sites are located at the points of a tetrahedron, approximately 72 Å apart.[13] In solutions of pH <5.6, Con A tetramers dissociate to yield dimers which

may also recognise mannose through complexation at two sites. Con A serves as a useful 'model lectin' as it recognition behaviour has been well studied.[14]

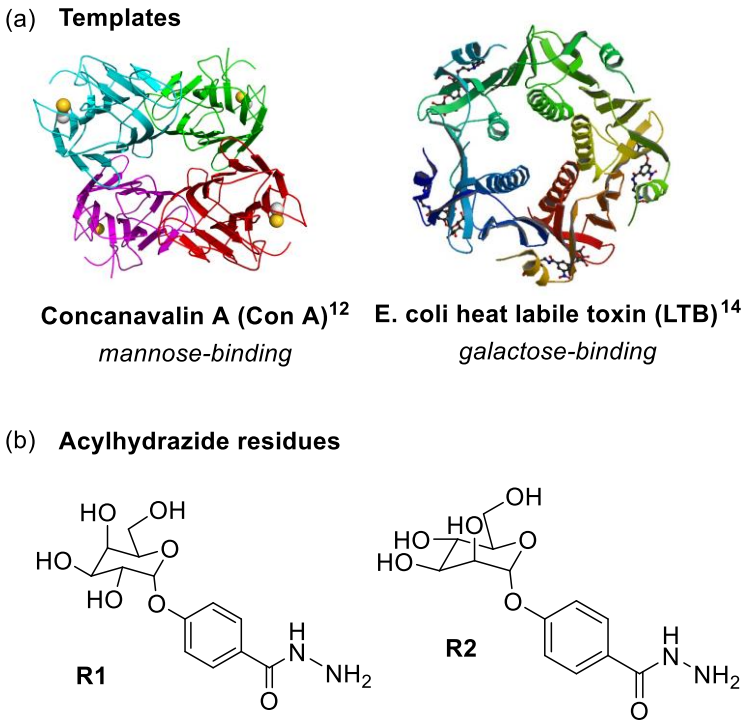

Fig 3 (a) Lectin templates used within PS-DCLs. (b) Acylhydrazide residues used to construct PS-DCLs.

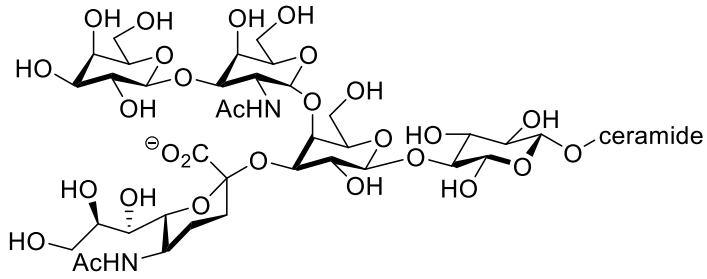

Fig. 4 Ganglioside **GM1**, a cell surface marker which binds to LTB, facilitating cell entry.

E. coli heat labile toxin (LTB)[15] belongs to the AB_5 family of toxins,[16] and exhibits recognition behaviour identical to that of cholera toxin.[17] The single A subunit is responsible for the toxicity of the protein, with the B-pentamer facilitating entry of the toxin into cells by binding to the galactose-terminated ganglioside **GM1** (Fig. 4). For the purposes of this investigation, a modified B_5 variant of the toxin, which does not contain the A subunit and is therefore non-toxic, has been used.*

Acylhydrazide residues **R1** and **R2**† display galactose and mannose units and may be expected to interact favourably with Con A and LTB, respectively. PS-DCLs incorporating **R1** and **R2** have been constructed on the aldehyde- functionalised polymer scaffold **P1** (Scheme 1). PS-DCLs generated for templation with Con A were prepared in a solution containing 2 mM $CaCl_2$, 100 mM NH_4OAc/AcOH (pH 4.5) in D_2O. PS-DCLs generated for templation with LTB were prepared in 100 mM NaCl, 100 mM NH_4OAc/AcOH (pH 4.5) in D_2O.

* Modified LTB supplied by T. McAllister and W. B. Turnbull, University of Leeds.
† Acylhydrazides **R1** and **R2** were supplied by M. Fascione, C. Sakonsinsiri and W. B. Turnbull, University of Leeds.

The residual composition of these carbohydrate-functionalised PS-DCLs may be determined indirectly using ^{1}H NMR spectroscopy. Integral analysis of resonances corresponding to the anomeric protons of **R1** and **R2** was used to determine the relative concentration of these residues in solution, allowing the relative proportion of each carbohydrate on the polymer scaffold to be determined. Equilibrium was attained overnight, with ^{1}H NMR spectroscopic analysis revealing **R1** and **R2** to be present in solution in a 1.0:1.0 ratio, implying that the residual composition of the polymer scaffolds is also 1.0:1.0. No aldehyde signal was observed, indicating that polymers are fully functionalised with carbohydrate residues. The composition of the PS-DCL was monitored over a period of 48 h, with no further deviation from this composition observed. This observation suggests that, in the absence of any template, the polymer scaffold displays no preference for the incorporation of either acylhydrazide **R1** or **R2**.

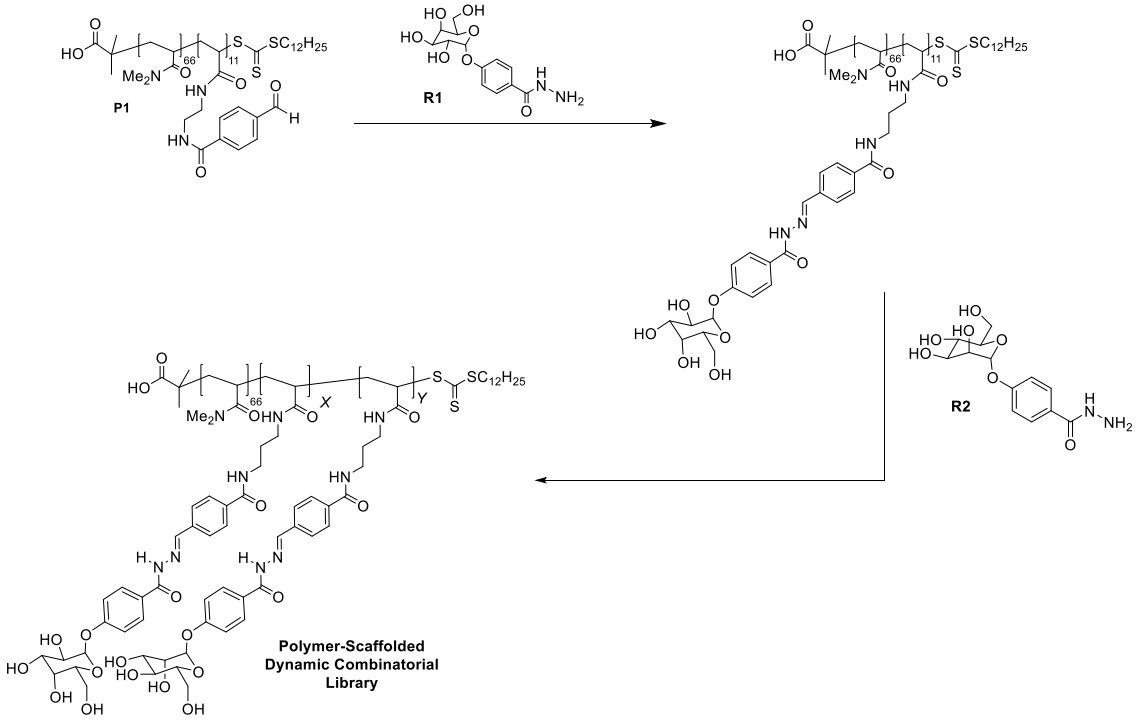

Scheme 1 Preparation of carbohydrate-functionalised PS-DCLs in 100 mM NH_4OAc/AcOH, pH 4.5, D_2O. PS-DCLs generated for templation with Con A were prepared in solutions which also contained 2 mM $CaCl_2$, while PS-DCLs generated for templation with LTB were prepared in solutions containing 100 mM NaCl.

5.3.2 Response of PS-DCLs to addition of lectin templates

Initial templating experiments were performed using Con A as a template. Upon addition of Con A, changes in the composition of the PS-DCL as a function of time were monitored using ^{1}H NMR spectroscopy, which revealed an increase in the relative concentration of **R1** compared to **R2** of 1.2:1.0 (Fig. 5). This observation

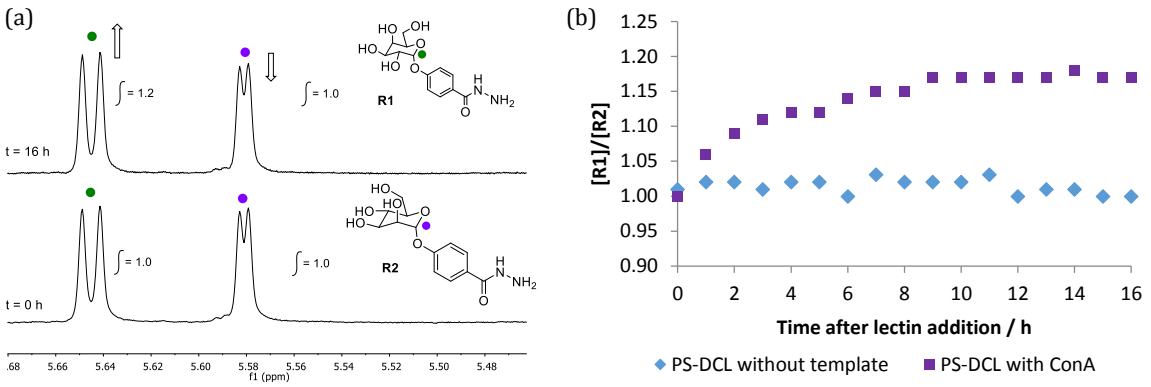

Fig. 5 (a) ^{1}H NMR spectroscopic analysis (500 MHz, D_2O, pH 4.5) of PS-DCL before (t = 0 h) and after (t = 16 h) addition of Con A, highlighting the changes in intensity of the diagnostic anomeric resonances of **R1** and **R2** 16 h after addition of template. (b) Effect of addition of Con A to a PS-DCL constructed on scaffold **P1** using acylhydrazides **R1** and **R2** as a function of time (purple squares). There was no observed change in the relative concentrations of **R1** and **R2** in the absence of template (blue diamonds).

suggests that polymer scaffolds have responded to the addition of Con A by preferentially incorporating the mannose-functionalised **R2** at the expense of the galactose-functionalised **R1**. It is proposed that this templating effect proceeds as a consequence of favourable interactions between Con A dimers and library members functionalised primarily with **R2**.

The templating effect of LTB upon the PS-DCL was also investigated. Upon addition of LTB, ^{1}H NMR spectroscopy revealed a decrease in the relative concentration of **R1** compared to **R2** of 0.8:1.0 from an initial ratio of 1.0:1.0 (Fig. 6). This observation suggests that polymer scaffolds have preferentially incorporated the galactose functionalised **R1**, rejecting the mannose-functionalised **R2**. This templating effect is likely to be a consequence of favourable interactions between LTB and polymers functionalised primarily with **R2**.

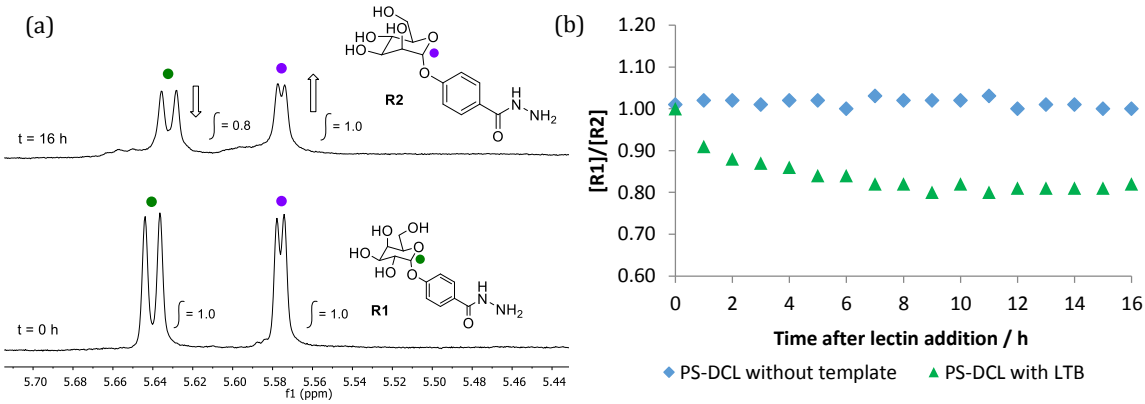

Fig. 6 (a) ^{1}H NMR spectroscopic analysis (500 MHz, D_2O, pH 4.5) of PS-DCL before (t = 0 h) and after (t = 16 h) addition of LTB, highlighting the changes in intensity of the diagnostic anomeric resonances of **R1** and **R2** 16 h after addition of template. (b) Effect of addition of LTB to a PS-DCL constructed on scaffold **P1** using acylhydrazides **R1** and **R2** as a function of time (green triangles). There was no observed change in the relative concentrations of **R1** and **R2** in the absence of template (blue diamonds).

These observations demonstrate that carbohydrate-functionalised PS-DCLs possess that same capacity for template-induced re-equilibration exhibited by other PS-DCLs,[1-3] and suggest that compositional exchange upon template addition is driven by favourable multivalent interactions between template and library members.

5.3.3 Establishing binding affinities of polymer scaffolds at various residual compositions

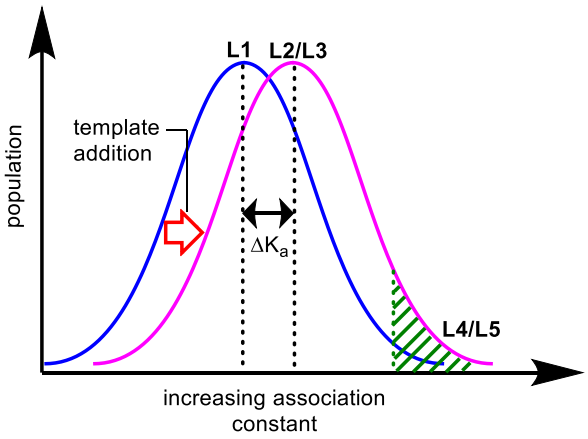

Fig. 7 'Static' libraries may be constructed at various points along proposed population distributions for templated and untemplated PS-DCLs, in order to establish relative binding affinities of polymers of such compositions.

As templation within PS-DCLs had previously been shown to occur by a thermodynamically driven process,[3] it was hypothesised that templated populations of carbohydrate-functionalised polymers would display improved binding affinities for the lectin template compared to untemplated populations. Libraries were prepared at various average compositions at different points along the proposed population distribution (Fig. 7) to establish if libraries with 'templated' compostion demonstrated higher binding affinities than libraries of 'untemplated' composition. It must be remembered, however, that these 'static' libraries have not been exposed to templates, and therefore lack any sequence-specific information acquired during the templating process. Sequence-specific information is thought to be particularly relevant to interactions between carbohydrates and lectins, as recognition occurs at multiple distinct sites, rather than across the whole surface as is likely to be the case in the electrostatically-driven recognition processes examined previously.[3]

Static libraries were constructed upon scaffold **P1** with compositions analogous to an untemplated PS-DCL (**L1**), a PS-DCL templated with Con A (**L2**) and a PS-DCL templated with LTB (**L3**). Libraries **L4** and **L5** were generated with compositions likely to reflect the strongly binding outliers of the templated populations *i.e.* functionalised only with the preferred carbohydrate. ^{1}H NMR spectroscopic analysis of **L1**-**L5** confirmed the desired residual compositions in each case. Static libraries **L1**-**L5** were reduced using $NaCNBH_3$ to prevent unwanted compositional exchange

upon exposure to templates, and purified by dialysis before titration against the relevant lectins (Table 1-2, Fig. 8(a)). Binding stoichiometries were determined by Job's method[18, 19] (Table 1-2, Fig. 8(b)) to be between 0.7:1.0 and 1.0:1.0 for each static library investigated, reflecting similar modes of binding. Titrations were performed under conditions similar to those used during templating (pH 4.5, Table 1), and also under neutral conditions (pH 7.1, Table 2), to investigate the hypothesis that static libraries would interact more favourably with Con A tetramers than Con A dimers as a consequence of increased multivalency.

Static libraries with compositions analogous to templated PS-DCLs (**L2** and **L3**) were shown to have greater binding affinities for the relevant lectin than the untemplated library (**L1**), suggesting that the compositional change induced by template addition leads to an increase in binding affinities between polymers within the library and templates.

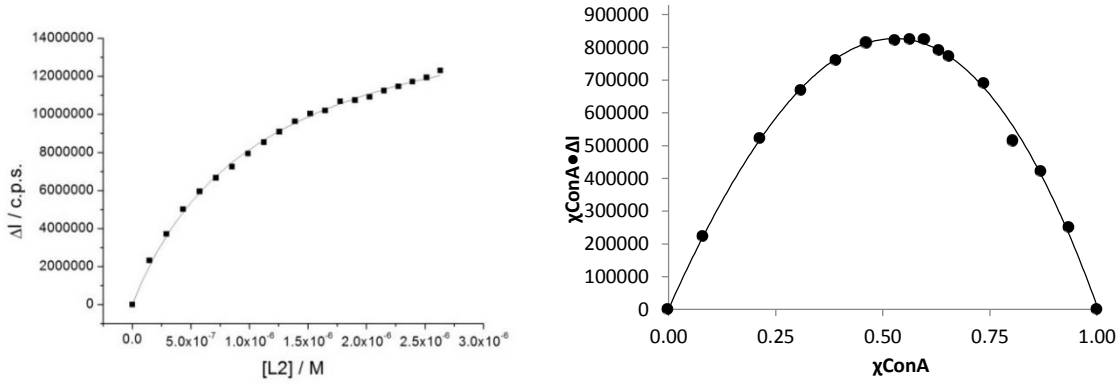

Fig. 8 (a) Sample binding isotherm obtained by titration of **L2** against Con A at pH 4.5. (b) Sample Job plot of **L2**-ConA binding at pH 4.5.

Library	Average Composition **R1**:**R2**	Template	K_a / M^{-1}	ΔG / kJ mol^{-1}	*n* (polymer: template)
L1	1.0 : 1.0	Con A	$4.45 \times 10^5 \pm 2.64 \times 10^4$	-31.7	1.0
L1	1.0 : 1.0	LTB	$1.68 \times 10^5 \pm 1.69 \times 10^4$	-29.3	1.0
L2	1.0 : 1.2	Con A	$5.32 \times 10^5 \pm 3.20 \times 10^4$	-32.1	0.8
L3	1.0 : 0.8	LTB	$6.27 \times 10^5 \pm 5.05 \times 10^4$	-35.5	1.0
L4	0 : 1.0	Con A	$5.26 \times 10^5 \pm 4.77 \times 10^4$	-32.1	1.0
L4	0 : 1.0	LTB	1.06 ± 985.8	-0.10	0.8
L5	1.0 : 0	Con A	$4.66 \pm 1.12 \times 10^4$	-9.36	0.7
L5	1.0 : 0	LTB	$2.42 \times 10^5 \pm 4.83 \times 10^3$	-30.2	0.8

Table 1 Association constants K_a and binding stoichiometries *n* of **L1**-**L5** towards Con A and LTB at pH 4.5. Con A titrations were performed in 100 mM NH_4OAc/AcOH pH 4.5, 2 mM $CaCl_2$. LTB titrations were performed in 100 mM NH_4OAc/AcOH pH 4.5, 100 mM NaCl.

Interestingly, polymers functionalised only with the preferred carbohydrate (**L4** and **L5**) do not present an improvement upon binding affinities exhibited by

polymers of templated composition (**L2** and **L3**). In the case of **L4**, which only displays mannose units, the K_a obtained upon titration against Con A is within error of that of **L2**, the polymer of templated composition. Static library **L5**, which is functionalised only with galactose units, binds to LTB with decreased affinity compared to **L2**, the static library prepared to model the composition of a PS-DCL templated with LTB.

Polymers functionalised with a single carbohydrate (**L4** and **L5**) do not display affinities towards the lectin which does not recognise the carbohydrate (**L4**-LTB, **L5**-Con A), confirming that recognition events within these systems are likely to be highly specific.‡

Binding of static libraries to Con A was investigated under neutral conditions (Table 2) to investigate the hypothesis that static libraries would interact more favourably with Con A tetramers rather than dimers, as a consequence of increased multivalency. These experiments were also conducted in the presence of Mn^{2+}, in an effort to optimise recognition. Contrary to expectation, increasing pH did not lead to a significant increase in association constants. This observation may suggest that polymers are not benefitting from increased multivalency in their interactions with Con A. It is possible that polymer scaffolds may not be long enough, or flexible enough, to simultaneously access all four binding sites of a Con A tetramer. Alternatively, the entropic penalty of rearrangement of the polymer scaffold to allow access of mannose residues to all four binding sites may outweigh the enthalpic gain of multi-site binding.

Library	Average Composition **R1**:**R2**	Template	K_a / M^{-1}	ΔG / kJ mol^{-1}	*n* (polymer: template)
L1	1.0 : 1.0	Con A	$4.12 \times 10^5 \pm 6.32 \times 10^4$	-31.5	1.0
L1	1.0 : 1.0	LTB	$1.64 \times 10^5 \pm 1.32 \times 10^4$	-29.3	0.8
L2	1.0 : 1.2	Con A	$4.77 \times 10^5 \pm 1.43 \times 10^4$	-31.9	1.0
L3	1.0 : 0.8	LTB	$1.76 \times 10^5 \pm 1.24 \times 10^4$	-29.4	1.0
L4	0 : 1.0	Con A	$6.62 \times 10^5 \pm 4.65 \times 10^4$	-32.7	1.0
L4	0 : 1.0	LTB	$0.625 \pm 4.27 \times 10^4$	1.10	1.0
L5	1.0 : 0	Con A	$0.181 \pm 5.53 \times 10^3$	4.17	0.7
L5	1.0 : 0	LTB	$2.45 \times 10^5 \pm 9.83 \times 10^3$	-30.2	0.8

Table 2 Association constants K_a and binding stoichiometries *n* of **L1**-**L5** towards Con A and LTB at pH 7.1. Con A titrations were carried out in 100 mM HEPES, pH 7.1, 1 mM $CaCl_2$, 1 mM $MnCl_2$. LTB titrations were carried out in 100 mM HEPES pH 7.1, 100 mM NaCl.

‡ Errors associated with these measurements are very large, as a consequence of very limited association between these polymers and lectins.

Binding of static libraries to LTB under neutral conditions was also investigated (Table 2). Under these conditions **L3**, the static library constructed at 'templated' composition, does not exhibit enhanced binding affinity for LTB when compared to **L1**, the 'untemplated' library analogue, with K_a values within error of one another. Static library **L5**, functionalised only with galactose residues, does exhibit a measurably enhanced affinity for LTB when compared to **L1** and **L3**. The contrast between these observations and those made at pH 4.5 suggest that the modes of interaction under the two sets of conditions may differ.

Studies of static libraries have yielded thought-provoking and somewhat unexpected results. Analysis of PS-DCLs which have been exposed to templates may provide more insightful information, particularly as sequence-specific effects may be presumed to be of significant importance in these systems.

5.3.4 Isolating the best-binding fraction of PS-DCLs

A key validation of the hypothesis that templating PS-DCLs presents a viable route to polymeric receptors for lectins is the isolation from a PS-DCL of the best-binding fraction of the library, and demonstration that these polymers exhibit significantly enhanced affinity for the lectin template.

A method was developed for the immobilisation of lectins onto solid-supports, using commercially available streptavidin-functionalised 96-well plates and biotinylated Con A or LTB.§ Functionalisation of wells with lectins produces 'templation vessels' where PS-DCLs may be placed to allow interaction with surface-immobilised templates. It was proposed that those library members which interacted most favourably with the template would become attached to the surfaces of the wells, presenting a straightforward route to their isolation from the rest of the system.

Templating experiments were performed using PS-DCLs constructed with acylhydrazides **R1** and **R2** upon polymer scaffold **P1**. PS-DCLs were shown to contain equal concentrations of **R1** and **R2** using ^{1}H NMR spectroscopy prior to templation, indicating that both carbohydrates are incorporated onto polymer scaffolds in equal proportions. After 18 h incubation at 5 °C in lectin-functionalised wells, ^{1}H NMR spectroscopic analysis revealed compositional change within both systems – a decrease in the concentration of **R2** compared to **R1** of 0.8:1.0 from an

§ Biotinyl-LTB was supplied by T. McAllister and W. B. Turnbull, University of Leeds.

initial ratio of 1.0:1.0 in Con A-functionalised wells, and a decrease in the relative concentration of **R1** compared to **R2** of 0.9:1.0 from an initial ratio of 1.0:1.0 in LTB-functionalised wells. In both cases, polymer scaffolds have preferentially incorporated the carbohydrate known to interact favourably with the lectin added. There was no significant change in the composition of PS-DCLs incubated in 96-well plates which had not been treated with biotinyl-LTB or biotinyl-Con A, eliminating the possibility that streptavidin could induce compositional change within PS-DCLs. PS-DCLs were removed from the wells, and the surfaces of the wells were washed with a denaturant solution (50 mM EDTA in D_2O in the case of ConA-functionalised wells, or 5.0 M guanidinium chloride, 0.5 M NaCl in D_2O in the case of LTB-functionalised wells) to disrupt interactions between templates and polymers bound to the surfaces of wells. These washings were shown using ^1H NMR spectroscopy to contain polymeric species which were reduced using $NaCNBH_3$ to prevent unwanted compositional change during binding studies, and purified by dialysis. Material isolated from the wells was shown by UV-Visible spectroscopy to comprise of carbohydrate-functionalised polymers and another component proposed to be a carbohydrate-functionalised polymer-lectin complex. The concentration of carbohydrate-functionalised polymers in the material isolated may be determined by absorbance (ε = 0.264 μM cm^{-1}).** These polymers (**L6**-**L7**) were then titrated against Con A or LTB (Table 3).

	Library	Residual composition **R1**:**R2**	Template	K_a / M^{-1}	ΔG / kJ mol^{-1}	ΔΔG / kJ mol^{-1}	*n*
pH 4.5	**L6**	unknown	Con A	$3.76 \times 10^6 \pm 2.26 \times 10^5$	-36.9	-5.2	1.2
	L7	unknown	LTB	$1.74 \times 10^6 \pm 6.97 \times 10^4$	-35.0	-5.7	0.8
pH 7.1	**L6**	unknown	Con A	$7.69 \times 10^6 \pm 4.63 \times 10^5$	-38.6	-7.1	0.8
	L7	unknown	LTB	$6.11 \times 10^6 \pm 9.38 \times 10^5$	-38.1	-8.8	1.0

Table 3 Association constants K_a and binding stoichiometries *n* for interactions between polymers from libraries **L6**-**L7** and lectins, as determined by fluorescence titration and Job analysis. ΔΔG values are calculated against ΔG for **L1** binding to the appropriate lectin. Con A titrations were performed in 100 mM NH_4OAc/AcOH, pH 4.5, 2mM $CaCl_2$ or 100 mM HEPES, pH 7.1, 1 mM $CaCl_2$, 1 mM $MnCl_2$. LTB titrations were performed in 100 mM NH_4OAc/AcOH, pH 4.5, 100 mM NaCl or 100 mM HEPES, pH 7.1, 100 mM NaCl.

Polymers isolated from the surfaces of wells have been shown to display significantly enhanced affinities for the relevant lectin, with an order of magnitude enhancement in binding affinities observed compared to the untemplated library **L1** (Tables 1 and 2) with enhancements in free energy of binding of 5.2 – 8.8 kJ mol^{-1} observed. The best binding fractions **L6** and **L7** display significantly improved

** See Experimental Details for Beer-Lambert analysis of glycopolymers.

recognition characteristics compared to polymers of 'templated' compositions **L2** and **L3** and polymers functionalised only with the preferred carbohydrate **L4** and **L5**. This observation suggests that sequence-specific effects are of prime importance in these systems, and that key residues must occupy specific positions upon polymer scaffolds in order to achieve significant enhancements in binding affinities.

These observations demonstrate that templating PS-DCLs may deliver polymers of markedly improved affinity to lectins and validates the concept as a route to the generation of macromolecular receptors for these species.

5.4 Conclusions

Carbohydrate-functionalised PS-DCLs have been prepared by the reversible conjugation of mannose- and galactose-functionalised acylhydrazide residues onto an aldehyde-functionalised polymer scaffold. Library members within these PS-DCLs may interconvert through acylhydrazone exchange as expected, and the residual composition of polymer scaffolds may be monitored indirectly using ^{1}H NMR spectroscopy.

Carbohydrate-functionalised PS-DCLs have been shown to adapt their composition in response to the addition of lectin templates, with polymer scaffolds preferentially incorporating the carbohydrate known to interact favourably with the lectin added. Experiments suggest that recognition processes between lectins and carbohydrate-functionalised polymers are highly specific, with carbohydrate residues interacting at key sites on the lectin.

Compositional change within PS-DCLs has been shown to deliver polymers of enhanced affinities for lectin templates. The immobilisation of lectins on 96-well plates to produce 'templation vessels' has enabled the isolation of the best-binding fraction of the PS-DCL, separating those polymers of highest affinities towards the template from the rest of the system. These polymers have been shown to display significantly enhanced affinities for the lectin added, with enhancements in free energy of binding of 5.2 – 8.8 kJ mol^{-1} observed. The development of a method to immobilise protein templates onto solid supports using commercially available materials will allow for the rapid expansion of the concept to provide polymeric receptors for a wide range of bacterial toxins and other proteins of interest. The use of 96-well plates for the immobilisation of templates will allow for the application

of high-throughput techniques for the discovery of macromolecular receptors using PS-DCLs. The best-binding fractions of PS-DCLs could be conveniently separated from the bulk of the library to undergo a second exposure to template in the presence of additional acylhydrazides, with the possibility of further enhancing the affinities of these polymers to the template.

These results demonstrate the validity of the PS-DCL concept as a route to the development of receptors for lectins. Polymers of enhanced affinities to Con A, a mannose-binding lectin, and LTB, a galactose-binding member of the AB_5 family of bacterial toxins, have been produced by templation of a PS-DCL constructed using two simple carbohydrate derivatives and a synthetic polymer scaffold. Incorporating more complex carbohydrate-recognition motifs, e.g. derivatives of ganglioside **GM1** (Fig. 4), may lead to polymeric receptors of even greater affinities towards AB_5 toxins.

5.5 Experimental Details

All chemicals were purchased from Sigma-Aldrich or Alfa Aesar and were used as received without further purification. Carbohydrate-functionalised acylhydrazides **R1** and **R2** were synthesised by Martin A. Fascione, Chadamas Sakonsinsiri and W. Bruce Turnbull, University of Leeds. LTB and biotinyl-LTB were supplied by Tom Mc Allister and W. Bruce Turnbull, University of Leeds. *N,N*-Dimethylacrylamide was purified by vacuum distillation at 60 ˚C. ^{1}H and ^{13}C NMR spectra of synthesised compounds were recorded on a Bruker Avance 300 spectrometer at 300 MHz and 75 MHz respectively, or on a JEOL ECS-400 spectrometer at 400 MHz and 100 MHz, with the residual solvent signal as an internal standard. High-resolution mass spectrometry was performed on a Waters LCT premier mass spectrometer (Waters Inc.). Gel permeation chromatography (GPC) was conducted on a Varian ProStar instrument (Varian Inc.) equipped with a Varian 325 UV-Vis dual wavelength detector (254 nm), a Dawn Heleos II multi-angle laser light scattering detector (Wyatt Technology Corp.), a Viscotek 3580 differential RI detector, and a pair of PL gel 5 μm Mixed D 300 × 7.5 mm columns with guard column (Polymer Laboratories Inc.) in series. Near monodisperse methyl methacrylate standards (Agilent Technologies) were used for calibration. Data collection was performed with Galaxie software (Varian Inc.) and chromatograms analyzed with Cirrus software (Varian Inc.) and Astra software (Wyatt Technology Corp.). Fluorescence spectroscopy was

carried out on a Fluoromax instrument, with corrected spectra used for all analysis. UV-Visible spectroscopy was performed on a Cary 100 Bio UV-Vis spectrophotometer.

^{1}H NMR spectra of PS-DCLs were measured using a JEOL Lambda spectrometer (^{1}H at 500 MHz) or on a JEOL ECS-400 spectrometer (^{1}H at 400 MHz), and analysed using MestreNova software. PS-DCLs were prepared so as to contain 12.5 mM concentrations of acylhydrazides **R1** and **R2,** with **P1** present at a concentration of 1.85 mM. Equilibration to a 1.0:1.0 ratio of **R1** to **R2** in solution was confirmed by ^{1}H NMR spectroscopic analysis prior to addition of templates. Con A and LTB were added to PS-DCLs at concentrations of 5.0 mg mL^{-1}.

Aldehyde-Functionalized Polymer Scaffold (**P1**)

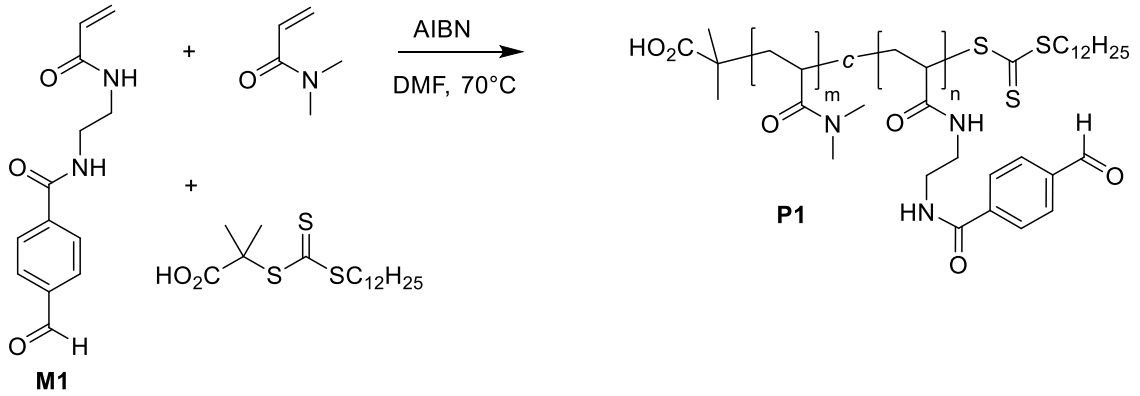

Scheme 2 Synthesis of aldehyde-functionalised copolymer **P1**.

S-1-Dodecyl-*S'*-(α,α-dimethyl-α''-acetic acid)trithiocarbonate[20] (DDMAT) (1 eq, 25.0 mg, 0.069 mmol) and AIBN (0.2 eq, 2.3 mg, 14 μmol) were added to a small schlenk tube. *N,N*-Dimethylacrylamide (DMA) (80 eq, 0.545 g, 5.50 mmol) and *N*-ethylacrylamide-2-(4-formylbenzamide) (**M1**) (20 eq, 0.363 g, 1.37 mmol) were then added followed by DMF (3 mL). The reaction mixture was degassed through five freeze-pump-thaw cycles before the vessel was backfilled with N_2, purged with N_2, and allowed to warm to room temperature. The reaction mixture was then placed in an oil bath at 70 ˚C, and the polymerisation was quenched after 22 h. The reaction mixture was dissolved in a minimal amount of THF-acetone and added dropwise to a large excess of ice-cold diethyl ether. The polymer was then isolated by filtration and the precipitation was repeated before drying under high vacuum. Polymer **P1** was obtained as a pale yellow solid. ^{1}H NMR (300 MHz, $CDCl_3$): 1.4 – 1.8 (br, CHC*H*$_2$, polymer backbone), 2.2 – 2.7 (br, C*H*CH$_2$, polymer backbone), 2.88 (br, N(C*H*$_3$)$_2$), 3.4 – 3.6 (br, (C*H*$_2$)$_2$), 7.88 (br, Ar), 8.07 (br, Ar), 8.59 (br, N*H*), 10.04 (br,

Ar). The composition of **P1** can be determined by comparing the integration of the aldehyde protons of **M1** with the integration of the N(CH_3)$_2$ protons of DMA. The monomer compositions were not determined to identical to the feed ratio of DMA:**M1**, most likely as a consequence of the difference in reactivity of the two monomers.

Polymer	**DDMAT** / eq.	**AIBN** / eq.	**DMA** / eq.	**M1** / eq.	n[a]	m[a]	n : m[a]	M_n[a] / g mol^{-1}	M_n[b] / g mol^{-1}	M_w[b] / g mol^{-1}	PDI[b] (M_w/M_n)
P1	1	0.2	80	20	11	66	1:6	9,800	23,600	29,600	1.25

Table 4 Characterisation of polymer scaffold **P1**. [a] As determined by ^{1}H NMR spectroscopy [b] As determined by gel permeation chromatography in DMF + 1 g L^{-1} LiBr (0.6 mL/ min) calibrated against near monodisperse poly(methyl methacrylate) standards. AIBN: azobis(isobutyronitrile), DMA: *N*,*N*-dimethylacrylamide, DDMAT: *S*-1-dodecyl-*S'*-(α,α-dimethyl-α''-acetic acid)trithiocarbonate.

General Procedure for Preparation of 'Static' Libraries **L1**-**L5**

L1-**L5** were prepared so as to contain 12.5 mM concentrations of acylhydrazides **R1** and **R2**, with polymer **P1** present at a concentration of 1.85 mM.

Polymer **P1** was combined with galactosyl derivative **R1** in 0.1 M NH_4OAc/AcOH deuterated buffer (pH 4.5, 0.5 mL) and sonicated until a clear solution was obtained. Mannosyl derivative **R2** was added to the reaction mixture, which was left overnight to equilibrate. Equilibration to the required ratio of **R1** and **R2** was confirmed by ^{1}H NMR spectroscopic analysis prior to reduction. $NaCNBH_3$ (10 eq. per aldehyde functionality) was added to the solution and the reaction mixture was left overnight at room temperature. Reduction was confirmed by ^{1}H NMR spectroscopic analysis prior to dialysis against H_2O and lyophilisation to yield static libraries **L1**-**L5**.

General Procedure for Lectin Functionalisation of 96-well plates

Wells were washed with D_2O (200 μL) before treatment with solution of biotinylated lectin (3.0 mg biotinyl-Con A/3000 μL D_2O, 0.25 mg biotinyl-LTB/3000 μL 100 mM NaCl, D_2O) (100 μL). Plates were incubated at 5 °C for 16 h before lectin solutions were removed and wells were washed with 100 mM NH_4OAc/AcOH deuterated buffer pH 4.5 before addition of PS-DCLs.

General Procedure for Isolation of Library Members from Lectin-functionalised Wells

The bulk of the PS-DCL was pipetted from the wells, and the surfaces of the wells were incubated for 1 h with a denaturant solution (50 mM EDTA in D_2O in the case of Con A, and 5.0 M guanidinium chloride, 0.5 M NaCl in D_2O in the case of LTB) (100 μL per well). ^{1}H NMR spectroscopic analysis revealed both sets of washings to

contain polymeric species which were purified by dialysis then lyophilised to yield **L6**-**L7**. Concentration of glycopolymers in material isolated from the wells was determined based on the absorbance of glycopolymers at 310 nm.

*Beer-Lambert Analysis of **L1***

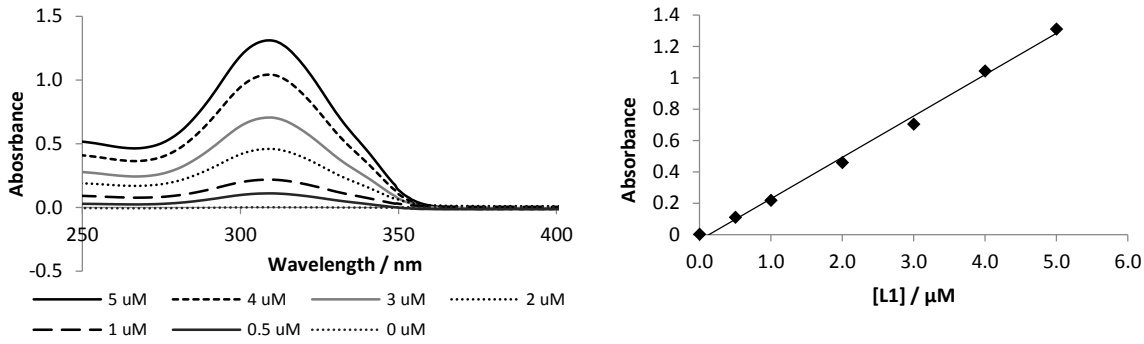

Fig. 9 (a) UV-Visible spectra of solutions of **L1** in the range 0 µM to 5.00 µM. (b) Beer-Lambert plot for **L1**.

Solutions of **L1** of known concentrations between 0 µM and 5.00 µM were prepared and their absorbance at 310 nm was determined (Fig. 9), allowing the molar extinction coefficient ε_{310} to be determined to be 0.264 $\mu M^{-1}\,cm^{-1}$.

General Procedure for Fluorescence Titrations

Solutions of Con A and LTB were prepared at 0.5 µM concentrations. Solutions of **L1**-**L7** were prepared by dissolving **L1**-**L7** in the appropriate lectin solution to ensure a constant concentration of lectin throughout the titration. The lectin solution (400 µL) was placed in a cuvette and the appropriate solution of **L1**-**L7** was added in small aliquots (5.0 µL). The samples were excited at a wavelength of 280 nm and the change in emission intensity at 340 nm was recorded. Control experiments were performed where solutions of **L1**-**L7** were titrated into a solution of the buffer in the absence of lectin. The change in intensity of fluorescence of the solution as a consequence of polymer addition was monitored, and these values were subtracted from those obtained during titrations of **L1**-**L7** with lectins. Titration curves may be found in Appendix C.

Binding stoichiometries (n) were determined by Job Plot analysis. Dissociation constants were calculated using non-linear regression methods, with data fitted to a modified Hill equation $y = V_{\max}\frac{x^n}{{K_d}^n + x^n}$. The binding stoichiometry n was obtained from the relevant Job Plot. This analysis yielded values of n between 0.8 and 1.2 for each set of polymers investigated. While the apparent binding stoichiometries of **L1**-

L7 with templates may not be identical, we believe that they are sufficiently similar, reflecting comparable modes of binding and thus allow for direct comparison of K_a values.

5.6 References

1. C. S. Mahon, A. W. Jackson, B. S. Murray and D. A. Fulton, *Chem. Commun.*, 2011, **47**, 7209-7211.
2. C. S. Mahon, A. W. Jackson, B. S. Murray and D. A. Fulton, *Polym. Chem.*, 2013, **4**, 368-377.
3. C. S. Mahon and D. A. Fulton, *Chem. Sci.*, 2013, **4**, 3661-3666.
4. M. Mammen, S.-K. Choi and G. M. Whitesides, *Angew. Chem., Int. Ed.*, 1998, **37**, 2754-2794.
5. A. Imberty and A. Varrot, *Curr. Opin. Struct. Biol.*, 2008, **18**, 567-576.
6. A. Imberty, Y. M. Chabre and R. Roy, *Chem. Eur. J.*, 2008, **14**, 7490-7499.
7. A. Bernardi, J. Jimenez-Barbero, A. Casnati, C. De Castro, T. Darbre, F. Fieschi, J. Finne, H. Funken, K.-E. Jaeger, M. Lahmann, T. K. Lindhorst, M. Marradi, P. Messner, A. Molinaro, P. V. Murphy, C. Nativi, S. Oscarson, S. Penades, F. Peri, R. J. Pieters, O. Renaudet, J.-L. Reymond, B. Richichi, J. Rojo, F. Sansone, C. Schaffer, W. B. Turnbull, T. Velasco-Torrijos, S. Vidal, S. Vincent, T. Wennekes, H. Zuilhof and A. Imberty, *Chem. Soc. Rev.*, 2013, **42**, 4709-4727.
8. C. J. O'Neal, M. G. Jobling, R. K. Holmes and W. G. J. Hol, *Science*, 2005, **309**, 1093-1096.
9. R. D. Astronomo and D. R. Burton, *Nat. Rev. Drug. Discov.*, 2010, **9**, 308-324.
10. J. D. Badjić, A. Nelson, S. J. Cantrill, W. B. Turnbull and J. F. Stoddart, *Acc. Chem. Res.*, 2005, **38**, 723-732.
11. U. Boas and P. M. H. Heegaard, *Chem. Soc. Rev.*, 2004, **33**, 43-63.
12. G. Moad, E. Rizzardo and S. H. Thang, *Aust. J. Chem.*, 2005, **58**, 379-410.
13. K. D. Hardman and C. F. Ainsworth, *Biochemistry*, 1972, **11**, 4910-4919.
14. V. Wittmann and R. J. Pieters, *Chem. Soc. Rev.*, 2013, **42**, 4492-4503.
15. E. A. Merritt, T. K. Sixma, K. H. Kalk, B. A. M. van Zanten and W. G. J. Hol, *Mol. Microbiol.*, 1994, **13**, 745-753.
16. E. A. Merritt and W. G. J. Hol, *Curr. Opin. Struct. Biol.*, 1995, **5**, 165-171.
17. T. R. Branson and W. B. Turnbull, *Chem. Soc. Rev.*, 2013, **42**, 4613-4622.
18. P. Job, *Ann. Chim.*, 1928, **9**, 113-203.
19. J. S. Renny, L. L. Tomasevich, E. H. Tallmadge and D. B. Collum, *Angew. Chem. Int. Ed.*, 2013, **52**, 11998-12013.
20. J. T. Lai, D. Filla and R. Shea, *Macromolecules*, 2002, **35**, 6754-6756.

Outlook

This outlook is adapted from the following article:

Clare S. Mahon and David A. Fulton, Mimicking Nature with Synthetic Macromolecules Capable of Recognition. *Nature Chem*., 2014, **6**, 665-672

This thesis has served to highlight the potential of Polymer-Scaffolded Dynamic Combinatorial Libraries (PS-DCLs) as a new route to the discovery of macromolecular receptors for synthetic polymers, toxins and other biologically important macromolecules. Significant progress has been made towards the realisation of the concept as a route towards the 'artificial antibody.' PS-DCLs have been shown to undergo compositional change[1, 2] in response to the addition of templates, preferentially incorporating residues which interact favourably with the template and rejecting those which do not. The templating process is driven by an increase in the total sum of affinities of all library members towards the template, and the thermodynamic control of the system is demonstrated by the return of PS-DCLs to their initial compositions upon removal of template.[3] Such dynamic behaviour offers scope for 'error-correction' within library members, a factor likely to improve the specificity and uniformity of binding sites within the receptors produced.

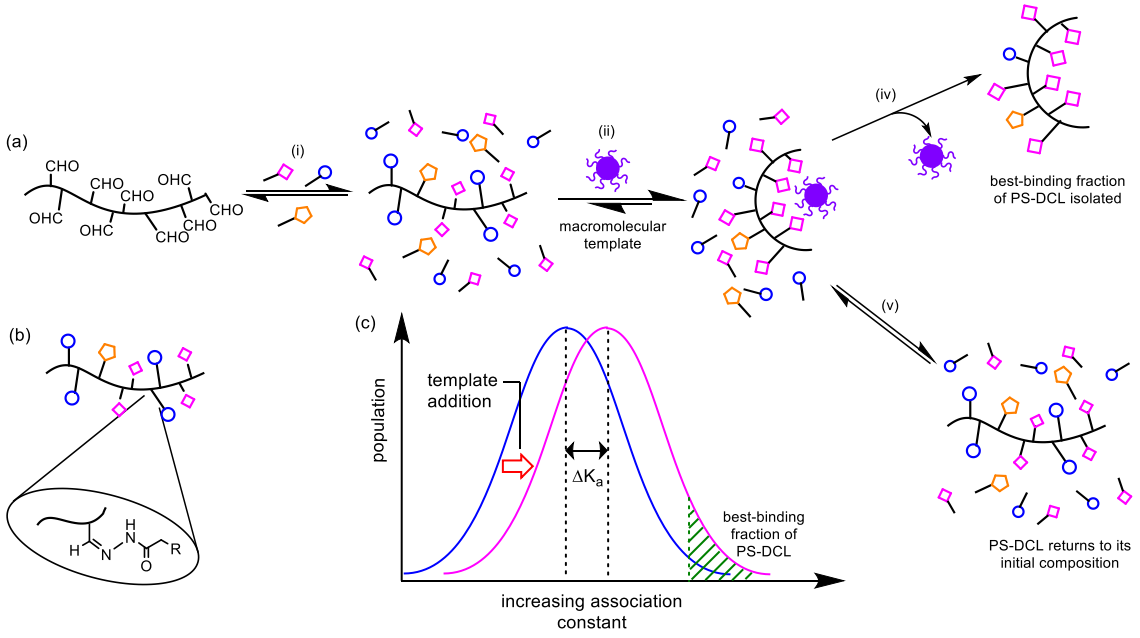

Fig. 1 Polymer-scaffolded dynamic combinatorial libraries (PS-DCLs) present a new route to the generation of macromolecular receptors. (a) The reversible conjugation of acylhydrazide residues onto a polymer scaffold, (i), generates a mixture of interconverting polymers – a PS-DCL. Addition of a macromolecular template, which may interact favourably with some library members, may induce a compositional shift (ii) so as to produce a population of polymers of enhanced binding affinities towards the template. The best-binding fraction of the population may be isolated from the rest of the system, (iv), through use of a solid-supported template. Removal of the template induces further compositional shift, (v), so as to return the system to its original, untemplated composition, demonstrating the dynamic nature of the templating process. (b) The dynamic nature of the acylhydrazone linkage allows for component exchange on polymer scaffolds, endowing the system with responsive behaviour. (c) The PS-DCL may be thought of as a population of polymers of varying affinities to a particular template. Addition of the template is proposed to shift the distribution towards increased binding affinities, with a significant proportion of the population displaying greatly enhanced binding affinities.

This proof-of-principle work has been performed with relatively simple PS-DCLs consisting of an aldehyde-functionalised polymer scaffold and just two acylhydrazide residues. Increasing the number of residues used for construction of PS-DCLs is anticipated to offer increased scope for the generation of better-binding polymeric receptors. Nature has assembled its collection of polymeric receptors using a palette of twenty amino acids and, whilst it may not be necessary to develop PS-DCLs of such complexity, one is encouraged to imagine that increasing diversity within PS-DCLs will enhance the recognition capabilities of the resultant polymeric receptors.

Most of the work detailed in this thesis has focussed on harnessing electrostatic interactions between library members and charged macromolecular templates.[1-3] The scope of the endeavour has since been expanded to exploit more specific interactions between carbohydrates and proteins, with notably larger enhancements in binding affinities observed for these systems (Chapter 5). Further development of the PS-DCL approach, such as the incorporation of more complex carbohydrates or the development of more 'amino acid-like' residues is anticipated to lead to further enhancements in binding affinities within library members.

The ultimate limitation of the DCL route to the generation of receptors lies (ironically!) within the thermodynamic nature of the templating process. The DCL is best thought of as a population of different species which vary in their affinities towards the template. Compositional exchange may shift this entire distribution to a measurable degree,[4] but the species of greatest interest to the chemist searching for receptors are the outliers in this population, which inevitably make up a small proportion of the library. The use of solid-supported templates for PS-DCLs has enabled the isolation of this best-binding fraction of the library, and whilst a relatively small proportion (~10% by mass) of the population is isolated, the dynamic nature of these systems should allow for the 'recycling' of the lower affinity fraction of the population, by exposing these polymers to the template once again the presence of more acylhydrazide residues.

The ideal route to the generation of synthetic macromolecular receptors would provide the scope for error-correction and refinement of binding sites afforded by a thermodynamically-controlled templating process, but somehow operate away from equilibrium so as to generate increased quantities of the favoured compounds.

This idea presents a considerable challenge, as thermodynamically controlled systems by their very nature respond to stimuli in order to minimise the energy of the entire system, rather than its individual components. Theoretical work[5-7] on DCLs has demonstrated that the best-binding species are not necessarily those that are amplified to the greatest extent upon exposure of the system to template, as a consequence of the complexity of the systems and factors such as competition for constituent units. Were these favoured species to display 'intelligent' behaviours such as the ability to self-replicate or catalyse their own formation,[8-11] "beating the Boltzmann distribution,"[12] as is required may well be possible. This considerable task may present one of the greatest challenges to our discipline of the twenty-first century.

References

1. C. S. Mahon, A. W. Jackson, B. S. Murray and D. A. Fulton, *Chem. Commun.*, 2011, **47**, 7209-7211.
2. C. S. Mahon, A. W. Jackson, B. S. Murray and D. A. Fulton, *Polym. Chem.*, 2013, **4**, 368-377.
3. C. S. Mahon and D. A. Fulton, *Chem. Sci.*, 2013, **4**, 3661-3666.
4. J. S. Moore and N. W. Zimmerman, *Org. Lett.*, 2000, **2**, 915-918.
5. P. T. Corbett, S. Otto and J. K. M. Sanders, *Org. Lett.*, 2004, **6**, 1825-1827.
6. P. T. Corbett, S. Otto and J. K. M. Sanders, *Chem. Eur. J.*, 2004, **10**, 3139-3143.
7. P. T. Corbett, J. K. M. Sanders and S. Otto, *J. Am. Chem. Soc.*, 2005, **127**, 9390-9392.
8. J. M. A. Carnall, C. A. Waudby, A. M. Belenguer, M. C. A. Stuart, J. J. P. Peyralans and S. Otto, *Science*, 2010, **327**, 1502-1506.
9. S. Xu and N. Giuseppone, *J. Am. Chem. Soc.*, 2008, **130**, 1826-1827.
10. R. Nguyen, L. Allouche, E. Buhler and N. Giuseppone, *Angew. Chem. Int. Ed.*, 2009, **48**, 1093-1096.
11. J. W. Sadownik and D. Philp, *Angew. Chem. Int. Ed.*, 2008, **47**, 9965-9970.
12. J. N. H. Reek and S. Otto, *Dynamic Combinatorial Chemistry*, Wiley-VCH, 2010.

Appendix A

^{1}H NMR analysis of PS-DCLs constructed on scaffolds **P1**-**P9**

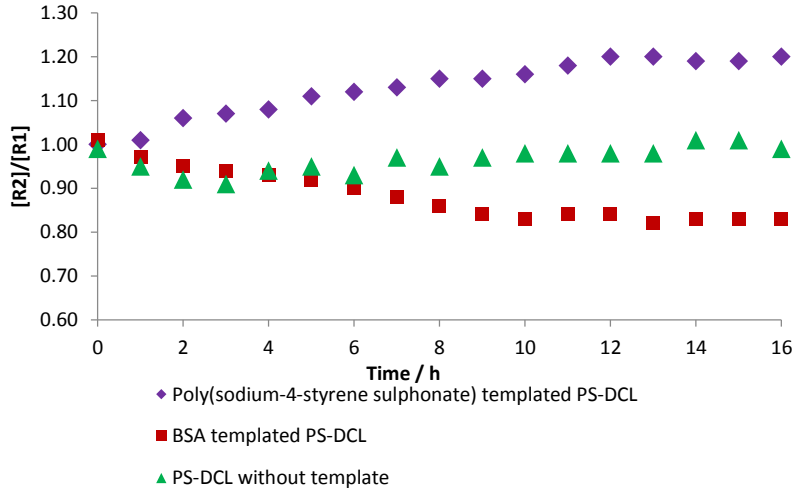

Fig. 1 ^{1}H NMR spectroscopic analysis of PS-DCLs constructed upon scaffold **P1**.

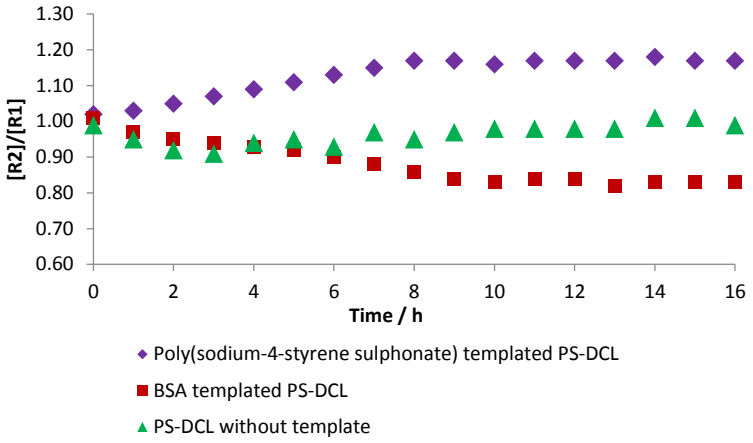

Fig. 2 ^{1}H NMR spectroscopic analysis of PS-DCLs constructed upon scaffold **P2**.

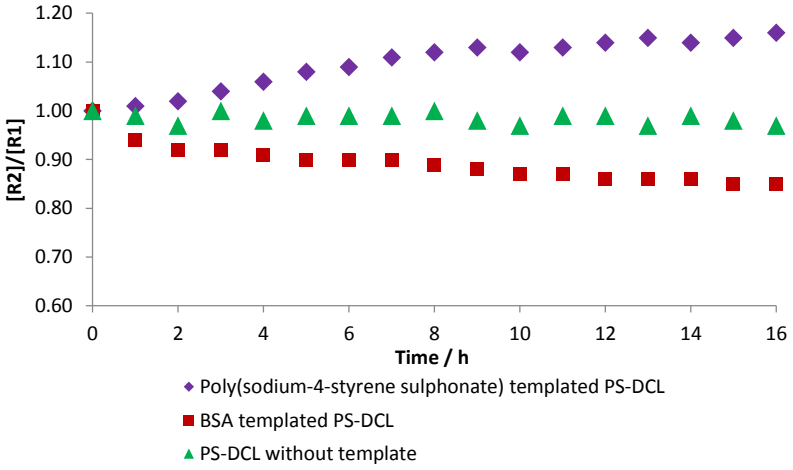

Fig. 3 ^{1}H NMR spectroscopic analysis of PS-DCLs constructed upon scaffold **P3**.

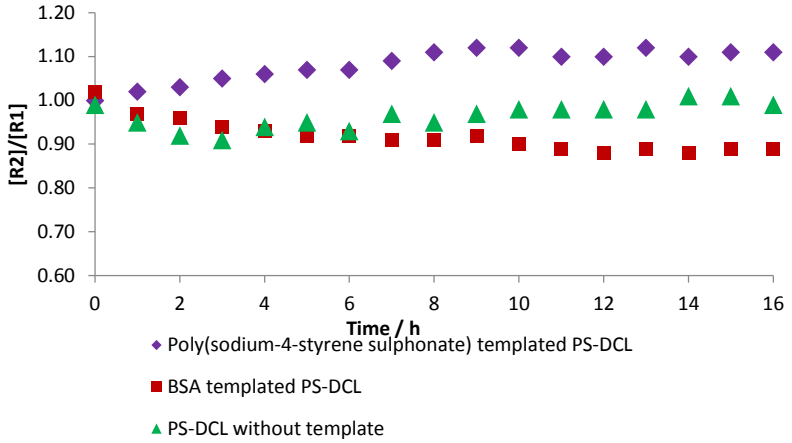

Fig. 4 ^{1}H NMR spectroscopic analysis of PS-DCLs constructed upon scaffold **P4**.

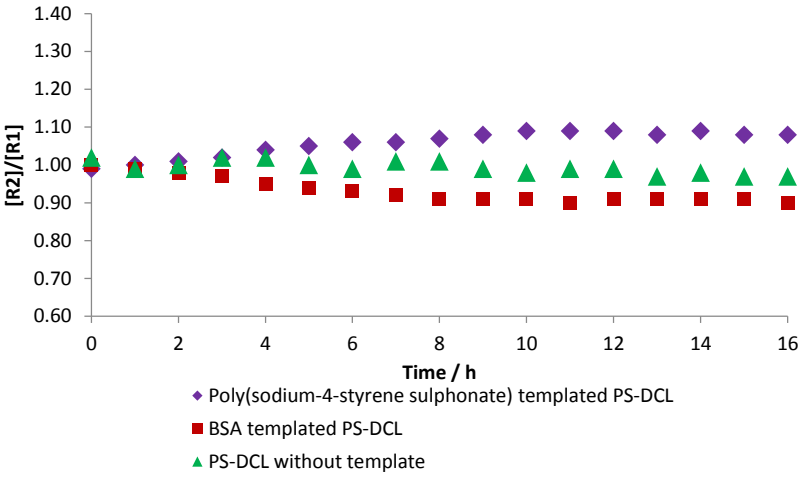

Fig. 5 ^{1}H NMR spectroscopic analysis of PS-DCLs constructed upon scaffold **P5**.

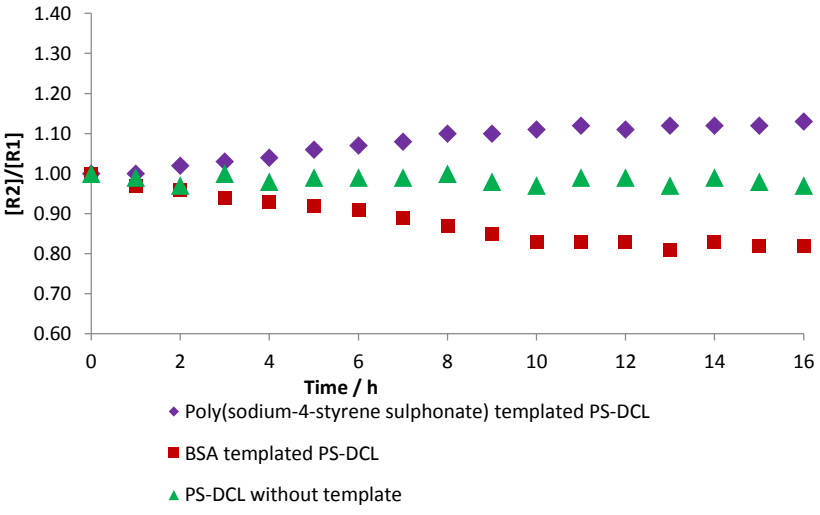

Fig. 6 ^{1}H NMR spectroscopic analysis of PS-DCLs constructed upon scaffold **P6**.

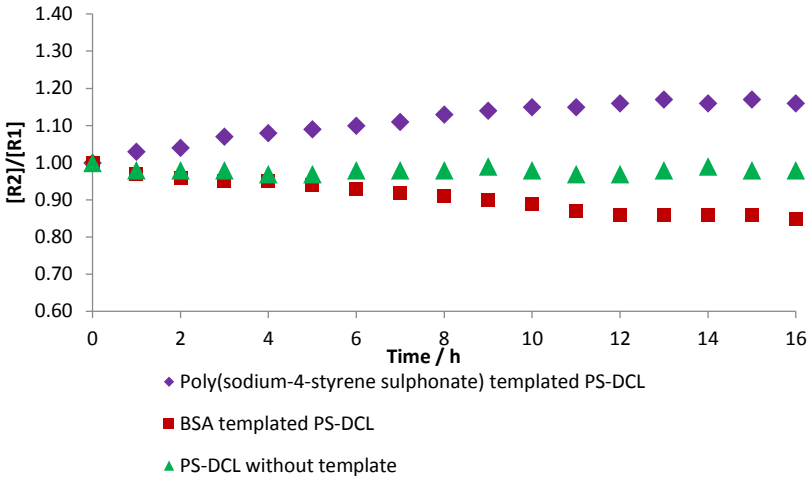

Fig. 7 ^{1}H NMR spectroscopic analysis of PS-DCLs constructed upon scaffold **P7**.

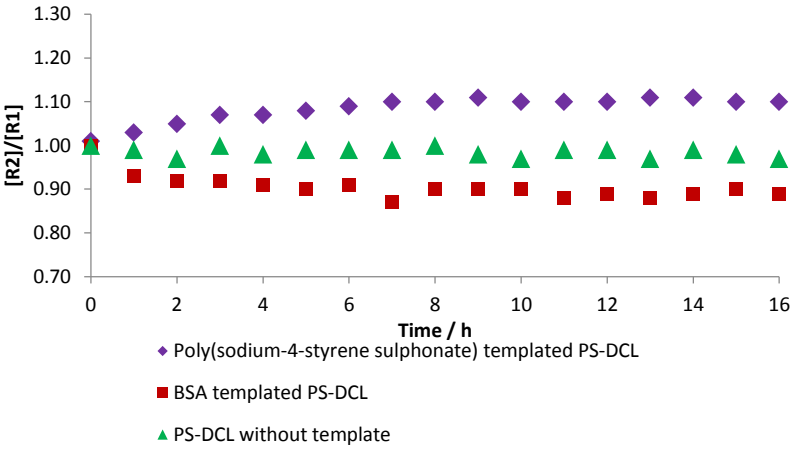

Fig. 8 ^{1}H NMR spectroscopic analysis of PS-DCLs constructed upon scaffold **P8**.

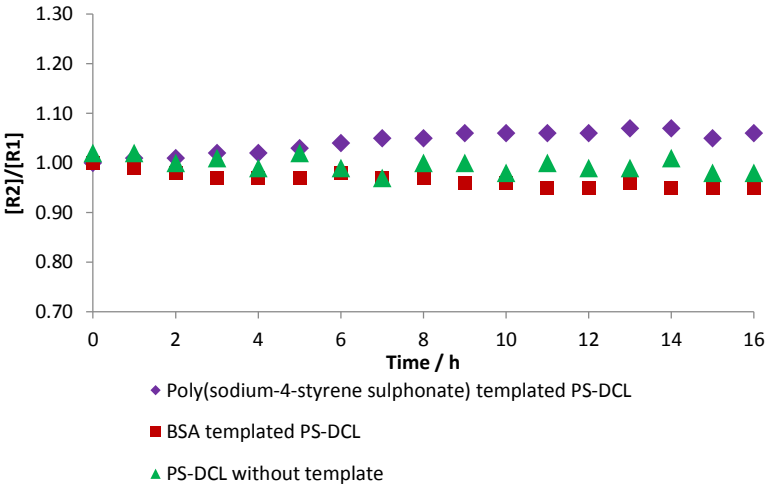

Fig. 9 ^{1}H NMR spectroscopic analysis of PS-DCLs constructed upon scaffold **P9**.

Appendix B

Binding Curves

Static library **L1** vs. poly(sodium-4-styrene sulphonate) (c.p.s.: counts per second).

[L1] / M	[poly(sodium-4-styrene sulphonate)] / M	[poly(sodium-4-styrene sulphonate)]/[L1]	Fluorescence Intensity / c.p.s.	ΔI / c.p.s.
2.00×10^{-6}	0	0.00	3537807	0
2.00×10^{-6}	2.93×10^{-7}	0.15	3642466	104659
2.00×10^{-6}	5.85×10^{-7}	0.29	3870747	332940
2.00×10^{-6}	8.75×10^{-7}	0.44	4008804	470997
2.00×10^{-6}	1.16×10^{-7}	0.58	4164744	626937
2.00×10^{-6}	1.45×10^{-6}	0.72	4257654	719847
2.00×10^{-6}	2.02×10^{-6}	1.01	4347440	809633
2.00×10^{-6}	2.58×10^{-6}	1.29	4442812	905005
2.00×10^{-6}	3.13×10^{-6}	1.57	4514359	976552
2.00×10^{-6}	3.68×10^{-6}	1.84	4570488	1032681
2.00×10^{-6}	4.23×10^{-6}	2.11	4574282	1036475
2.00×10^{-6}	4.76×10^{-6}	2.38	4631430	1093623
2.00×10^{-6}	5.29×10^{-6}	2.65	4598718	1060911
2.00×10^{-6}	5.82×10^{-6}	2.91	4620836	1083029
2.00×10^{-6}	6.34×10^{-6}	3.17	4564236	1026429
2.00×10^{-6}	6.85×10^{-6}	3.42	4616555	1078748
2.00×10^{-6}	7.36×10^{-6}	3.68	4618193	1080386

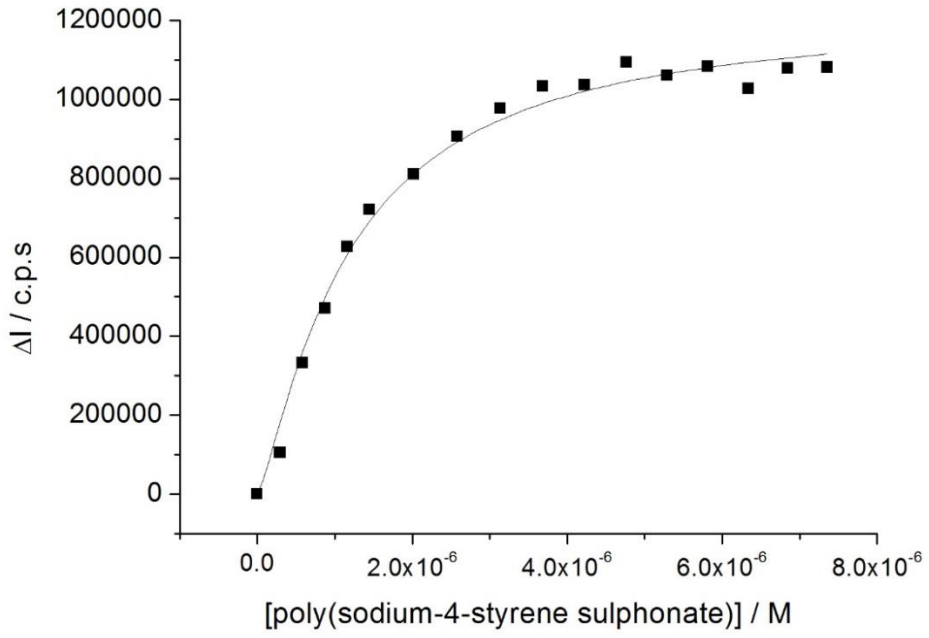

$K_a = 7.04 \times 10^5 \pm 9.88 \times 10^4$ M^{-1}

$n = 1.0$

Static library **L2** vs. poly(sodium-4-styrene sulphonate) (c.p.s.: counts per second).

[L2] / M	[poly(sodium-4-styrene sulphonate)] / M	[poly(sodium-4-styrene sulphonate)]/[L2]	Fluorescence Intensity (I) / c.p.s.	ΔI / c.p.s.
2.00×10^{-6}	0	0.00	1540071	0
2.00×10^{-6}	2.93×10^{-7}	0.15	1639455	99384
2.00×10^{-6}	5.85×10^{-7}	0.29	1773927	233856
2.00×10^{-6}	8.75×10^{-7}	0.44	1870753	330682
2.00×10^{-6}	1.16×10^{-6}	0.58	1913888	373817
2.00×10^{-6}	1.45×10^{-6}	0.72	1963324	423253
2.00×10^{-6}	2.02×10^{-6}	1.01	2050334	510263
2.00×10^{-6}	2.58×10^{-6}	1.29	2073104	533033
2.00×10^{-6}	3.13×10^{-6}	1.57	2133966	593895
2.00×10^{-6}	3.68×10^{-6}	1.84	2159198	619127
2.00×10^{-6}	4.23×10^{-6}	2.11	2146625	606554
2.00×10^{-6}	4.76×10^{-6}	2.38	2168327	628256
2.00×10^{-6}	5.29×10^{-6}	2.65	2182379	642308
2.00×10^{-6}	5.82×10^{-6}	2.91	2157766	617695
2.00×10^{-6}	6.34×10^{-6}	3.17	2116117	576046
2.00×10^{-6}	6.85×10^{-6}	3.42	2172727	632656

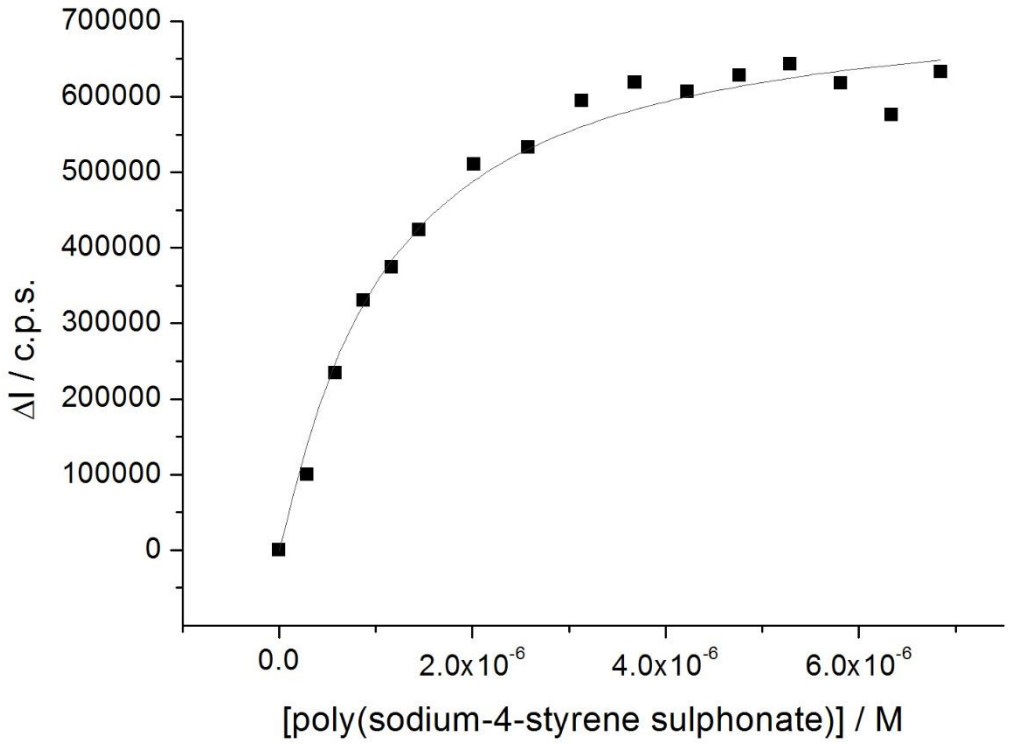

$K_a = 9.35 \times 10^5 \pm 9.0 \times 10^4$ M^{-1}

$n = 1.1$

Static library **L4** vs. poly(sodium-4-styrene sulphonate) (c.p.s.: counts per second).

[L4] / M	[poly(sodium-4-styrene sulphonate)] / M	[poly(sodium-4-styrene sulphonate]/[L4]	Fluorescence Intensity (I) / c.p.s.	ΔI / c.p.s.
2.00×10^{-6}	0	0.00	1087348	0
2.00×10^{-6}	2.93×10^{-7}	0.15	1191912	104564
2.00×10^{-6}	5.85×10^{-7}	0.29	1286722	199374
2.00×10^{-6}	8.75×10^{-7}	0.44	1309036	221688
2.00×10^{-6}	1.16×10^{-6}	0.58	1331960	244612
2.00×10^{-6}	1.45×10^{-6}	0.72	1370398	283050
2.00×10^{-6}	2.02×10^{-6}	1.01	1387494	300146
2.00×10^{-6}	2.58×10^{-6}	1.29	1418646	331298
2.00×10^{-6}	3.13×10^{-6}	1.57	1433288	345940
2.00×10^{-6}	3.68×10^{-6}	1.84	1418220	330872
2.00×10^{-6}	4.23×10^{-6}	2.11	1443798	356450
2.00×10^{-6}	4.76×10^{-6}	2.38	1439798	352450
2.00×10^{-6}	5.29×10^{-6}	2.65	1417974	330626

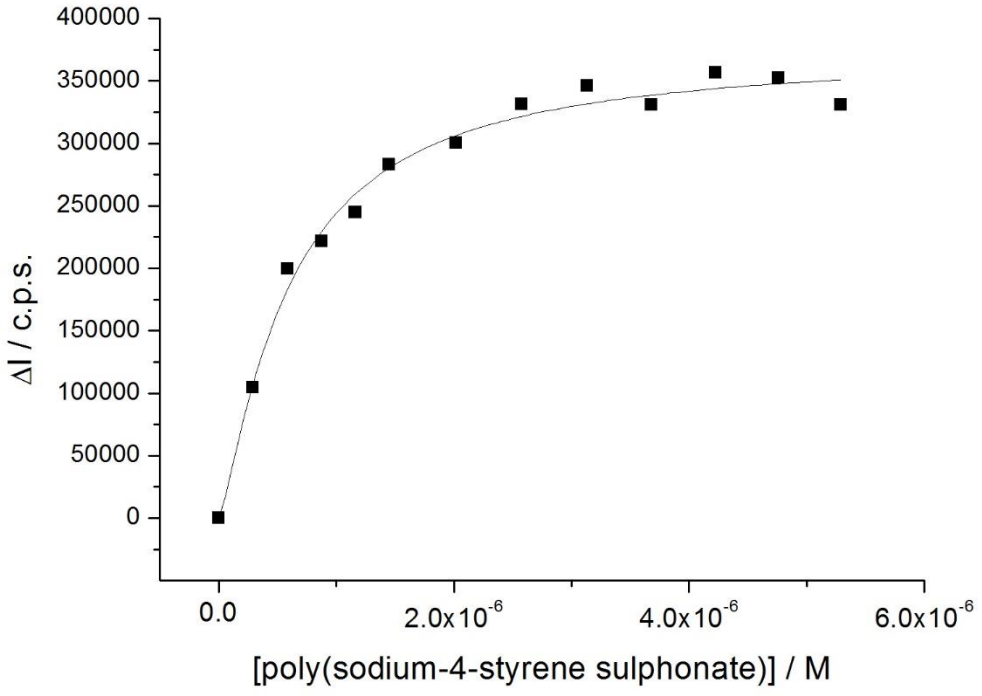

$K_a = 1.67 \times 10^6 \pm 1.25 \times 10^5$ M^{-1}

$n = 1.3$

Polymer mixture **L6** vs. poly(sodium-4-styrene sulphonate) (c.p.s.: counts per second).

[L6] / M	[poly(sodium-4-styrene sulphonate)] / M	[poly(sodium-4-styrene sulphonate]/[L6]	Fluorescence Intensity (I) / c.p.s.	ΔI / c.p.s.
2.00×10^{-6}	0	0.00	464152	0
2.00×10^{-6}	2.93×10^{-7}	0.15	494673	30521
2.00×10^{-6}	5.85×10^{-7}	0.29	543071	78919
2.00×10^{-6}	1.16×10^{-6}	0.58	587202	123050
2.00×10^{-6}	1.73×10^{-6}	0.87	593755	129603
2.00×10^{-6}	2.30×10^{-6}	1.15	628664	164512
2.00×10^{-6}	2.86×10^{-6}	1.43	639107	174955
2.00×10^{-6}	3.41×10^{-6}	1.70	639082	174930
2.00×10^{-6}	3.95×10^{-6}	1.98	627723	163571
2.00×10^{-6}	4.49×10^{-6}	2.25	629238	165086
2.00×10^{-6}	5.03×10^{-6}	2.51	633136	168984
2.00×10^{-6}	5.56×10^{-6}	2.78	644331	180179
2.00×10^{-6}	6.08×10^{-6}	3.04	637318	173166

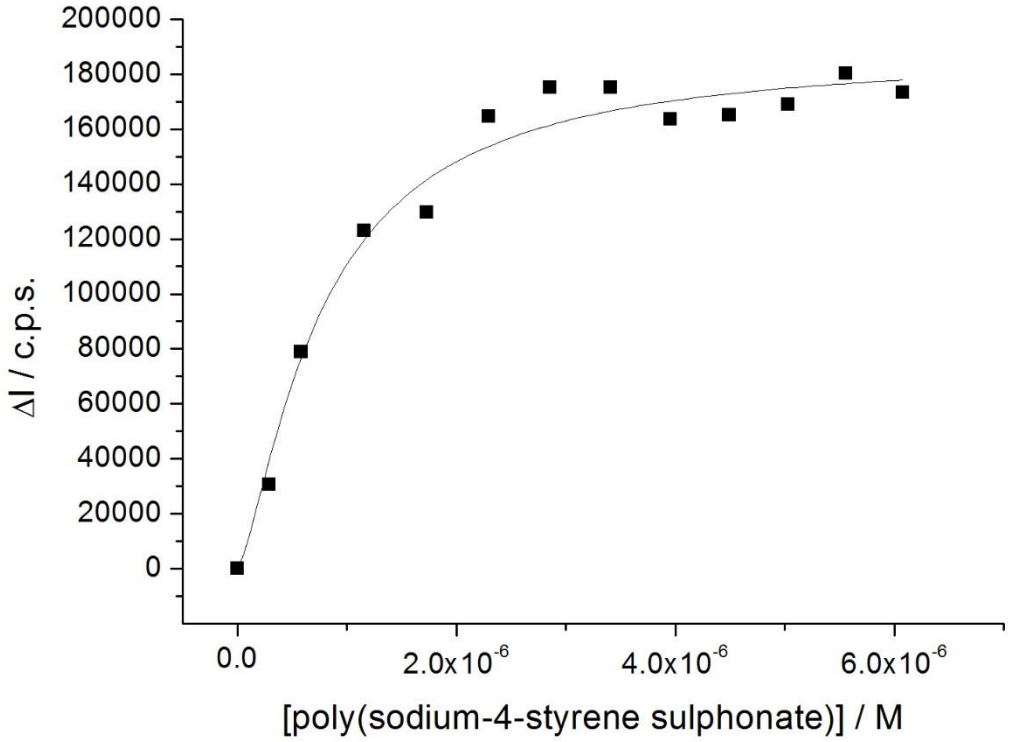

$K_a = 1.30 \times 10^6 \pm 1.36 \times 10^5$ M^{-1}

$n = 1.4$

Static library **L1** vs. BSA (c.p.s.: counts per second).

[L1] / M	[BSA] / M	[BSA]/ [L1]	Fluorescence Intensity (I) / c.p.s.	ΔI / c.p.s.
2.00×10^{-6}	0	0.00	3065446	0
2.00×10^{-6}	1.47×10^{-6}	0.73	3069582	4136
2.00×10^{-6}	2.92×10^{-6}	1.46	3139572	74126
2.00×10^{-6}	5.81×10^{-6}	2.91	3209374	143928
2.00×10^{-6}	8.67×10^{-6}	4.34	3252743	187297
2.00×10^{-6}	1.15×10^{-5}	5.75	3317988	252542
2.00×10^{-6}	1.43×10^{-5}	7.14	3343153	277707
2.00×10^{-6}	1.70×10^{-5}	8.52	3333952	268506
2.00×10^{-6}	1.98×10^{-5}	9.89	3364854	299408
2.00×10^{-6}	2.25×10^{-5}	11.24	3401473	336027
2.00×10^{-6}	2.51×10^{-5}	12.57	3413691	348245
2.00×10^{-6}	2.78×10^{-5}	13.89	3418900	353454
2.00×10^{-6}	3.04×10^{-5}	15.19	3414291	348845
2.00×10^{-6}	3.30×10^{-5}	16.48	3441025	375579
2.00×10^{-6}	3.55×10^{-5}	17.76	3450656	385210

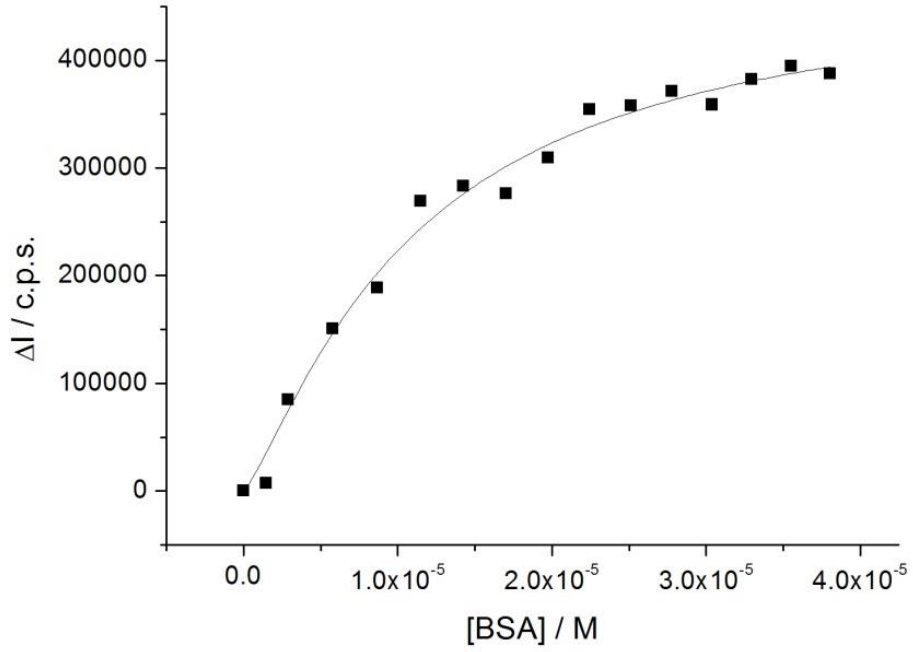

$K_a = 9.01 \times 10^4 \pm 7.93 \times 10^3$ M^{-1}

$n = 1.3$

Static library **L3** vs. BSA (c.p.s.: counts per second).

[L3] / M	[BSA] / M	[BSA]/[L3]	Fluorescence Intensity (I) / c.p.s.	ΔI / c.p.s.
2.00×10^{-6}	0	0.00	2243228	0
2.00×10^{-6}	1.47×10^{-6}	0.73	2353227	109999
2.00×10^{-6}	2.92×10^{-6}	1.46	2463226	219998
2.00×10^{-6}	5.81×10^{-6}	2.91	2532685	289457
2.00×10^{-6}	8.67×10^{-6}	4.34	2586485	343257
2.00×10^{-6}	1.15×10^{-5}	5.75	2673261	430033
2.00×10^{-6}	1.43×10^{-5}	7.14	2668894	425666
2.00×10^{-6}	1.70×10^{-5}	8.52	2750582	507354
2.00×10^{-6}	1.98×10^{-5}	9.89	2776332	533104
2.00×10^{-6}	2.25×10^{-5}	11.24	2775988	532760
2.00×10^{-6}	2.51×10^{-5}	12.57	2798865	555637

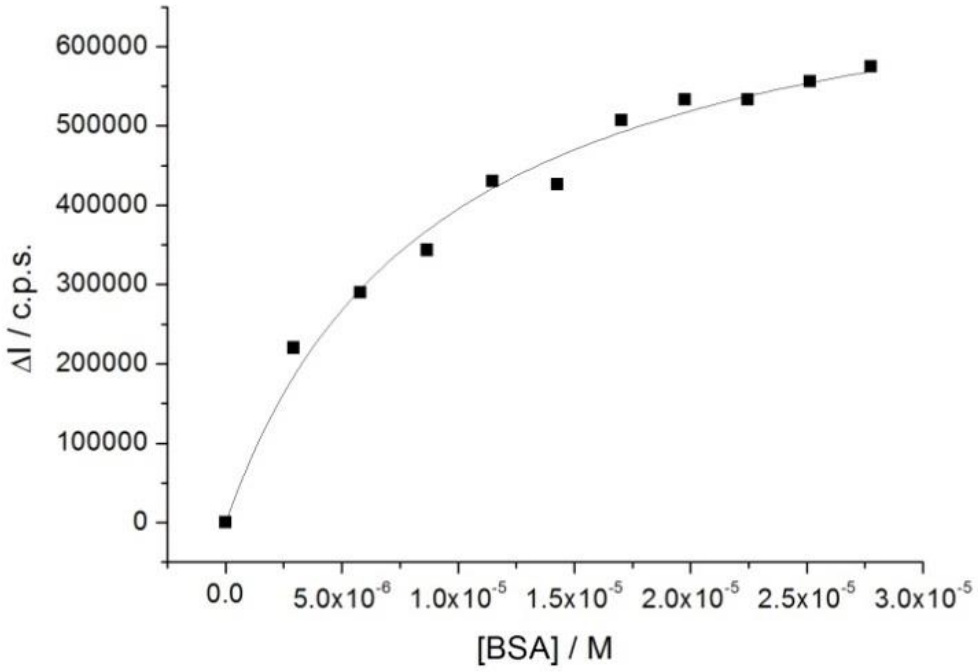

$K_a = 1.10 \times 10^5 \pm 1.50 \times 10^4$ M^{-1}

$n = 1.0$

Static library **L5** vs. BSA (c.p.s.: counts per second).

[L5] / M	[BSA] / M	[BSA]/[L5]	Fluorescence Intensity (I) / c.p.s.	ΔI / c.p.s.
2.00×10^{-6}	0	0.00	1215729	0
2.00×10^{-6}	1.47×10^{-6}	0.73	1314395	98666
2.00×10^{-6}	2.92×10^{-6}	1.46	1330762	115033
2.00×10^{-6}	5.81×10^{-6}	2.91	1381193	165464
2.00×10^{-6}	8.67×10^{-6}	4.34	1431676	215947
2.00×10^{-6}	1.15×10^{-5}	5.75	1480943	265214
2.00×10^{-6}	1.43×10^{-5}	7.14	1494896	279167
2.00×10^{-6}	1.70×10^{-5}	8.52	1528153	312424
2.00×10^{-6}	1.98×10^{-5}	9.89	1533098	317369
2.00×10^{-6}	2.25×10^{-5}	11.24	1561111	345382
2.00×10^{-6}	2.51×10^{-5}	12.57	1559255	343526
2.00×10^{-6}	2.78×10^{-5}	13.89	1601291	385562
2.00×10^{-6}	3.04×10^{-5}	15.19	1612937	397208
2.00×10^{-6}	3.30×10^{-5}	16.48	1609575	393846
2.00×10^{-6}	3.55×10^{-5}	17.76	1638573	422844
2.00×10^{-6}	3.80×10^{-5}	19.02	1629177	413448

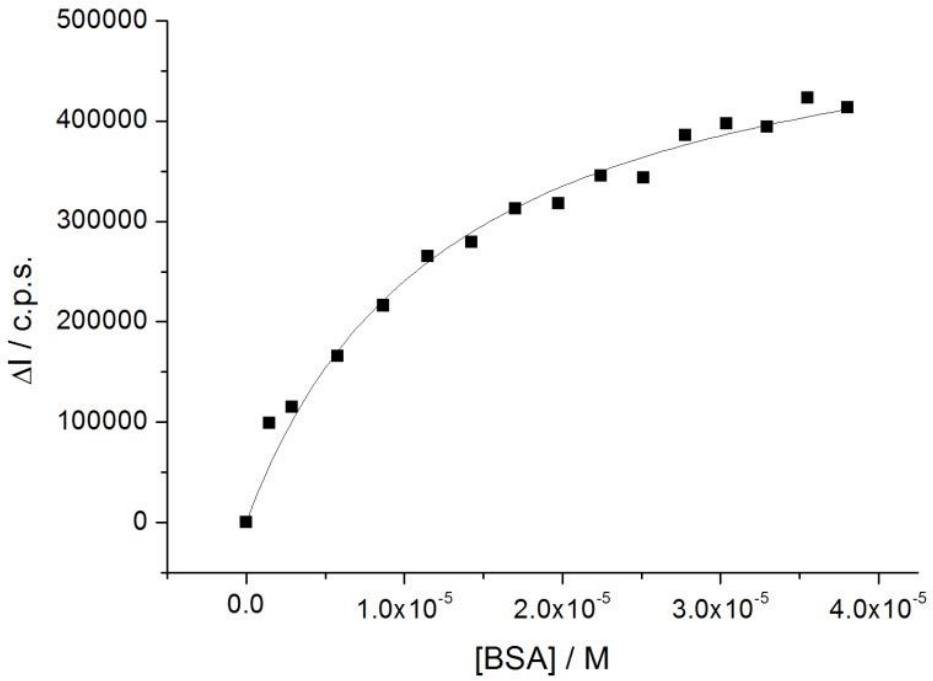

$K_a = 7.75 \times 10^4 \pm 9.16 \times 10^3$ M^{-1}

$n = 1.0$

Static library **L1** vs. poly(2-(acryloyloxyethyl)trimethylammonium chloride) (c.p.s.: counts per second).

[L1] / M	[poly(2-(acryoyloxyethyl) trimethylammonium chloride] / M	[poly(2-(acryoyloxyethyl) trimethylammonium chloride)] / [L1]	Fluorescence Intensity (I) / c.p.s.	ΔI / c.p.s.
2.00×10^{-6}	0	0.00	4482091	0
2.00×10^{-6}	2.93×10^{-7}	0.15	4313538	168553
2.00×10^{-6}	5.85×10^{-7}	0.29	4266227	215864
2.00×10^{-6}	1.16×10^{-6}	0.58	4223300	258791
2.00×10^{-6}	1.73×10^{-6}	0.87	4144447	337644
2.00×10^{-6}	2.30×10^{-6}	1.15	4087402	394689
2.00×10^{-6}	2.86×10^{-6}	1.43	4043705	438386
2.00×10^{-6}	3.41×10^{-6}	1.70	4038646	443445
2.00×10^{-6}	3.95×10^{-6}	1.98	4058332	423759
2.00×10^{-6}	4.49×10^{-6}	2.25	3992025	490066
2.00×10^{-6}	5.03×10^{-6}	2.51	3970219	511872

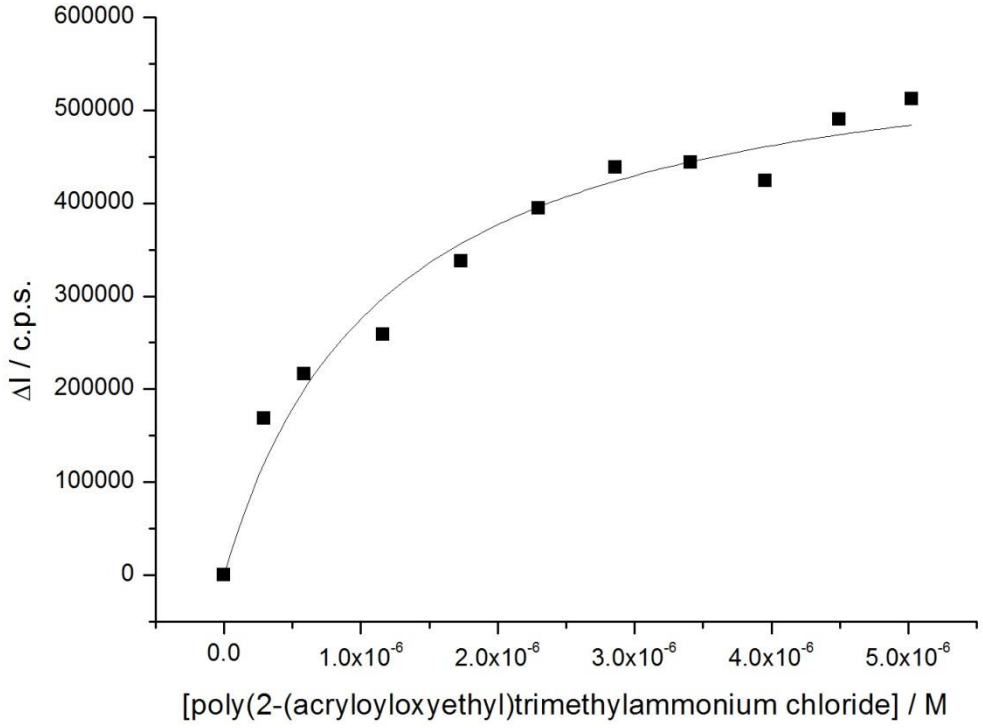

$K_a = 6.12 \times 10^5 \pm 8.84 \times 10^4$ M^{-1}

$n = 1.0$

Static library **L3** vs. poly(2-(acryloyloxyethyl)trimethylammonium chloride) (c.p.s.: counts per second).

[L3] / M	[poly(2-(acryoyloxyethyl) trimethylammonium chloride] / M	[poly(2-(acryoyloxyethyl) trimethylammonium chloride)] / [L3]	Fluorescence Intensity (I) / c.p.s.	ΔI / c.p.s.
2.00×10^{-6}	0	0.00	2870080	0
2.00×10^{-6}	2.93×10^{-7}	0.15	2772619	97461
2.00×10^{-6}	5.85×10^{-7}	0.29	2767843	102237
2.00×10^{-6}	1.16×10^{-6}	0.58	2732949	137131
2.00×10^{-6}	1.73×10^{-6}	0.87	2702118	167962
2.00×10^{-6}	2.30×10^{-6}	1.15	2680452	189628
2.00×10^{-6}	3.41×10^{-6}	1.70	2651952	218128
2.00×10^{-6}	3.95×10^{-6}	1.98	2647400	222680
2.00×10^{-6}	5.03×10^{-6}	2.51	2614966	255114
2.00×10^{-6}	5.56×10^{-6}	2.78	2622390	247690

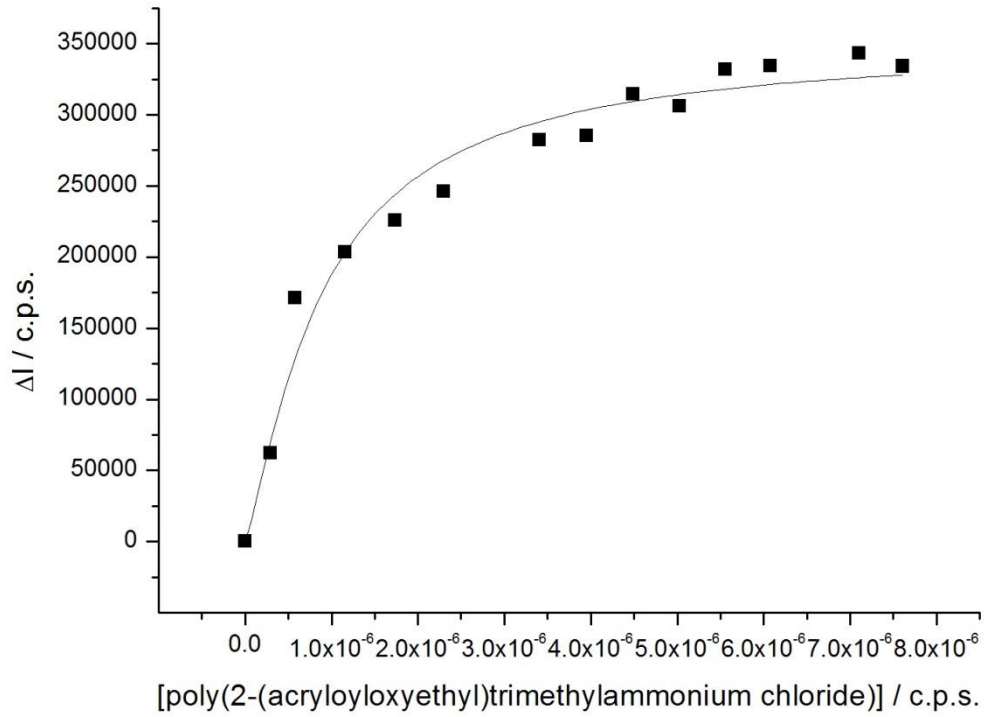

$K_a = 1.12 \times 10^6 \pm 1.41 \times 10^5$ M^{-1}

$n = 1.3$

Static library **L5** vs. poly(2-(acryloyloxyethyl)trimethylammonium chloride (c.p.s.: counts per second).

[L5] / M	[poly(2-(acryoyloxyethyl) trimethylammonium chloride] / M	[poly(2-(acryoyloxyethyl) trimethylammonium chloride)] / [L5]	Fluorescence Intensity (I) / c.p.s.	ΔI / c.p.s.
2.00×10^{-6}	0	0.00	1309275	0
2.00×10^{-6}	2.93×10^{-7}	0.15	1294182	15093
2.00×10^{-6}	5.85×10^{-7}	0.29	1261283	47992
2.00×10^{-6}	1.16×10^{-6}	0.58	1218063	91212
2.00×10^{-6}	1.73×10^{-6}	0.87	1195902	113373
2.00×10^{-6}	2.30×10^{-6}	1.15	1195156	114119
2.00×10^{-6}	2.86×10^{-6}	1.43	1192211	117064
2.00×10^{-6}	3.41×10^{-6}	1.70	1151811	157464
2.00×10^{-6}	3.95×10^{-6}	1.98	1174103	135172
2.00×10^{-6}	4.49×10^{-6}	2.25	1152814	156461
2.00×10^{-6}	5.03×10^{-6}	2.51	1158726	150549
2.00×10^{-6}	5.56×10^{-6}	2.78	1159458	149817
2.00×10^{-6}	6.08×10^{-6}	3.04	1162044	147231
2.00×10^{-6}	6.59×10^{-6}	3.30	1148376	160899
2.00×10^{-6}	7.10×10^{-6}	3.55	1150980	158295

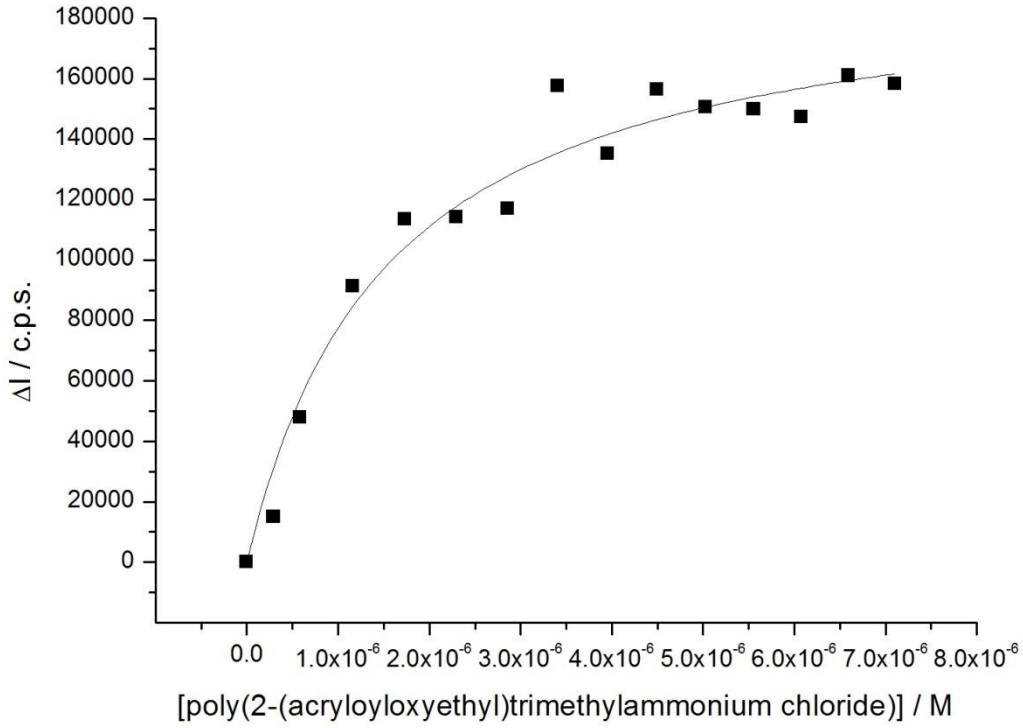

$K_a = 6.51 \times 10^5 \pm 1.25 \times 10^5$ M^{-1}

$n = 1.0$

Polymer mixture **L7** vs. poly(2-(acryloyloxyethyl)trimethylammonium chloride) (c.p.s.: counts per second).

[L7] / M	[poly(2-(acryoyloxyethyl) trimethylammonium chloride] / M	[poly(2-(acryoyloxyethyl) trimethylammonium chloride)] / [L7]	Fluorescence Intensity (I) / c.p.s.	ΔI / c.p.s.
2.00×10^{-6}	0	0.00	298425	0
2.00×10^{-6}	2.93×10^{-7}	0.15	276740	21685
2.00×10^{-6}	5.85×10^{-7}	0.29	272683	25742
2.00×10^{-6}	1.16×10^{-6}	0.58	265441	32984
2.00×10^{-6}	1.73×10^{-6}	0.87	247251	51174
2.00×10^{-6}	2.30×10^{-6}	1.15	249043	49382
2.00×10^{-6}	2.86×10^{-6}	1.43	249715	48710
2.00×10^{-6}	3.41×10^{-6}	1.70	247341	51084
2.00×10^{-6}	3.95×10^{-6}	1.98	242232	56193
2.00×10^{-6}	4.49×10^{-6}	2.25	233900	64525
2.00×10^{-6}	5.03×10^{-6}	2.51	239750	58675
2.00×10^{-6}	6.08×10^{-6}	3.04	234342	64083
2.00×10^{-6}	6.59×10^{-6}	3.30	237736	60689
2.00×10^{-6}	7.10×10^{-6}	3.55	237260	61165

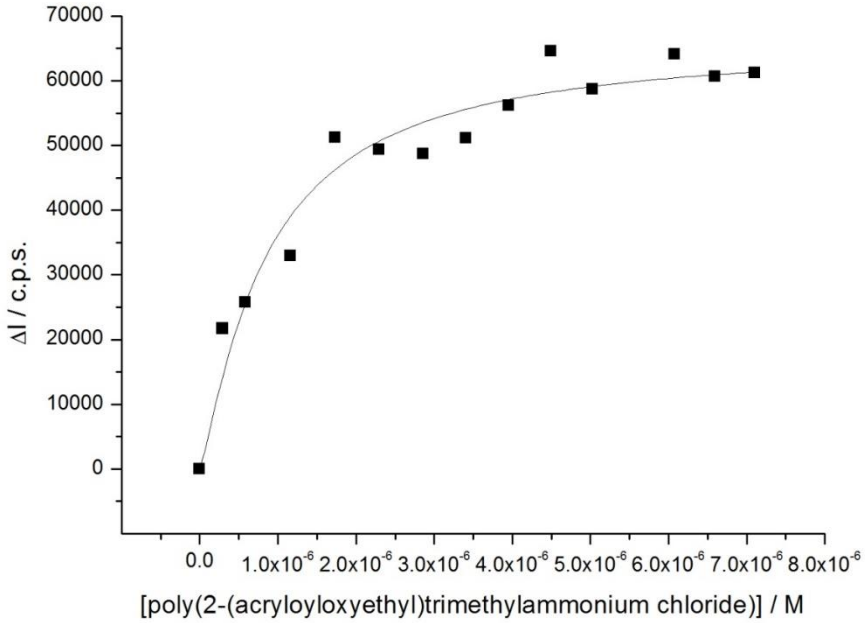

$K_a = 1.17 \times 10^6 \pm 1.98 \times 10^5$ M^{-1}

$n = 1.2$

Appendix C

Binding Curves

Static library **L1** vs. Con A (c.p.s.: counts per second).
100 mM NH_4OAc/AcOH, pH 4.5, 2 mM $CaCl_2$.

[ConA] / M	[L1] / M	[L1]/[ConA]	Fluorescence Intensity / c.p.s.	ΔI / c.p.s.
5.00×10^{-7}	0	0.00	24911023	0
5.00×10^{-7}	1.46×10^{-7}	0.29	23960979	950044
5.00×10^{-7}	2.91×10^{-7}	0.58	22126679	2784344
5.00×10^{-7}	4.34×10^{-7}	0.87	20639898	4271125
5.00×10^{-7}	5.75×10^{-7}	1.15	19112721	5798302
5.00×10^{-7}	7.14×10^{-7}	1.43	18225714	6685309
5.00×10^{-7}	8.52×10^{-7}	1.70	17809433	7101590
5.00×10^{-7}	9.89×10^{-7}	1.98	16679502	8231521
5.00×10^{-7}	1.12×10^{-6}	2.25	16363181	8547842
5.00×10^{-7}	1.26×10^{-6}	2.51	15621715	9289308
5.00×10^{-7}	1.39×10^{-6}	2.78	15008760	9902263
5.00×10^{-7}	1.52×10^{-6}	3.04	14317076	10593947
5.00×10^{-7}	1.65×10^{-6}	3.30	13913730	10997293
5.00×10^{-7}	1.78×10^{-6}	3.55	13112271	11798752
5.00×10^{-7}	1.90×10^{-6}	3.80	12844170	12066853
5.00×10^{-7}	2.03×10^{-6}	4.05	12421210	12489813
5.00×10^{-7}	2.15×10^{-6}	4.30	12066864	12844159
5.00×10^{-7}	2.27×10^{-6}	4.55	11555018	13356005
5.00×10^{-7}	2.39×10^{-6}	4.79	11272457	13638566
5.00×10^{-7}	2.51×10^{-6}	5.03	10932849	13978174
5.00×10^{-7}	2.63×10^{-6}	5.26	10922158	13988865

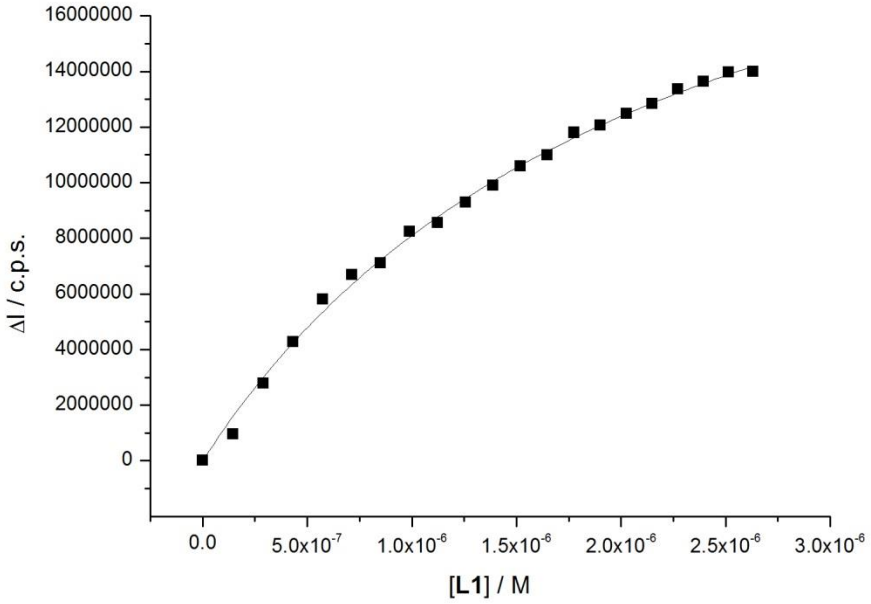

$K_a = 4.45 \times 10^5 \pm 2.64 \times 10^4\ M^{-1}$

$n = 1.0$

Static library **L1** vs. LTB (c.p.s.: counts per second).
100 mM NH_4OAc/AcOH, pH 4.5, 100 mM NaCl.

[LTB] / M	[L1] / M	[L1]/[LTB]	Fluorescence Intensity / c.p.s.	ΔI / c.p.s.
5.00×10^{-7}	0	0.00	22164883	0
5.00×10^{-7}	5.92×10^{-7}	1.18	20856802	1308081
5.00×10^{-7}	1.18×10^{-6}	2.36	19923931	2240952
5.00×10^{-7}	1.77×10^{-6}	3.54	19059505	3105378
5.00×10^{-7}	2.35×10^{-6}	4.70	18696704	3468179
5.00×10^{-7}	2.93×10^{-6}	5.86	17883253	4281630
5.00×10^{-7}	3.51×10^{-6}	7.02	17206184	4958699
5.00×10^{-7}	4.08×10^{-6}	8.17	16786880	5378003
5.00×10^{-7}	4.66×10^{-6}	9.31	16459046	5705837
5.00×10^{-7}	5.23×10^{-6}	10.5	15869460	6295423
5.00×10^{-7}	5.79×10^{-6}	11.6	15740215	6424668

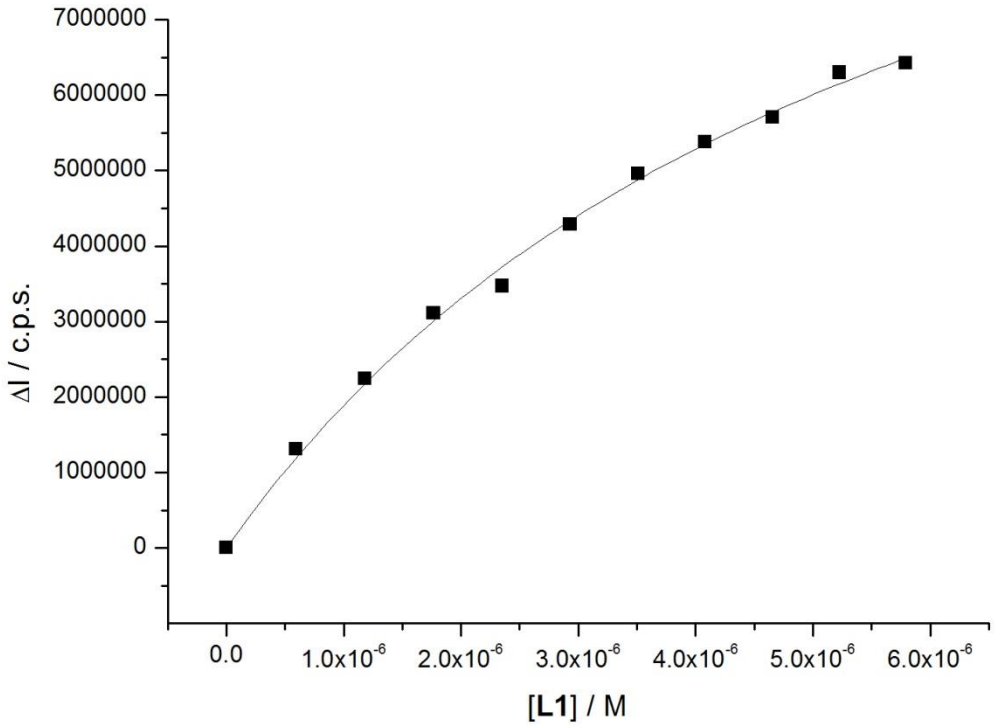

$K_a = 1.68 \times 10^5 \pm 1.69 \times 10^4$ M^{-1}

$n = 1.0$

Static library **L2** vs. Con A (c.p.s.: counts per second).
100 mM $NH_4OAc/AcOH$, pH 4.5, 2 mM $CaCl_2$.

[ConA] / M	[L2] / M	[L2]/[ConA]	Fluorescence Intensity / c.p.s.	ΔI / c.p.s.
5.00×10^{-7}	0	0.00	29025026	0
5.00×10^{-7}	1.46×10^{-7}	0.29	27504128	1520898
5.00×10^{-7}	2.91×10^{-7}	0.58	26101405	2923621
5.00×10^{-7}	4.34×10^{-7}	0.87	25298087	3726939
5.00×10^{-7}	5.75×10^{-7}	1.15	23691479	5333547
5.00×10^{-7}	7.14×10^{-7}	1.43	22780636	6244390
5.00×10^{-7}	8.52×10^{-7}	1.70	21988201	7036825
5.00×10^{-7}	9.89×10^{-7}	1.98	21215624	7809402
5.00×10^{-7}	1.12×10^{-6}	2.25	20470931	8554095
5.00×10^{-7}	1.26×10^{-6}	2.51	19556882	9468144
5.00×10^{-7}	1.39×10^{-6}	2.78	18792290	10232736
5.00×10^{-7}	1.52×10^{-6}	3.04	18197167	10827859
5.00×10^{-7}	1.65×10^{-6}	3.30	17488722	11536304
5.00×10^{-7}	1.78×10^{-6}	3.55	16974468	12050558
5.00×10^{-7}	1.90×10^{-6}	3.80	16388004	12637022
5.00×10^{-7}	2.03×10^{-6}	4.05	15912844	13112182
5.00×10^{-7}	2.15×10^{-6}	4.30	15344856	13680170
5.00×10^{-7}	2.27×10^{-6}	4.55	14852847	14172179
5.00×10^{-7}	2.39×10^{-6}	4.79	14597449	14427577
5.00×10^{-7}	2.51×10^{-6}	5.03	14098280	14926746
5.00×10^{-7}	2.63×10^{-6}	5.26	13661568	15363458

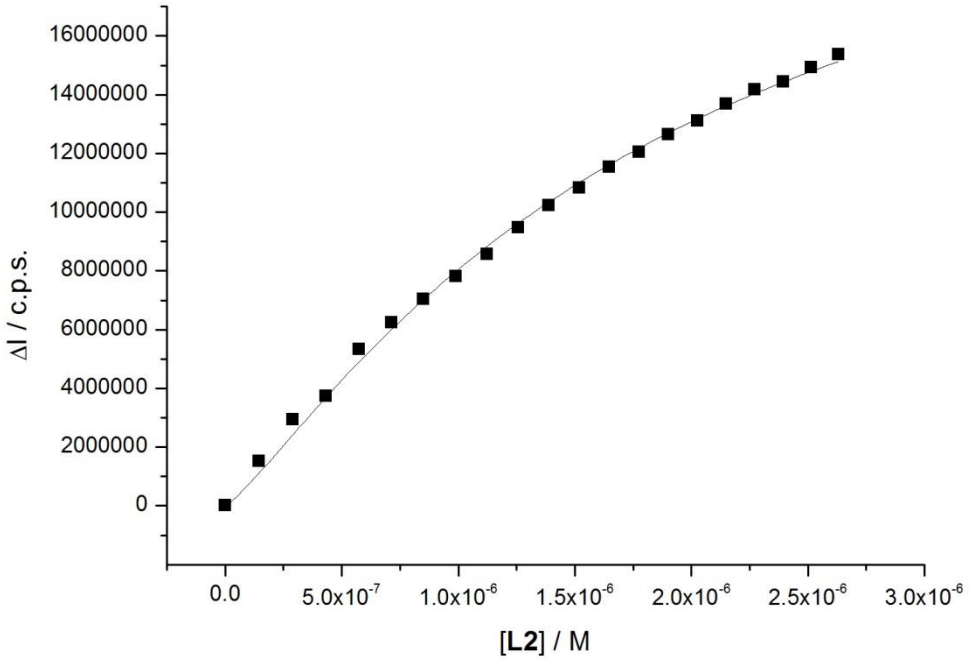

$K_a = 5.32 \times 10^5 \pm 3.20 \times 10^4$ M^{-1}

$n = 0.8$

Static library **L3** vs. LTB (c.p.s.: counts per second).
100 mM NH_4OAc/AcOH, pH 4.5, 100 mM NaCl.

[LTB] / M	[L3] / M	[L3]/[LTB]	Fluorescence Intensity / c.p.s.	ΔI / c.p.s.
5.00×10^{-7}	0	0.00	16867283	0
5.00×10^{-7}	1.86×10^{-7}	0.37	14521991	2345292
5.00×10^{-7}	3.68×10^{-7}	0.74	13559240	3308043
5.00×10^{-7}	5.46×10^{-7}	1.09	12426922	4440361
5.00×10^{-7}	7.21×10^{-7}	1.44	11852483	5014800
5.00×10^{-7}	8.93×10^{-7}	1.79	10905436	5961847
5.00×10^{-7}	1.06×10^{-6}	2.12	10499772	6367511
5.00×10^{-7}	1.23×10^{-6}	2.45	9801183	7066100
5.00×10^{-7}	1.39×10^{-6}	2.78	9340755	7526528
5.00×10^{-7}	1.55×10^{-6}	3.10	9111654	7755629
5.00×10^{-7}	1.70×10^{-6}	3.41	8782440	8084843
5.00×10^{-7}	1.86×10^{-6}	3.72	8499104	8368179
5.00×10^{-7}	2.01×10^{-6}	4.02	8202676	8664607
5.00×10^{-7}	2.16×10^{-6}	4.31	7694166	9173117
5.00×10^{-7}	2.30×10^{-6}	4.61	7411897	9455386
5.00×10^{-7}	2.45×10^{-6}	4.89	7190938	9676345
5.00×10^{-7}	2.59×10^{-6}	5.17	6855491	10011792
5.00×10^{-7}	2.72×10^{-6}	5.45	6522955	10344328
5.00×10^{-7}	2.86×10^{-6}	5.72	6324065	10543218
5.00×10^{-7}	2.99×10^{-6}	5.99	6065189	10802094
5.00×10^{-7}	3.13×10^{-6}	6.25	5585472	11281811

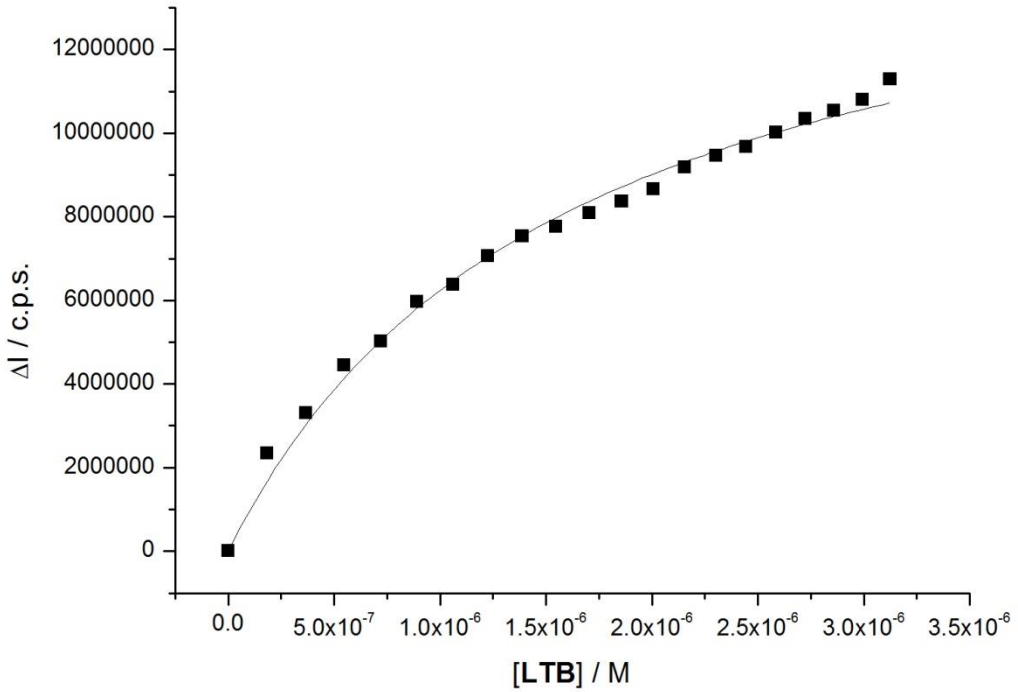

$K_a = 6.27 \times 10^5 \pm 5.05 \times 10^4$ M^{-1}

$n = 1.0$

Static library **L4** vs. Con A (c.p.s.: counts per second).
100 mM $NH_4OAc/AcOH$, pH 4.5, 2 mM $CaCl_2$.

[Con A] / M	[L4] / M	[L4]/[Con A]	Fluorescence Intensity / c.p.s.	ΔI / c.p.s.
5.00×10^{-7}	0	0.00	25735132	0
5.00×10^{-7}	1.46×10^{-7}	0.29	24243899	1491233
5.00×10^{-7}	2.91×10^{-7}	0.58	23387902	2347230
5.00×10^{-7}	4.34×10^{-7}	0.87	22763213	2971919
5.00×10^{-7}	5.75×10^{-7}	1.15	22112881	3622251
5.00×10^{-7}	7.14×10^{-7}	1.43	21395186	4339946
5.00×10^{-7}	8.52×10^{-7}	1.70	20758873	4976259
5.00×10^{-7}	9.89×10^{-7}	1.98	20304307	5430825
5.00×10^{-7}	1.12×10^{-6}	2.25	19844872	5890260
5.00×10^{-7}	1.26×10^{-6}	2.51	19537970	6197162
5.00×10^{-7}	1.39×10^{-6}	2.78	19022190	6712942
5.00×10^{-7}	1.52×10^{-6}	3.04	18637008	7098124
5.00×10^{-7}	1.65×10^{-6}	3.30	18120742	7614390
5.00×10^{-7}	1.78×10^{-6}	3.55	17853377	7881755

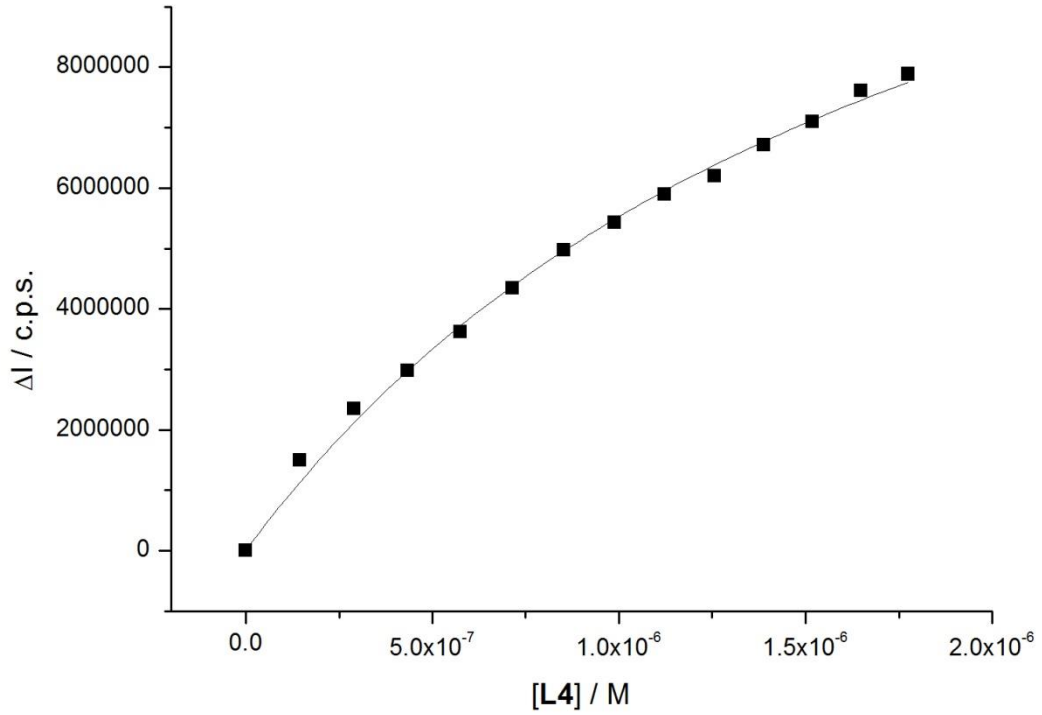

$K_a = 5.26 \times 10^5 \pm 4.77 \times 10^4$ M^{-1}

$n = 1.0$

Static library **L4** vs. LTB (c.p.s.: counts per second).
100 mM NH_4OAc/AcOH, pH 4.5, 100 mM NaCl.

[LTB] / M	[L4] / M	[L4]/[LTB]	Fluorescence Intensity / c.p.s.	ΔI / c.p.s.
5.00×10^{-7}	0	0.00	20303483	0
5.00×10^{-7}	2.97×10^{-7}	0.59	19503968	799515
5.00×10^{-7}	5.92×10^{-7}	1.18	19083764	1219719
5.00×10^{-7}	8.87×10^{-7}	1.77	18528216	1775267
5.00×10^{-7}	1.18×10^{-6}	2.36	18181802	2121681
5.00×10^{-7}	1.48×10^{-6}	2.95	17936194	2367289
5.00×10^{-7}	1.77×10^{-6}	3.54	17650519	2652964
5.00×10^{-7}	2.06×10^{-6}	4.12	17336033	2967450
5.00×10^{-7}	2.35×10^{-6}	4.70	16883891	3419592
5.00×10^{-7}	2.64×10^{-6}	5.28	16740494	3562989
5.00×10^{-7}	2.93×10^{-6}	5.86	16359046	3944437
5.00×10^{-7}	3.22×10^{-6}	6.44	16174128	4129355
5.00×10^{-7}	3.51×10^{-6}	7.02	15918091	4385392
5.00×10^{-7}	3.80×10^{-6}	7.60	15671554	4631929
5.00×10^{-7}	4.08×10^{-6}	8.17	15256107	5047376
5.00×10^{-7}	4.37×10^{-6}	8.74	14920257	5383226
5.00×10^{-7}	4.66×10^{-6}	9.31	14707362	5596121
5.00×10^{-7}	4.94×10^{-6}	9.88	14481955	5821528
5.00×10^{-7}	5.23×10^{-6}	10.5	14245699	6057784
5.00×10^{-7}	5.51×10^{-6}	11.0	14094336	6209147
5.00×10^{-7}	5.79×10^{-6}	11.6	13818802	6484681

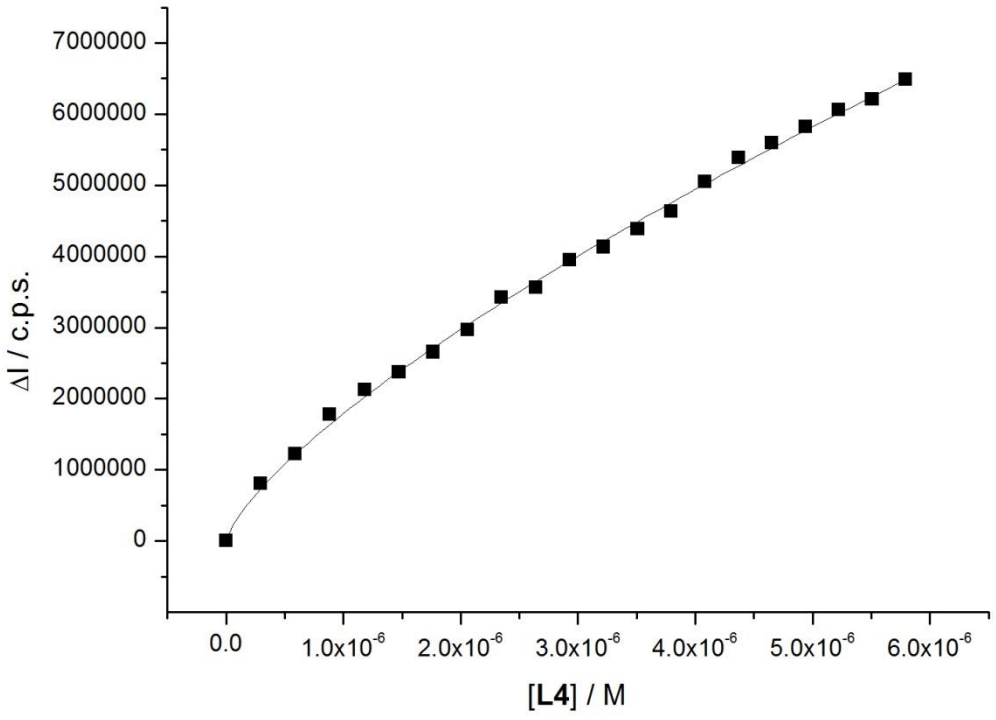

K_a = 1.06 ± 985.8 M^{-1}

n = 0.8

Static library **L5** vs. Con A (c.p.s.: counts per second).
100 mM $NH_4OAc/AcOH$, pH 4.5, 2 mM $CaCl_2$.

[ConA] / M	[L5] / M	[L5]/[ConA]	Fluorescence Intensity / c.p.s.	ΔI / c.p.s.
5.00×10^{-7}	0	0.00	21696619	0
5.00×10^{-7}	1.46×10^{-7}	0.29	19948963	1747656
5.00×10^{-7}	2.91×10^{-7}	0.58	18799701	2896918
5.00×10^{-7}	4.34×10^{-7}	0.87	17754174	3942445
5.00×10^{-7}	5.75×10^{-7}	1.15	17156181	4540438
5.00×10^{-7}	7.14×10^{-7}	1.43	16398500	5298119
5.00×10^{-7}	8.52×10^{-7}	1.70	15667055	6029564
5.00×10^{-7}	9.89×10^{-7}	1.98	15179674	6516945
5.00×10^{-7}	1.12×10^{-6}	2.25	14713588	6983031
5.00×10^{-7}	1.26×10^{-6}	2.51	14074958	7621661
5.00×10^{-7}	1.39×10^{-6}	2.78	13483935	8212684
5.00×10^{-7}	1.52×10^{-6}	3.04	13018135	8678484
5.00×10^{-7}	1.65×10^{-6}	3.30	12568757	9127862
5.00×10^{-7}	1.78×10^{-6}	3.55	11986834	9709785
5.00×10^{-7}	1.90×10^{-6}	3.80	11569362	10127257
5.00×10^{-7}	2.03×10^{-6}	4.05	11092850	10603769

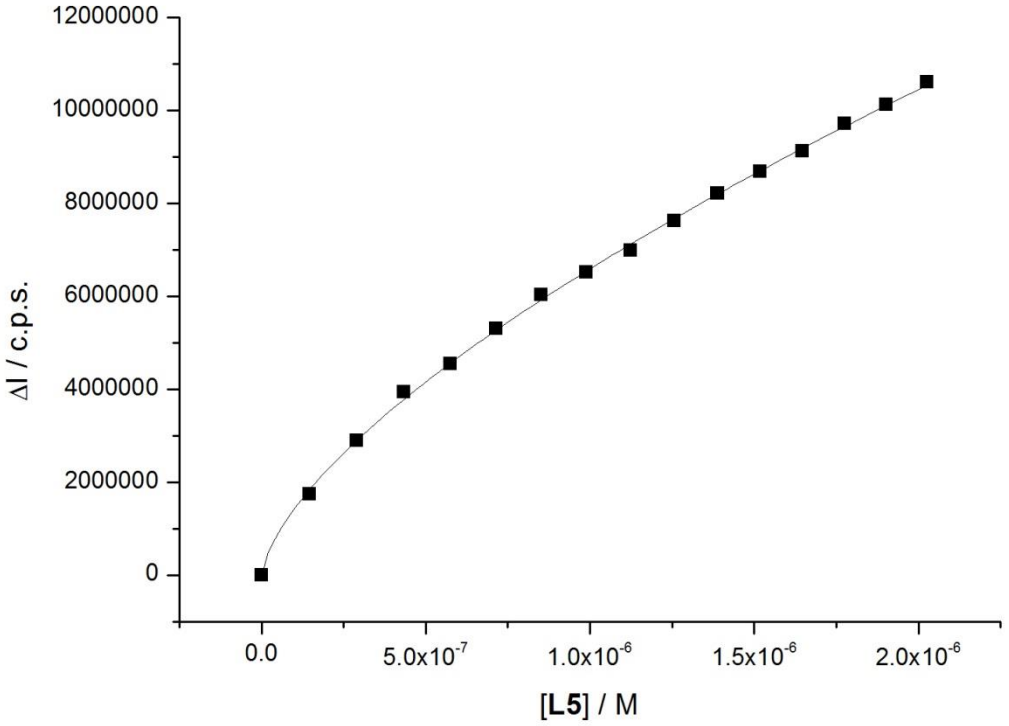

$K_a = 4.66 \pm 1.12 \times 10^4\ M^{-1}$

$n = 0.7$

Static library **L5** vs. LTB (c.p.s.: counts per second).
100 mM NH_4OAc/AcOH, pH 4.5, 100 mM NaCl.

[LTB] / M	[L5] / M	[L5]/[LTB]	Fluorescence Intensity / c.p.s.	ΔI / c.p.s.
5.00×10^{-7}	0	0.00	20474226	0
5.00×10^{-7}	2.97×10^{-7}	0.59	20264918	209308
5.00×10^{-7}	5.92×10^{-7}	1.18	19581988	892238
5.00×10^{-7}	8.87×10^{-7}	1.77	18919642	1554584
5.00×10^{-7}	1.18×10^{-6}	2.36	18264098	2210128
5.00×10^{-7}	1.48×10^{-6}	2.95	17478161	2996065
5.00×10^{-7}	1.77×10^{-6}	3.54	16636589	3837637
5.00×10^{-7}	2.06×10^{-6}	4.12	16011452	4462774
5.00×10^{-7}	2.35×10^{-6}	4.70	15528517	4945709
5.00×10^{-7}	2.64×10^{-6}	5.28	15003323	5470903
5.00×10^{-7}	2.93×10^{-6}	5.86	14154199	6320027
5.00×10^{-7}	3.22×10^{-6}	6.44	13905832	6568394
5.00×10^{-7}	3.51×10^{-6}	7.02	13213927	7260299
5.00×10^{-7}	3.80×10^{-6}	7.60	12857599	7616627
5.00×10^{-7}	4.08×10^{-6}	8.17	12006866	8467360
5.00×10^{-7}	4.37×10^{-6}	8.74	11627804	8846422
5.00×10^{-7}	4.66×10^{-6}	9.31	11252340	9221886
5.00×10^{-7}	4.94×10^{-6}	9.88	11017429	9456797
5.00×10^{-7}	5.23×10^{-6}	10.5	10796591	9677635
5.00×10^{-7}	5.51×10^{-6}	11.0	10333571	10140655
5.00×10^{-7}	5.79×10^{-6}	11.6	10042490	10431736

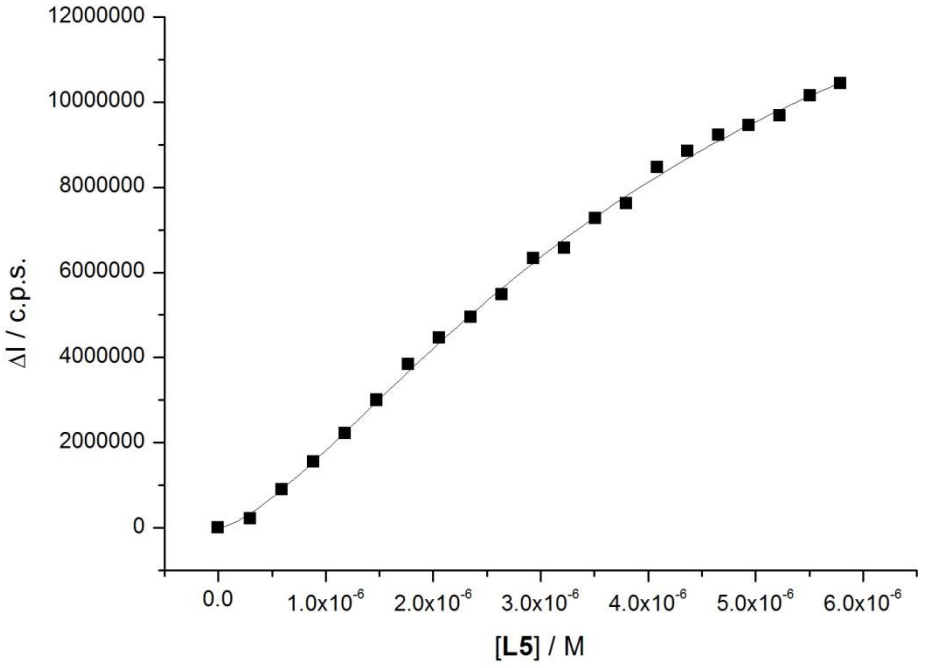

$K_a = 2.42 \times 10^5 \pm 4.83 \times 10^3\ M^{-1}$

$n = 0.8$

Polymer mixture **L6** vs. Con A (c.p.s.: counts per second).
100 mM $NH_4OAc/AcOH$, pH 4.5, 2 mM $CaCl_2$.

[ConA] / M	[L6] / M	[L6]/[ConA]	Fluorescence Intensity / c.p.s.	ΔI / c.p.s.
5.00×10^{-7}	0	0.00	27033840	0
5.00×10^{-7}	2.78×10^{-8}	0.06	25962039	1071801
5.00×10^{-7}	5.52×10^{-8}	0.12	24622579	2411261
5.00×10^{-7}	8.24×10^{-8}	0.16	23918500	3115340
5.00×10^{-7}	1.09×10^{-7}	0.22	23290152	3743688
5.00×10^{-7}	1.36×10^{-7}	0.28	22683587	4350253
5.00×10^{-7}	1.62×10^{-7}	0.32	21884039	5149801
5.00×10^{-7}	1.88×10^{-7}	0.38	21413895	5619945
5.00×10^{-7}	2.13×10^{-7}	0.42	20971402	6062438
5.00×10^{-7}	2.39×10^{-7}	0.48	20545434	6488406
5.00×10^{-7}	2.64×10^{-7}	0.52	20278383	6755457
5.00×10^{-7}	2.89×10^{-7}	0.58	19515794	7518046
5.00×10^{-7}	3.13×10^{-7}	0.62	19093892	7939948
5.00×10^{-7}	3.37×10^{-7}	0.68	18972708	8061132
5.00×10^{-7}	3.61×10^{-7}	0.72	18600580	8433260
5.00×10^{-7}	3.85×10^{-7}	0.78	18187090	8846750
5.00×10^{-7}	4.09×10^{-7}	0.82	17886671	9147169
5.00×10^{-7}	4.32×10^{-7}	0.86	17671436	9362404
5.00×10^{-7}	4.55×10^{-7}	0.90	17260411	9773429
5.00×10^{-7}	4.78×10^{-7}	0.96	17015640	10018200
5.00×10^{-7}	5.00×10^{-7}	1.00	16895578	10138262

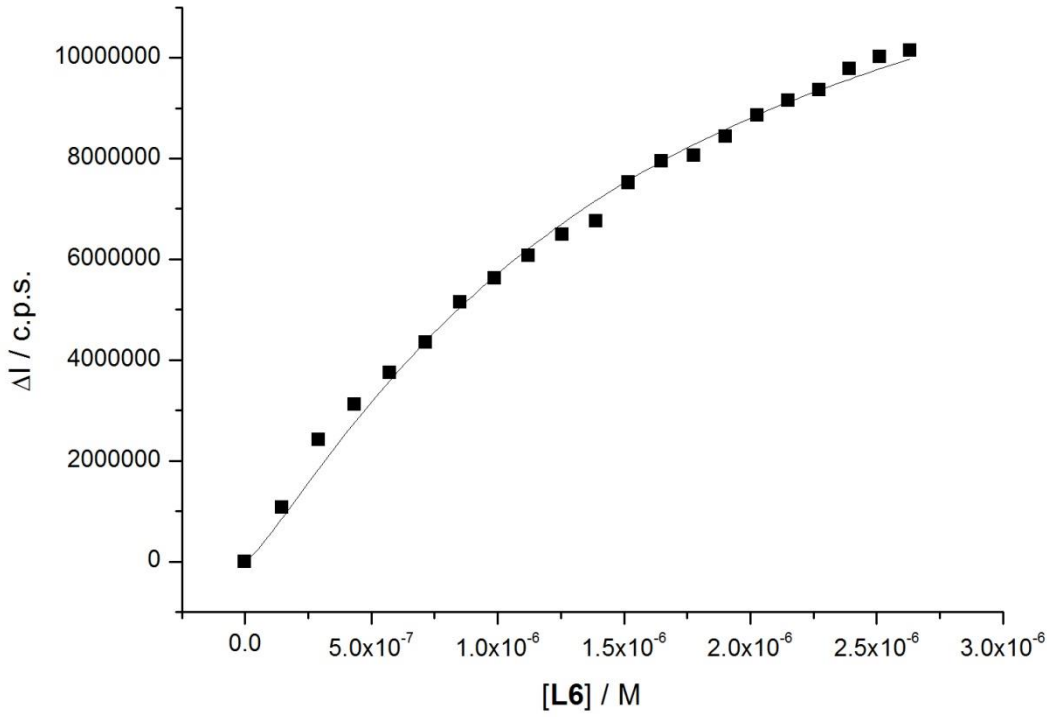

$K_a = 3.76 \times 10^6 \pm 2.26 \times 10^5\ M^{-1}$

$n = 1.2$

Polymer mixture **L7** vs. LTB (c.p.s.: counts per second).
100 mM $NH_4OAc/AcOH$, pH 4.5, 100 mM NaCl.

[LTB] / M	[L7] / M	[L7]/[LTB]	Fluorescence Intensity / c.p.s.	ΔI / c.p.s.
5.00×10^{-7}	0	0.00	20691937	0
5.00×10^{-7}	6.16×10^{-8}	0.12	20115232	576705
5.00×10^{-7}	1.23×10^{-7}	0.25	19571118	1120819
5.00×10^{-7}	1.84×10^{-7}	0.37	19009529	1682408
5.00×10^{-7}	2.45×10^{-7}	0.49	18583273	2108664
5.00×10^{-7}	3.06×10^{-7}	0.61	18361410	2330527
5.00×10^{-7}	3.67×10^{-7}	0.73	17831302	2860635
5.00×10^{-7}	4.28×10^{-7}	0.86	17558538	3133399
5.00×10^{-7}	4.88×10^{-7}	0.98	17164256	3527681
5.00×10^{-7}	5.49×10^{-7}	1.10	16822796	3869141
5.00×10^{-7}	6.09×10^{-7}	1.22	16629690	4062247
5.00×10^{-7}	6.69×10^{-7}	1.34	16408350	4283587
5.00×10^{-7}	7.29×10^{-7}	1.46	16217030	4474907
5.00×10^{-7}	7.89×10^{-7}	1.58	16082529	4609408
5.00×10^{-7}	8.48×10^{-7}	1.70	15860147	4831790
5.00×10^{-7}	9.08×10^{-7}	1.82	15679638	5012299
5.00×10^{-7}	9.67×10^{-7}	1.93	15436391	5255546
5.00×10^{-7}	1.03×10^{-6}	2.05	15222046	5469891

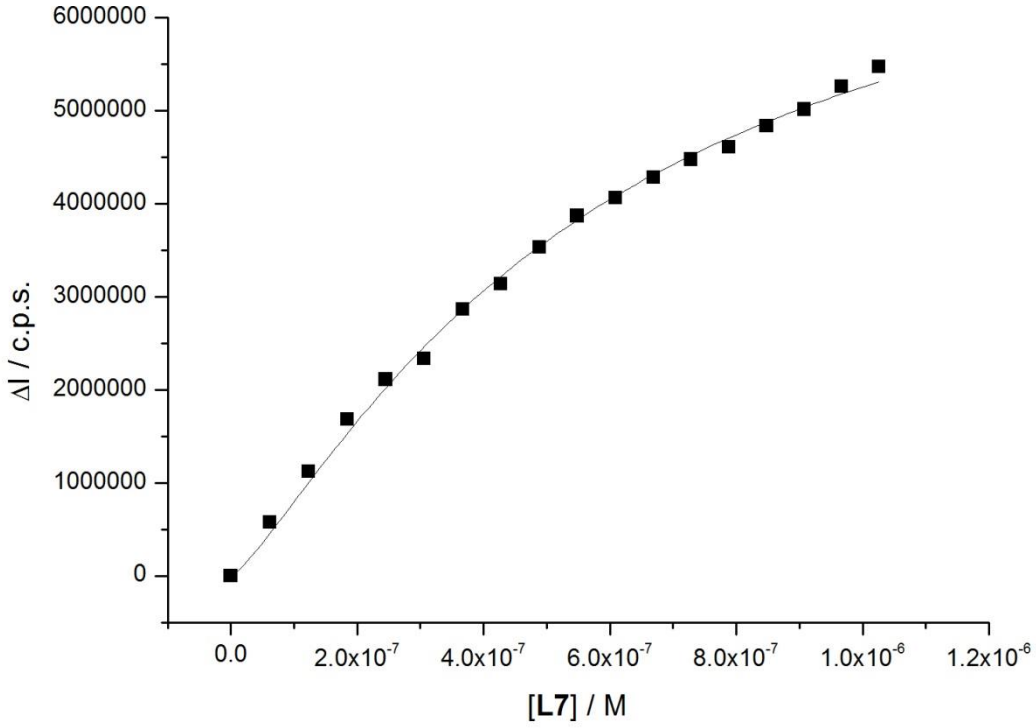

$K_a = 1.74 \times 10^6 \pm 6.97 \times 10^4\ M^{-1}$

$n = 0.8$

Static library **L1** vs. Con A (c.p.s.: counts per second).
100 mM HEPES, pH 7.1, 1 mM $CaCl_2$, 1 mM $MnCl_2$.

[ConA] / M	[L1] / M	[L1]/[ConA]	Fluorescence Intensity / c.p.s.	ΔI / c.p.s.
2.50×10^{-7}	0	0.00	25865657	0
2.50×10^{-7}	1.46×10^{-7}	0.58	27741925	31494461
2.50×10^{-7}	2.91×10^{-7}	1.16	25206491	28959027
2.50×10^{-7}	4.34×10^{-7}	1.73	23997704	27750240
2.50×10^{-7}	5.75×10^{-7}	2.30	22686388	26438924
2.50×10^{-7}	7.14×10^{-7}	2.86	21075193	24827729
2.50×10^{-7}	8.52×10^{-7}	3.41	19927016	23679552
2.50×10^{-7}	9.89×10^{-7}	3.95	19166947	22919483
2.50×10^{-7}	1.12×10^{-6}	4.49	18045015	21797551
2.50×10^{-7}	1.26×10^{-6}	5.03	17292983	21045519
2.50×10^{-7}	1.39×10^{-6}	5.56	16274433	20026969
2.50×10^{-7}	1.52×10^{-6}	6.08	15612615	19365151
2.50×10^{-7}	1.65×10^{-6}	6.59	14779346	18531882
2.50×10^{-7}	1.78×10^{-6}	7.10	14215958	17968494
2.50×10^{-7}	1.90×10^{-6}	7.61	13551008	17303544
2.50×10^{-7}	2.03×10^{-6}	8.11	13316282	17068818
2.50×10^{-7}	2.15×10^{-6}	8.60	12594927	16347463
2.50×10^{-7}	2.27×10^{-6}	9.09	12164734	15917270
2.50×10^{-7}	2.39×10^{-6}	9.57	11707435	15459971
2.50×10^{-7}	2.51×10^{-6}	10.1	11368272	15120808
2.50×10^{-7}	2.63×10^{-6}	10.5	10946190	14698726

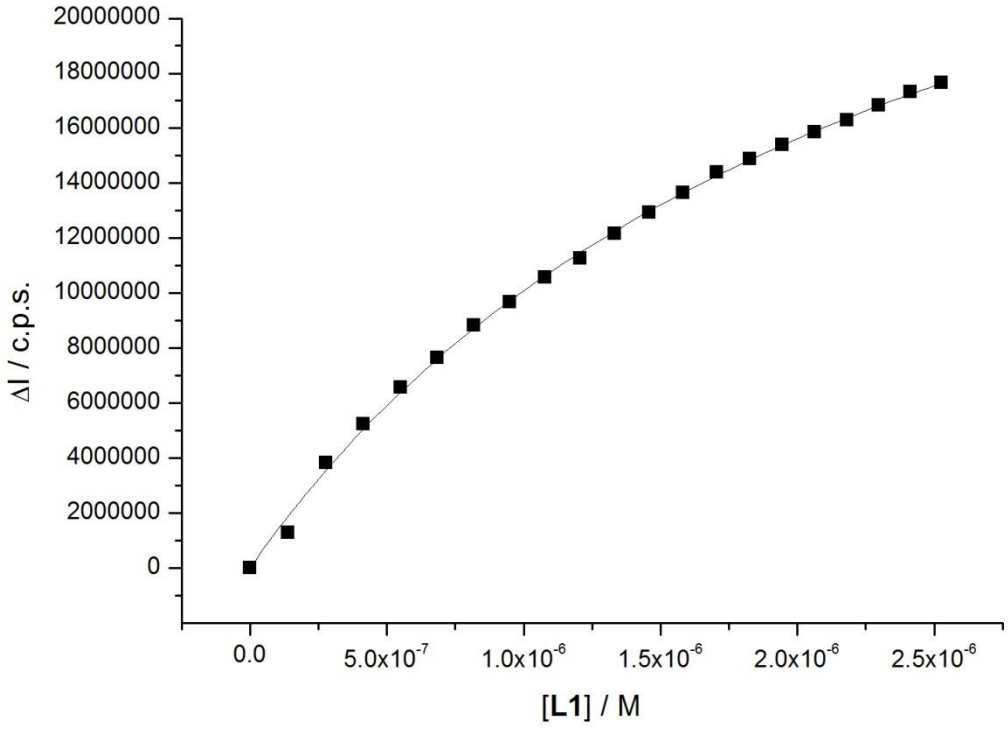

$K_a = 4.12 \times 10^5 \pm 6.32 \times 10^4\ M^{-1}$

$n = 1.0$

Static library **L1** vs. LTB (c.p.s.: counts per second).
100 mM HEPES, pH 7.1, 1 mM $CaCl_2$, 100 mM NaCl.

[LTB] / M	[L1] / M	[L1]/[LTB]	Fluorescence Intensity / c.p.s.	ΔI / c.p.s.
5.00×10^{-7}	0	0.00	24635400	0
5.00×10^{-7}	2.97×10^{-7}	0.59	23561263	1074137
5.00×10^{-7}	5.92×10^{-7}	1.18	22800791	1834609
5.00×10^{-7}	8.87×10^{-7}	1.77	21988911	2646489
5.00×10^{-7}	1.18×10^{-6}	2.36	21352531	3282869
5.00×10^{-7}	1.48×10^{-6}	2.95	20561387	4074013
5.00×10^{-7}	1.77×10^{-6}	3.54	20277216	4358184
5.00×10^{-7}	2.06×10^{-6}	4.12	19769881	4865519
5.00×10^{-7}	2.35×10^{-6}	4.70	19313969	5321431
5.00×10^{-7}	2.64×10^{-6}	5.28	19049536	5585864
5.00×10^{-7}	2.93×10^{-6}	5.86	18520105	6115295
5.00×10^{-7}	3.22×10^{-6}	6.44	18306609	6328791
5.00×10^{-7}	3.51×10^{-6}	7.02	17997043	6638357
5.00×10^{-7}	3.80×10^{-6}	7.60	17371509	7263891
5.00×10^{-7}	4.08×10^{-6}	8.17	17091921	7543479
5.00×10^{-7}	4.37×10^{-6}	8.74	16764718	7870682
5.00×10^{-7}	4.66×10^{-6}	9.31	16212818	8422582
5.00×10^{-7}	4.94×10^{-6}	9.88	15937195	8698205
5.00×10^{-7}	5.23×10^{-6}	10.5	15789456	8845944
5.00×10^{-7}	5.51×10^{-6}	11.0	15443819	9191581
5.00×10^{-7}	5.79×10^{-6}	11.6	15046132	9589268

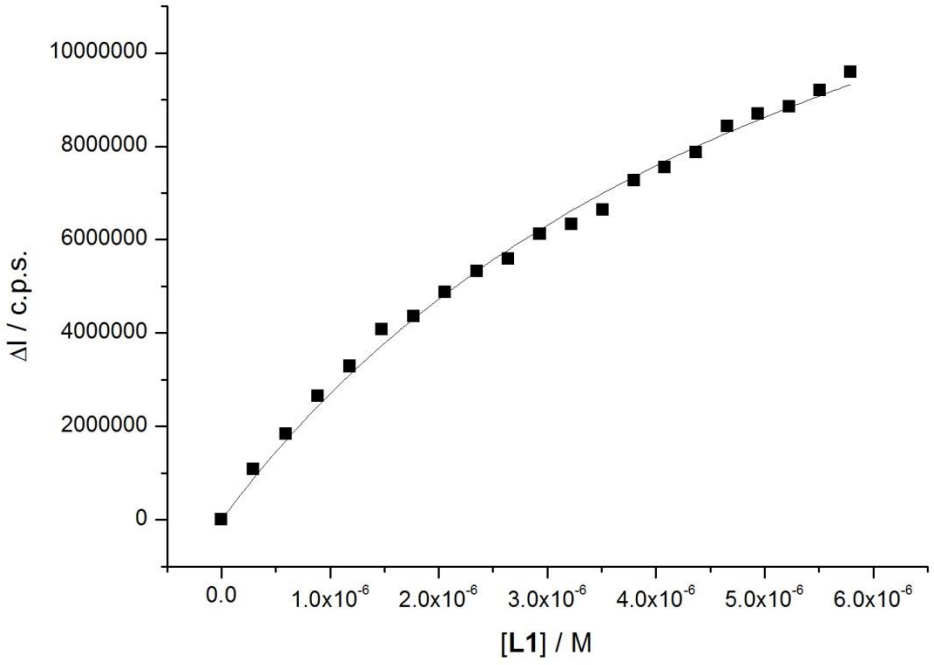

$K_a = 1.64 \times 10^5 \pm 1.32 \times 10^4\ M^{-1}$

$n = 0.8$

Static library **L2** vs. Con A (c.p.s.: counts per second).
100 mM HEPES, pH 7.1, 1 mM $CaCl_2$, 1 mM $MnCl_2$.

[ConA] / M	[L1] / M	[L1]/[ConA]	Fluorescence Intensity / c.p.s.	ΔI / c.p.s.
2.50×10^{-7}	0	0.00	25865657	0
2.50×10^{-7}	1.46×10^{-7}	0.58	27741925	1876268
2.50×10^{-7}	2.91×10^{-7}	1.16	25206491	4411702
2.50×10^{-7}	4.34×10^{-7}	1.73	23997704	5620489
2.50×10^{-7}	5.75×10^{-7}	2.30	22686388	6931805
2.50×10^{-7}	7.14×10^{-7}	2.86	21075193	8543000
2.50×10^{-7}	8.52×10^{-7}	3.41	19927016	9691177
2.50×10^{-7}	9.89×10^{-7}	3.95	19166947	10451246
2.50×10^{-7}	1.12×10^{-6}	4.49	18045015	11573178
2.50×10^{-7}	1.26×10^{-6}	5.03	17292983	12325210
2.50×10^{-7}	1.39×10^{-6}	5.56	16274433	13343760
2.50×10^{-7}	1.52×10^{-6}	6.08	15612615	14005578
2.50×10^{-7}	1.65×10^{-6}	6.59	14779346	14838847
2.50×10^{-7}	1.78×10^{-6}	7.10	14215958	15402235
2.50×10^{-7}	1.90×10^{-6}	7.61	13551008	16067185
2.50×10^{-7}	2.03×10^{-6}	8.11	13316282	16301911
2.50×10^{-7}	2.15×10^{-6}	8.60	12594927	17023266
2.50×10^{-7}	2.27×10^{-6}	9.09	12164734	17453459
2.50×10^{-7}	2.39×10^{-6}	9.57	11707435	17910758
2.50×10^{-7}	2.51×10^{-6}	10.1	11368272	18249921
2.50×10^{-7}	2.63×10^{-6}	10.5	10946190	18672003

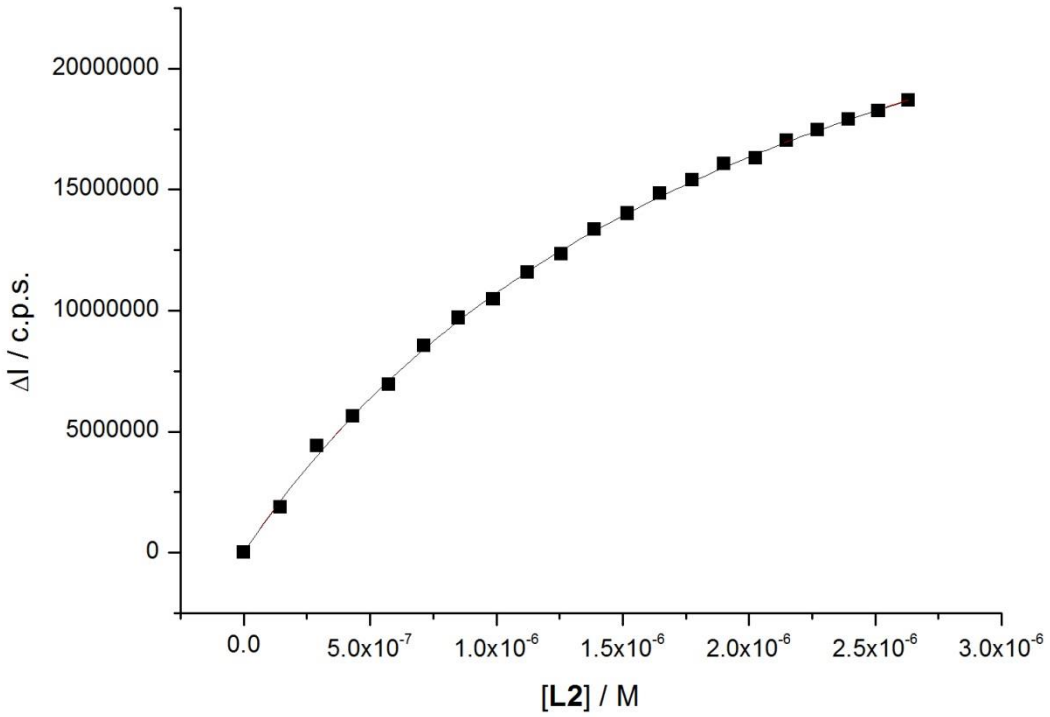

$K_a = 4.77 \times 10^5 \pm 1.43 \times 10^4\ M^{-1}$

$n = 1.0$

Static library **L3** vs. LTB (c.p.s.: counts per second).
100 mM HEPES, pH 7.1, 1 mM $CaCl_2$, 100 mM NaCl.

[LTB] / M	[L3] / M	[L1]/[LTB]	Fluorescence Intensity / c.p.s.	ΔI / c.p.s.
5.00×10^{-7}	0	0.00	25234446	0
5.00×10^{-7}	2.97×10^{-7}	0.59	23518662	1715784
5.00×10^{-7}	5.92×10^{-7}	1.18	22382614	2851832
5.00×10^{-7}	8.87×10^{-7}	1.77	22106351	3128095
5.00×10^{-7}	1.18×10^{-6}	2.36	20912294	4322152
5.00×10^{-7}	1.48×10^{-6}	2.95	19783649	5450797
5.00×10^{-7}	1.77×10^{-6}	3.54	19499317	5735129
5.00×10^{-7}	2.06×10^{-6}	4.12	18572947	6661499
5.00×10^{-7}	2.35×10^{-6}	4.70	17845253	7389193
5.00×10^{-7}	2.64×10^{-6}	5.28	17238958	7995488
5.00×10^{-7}	2.93×10^{-6}	5.86	16287585	8946861
5.00×10^{-7}	3.22×10^{-6}	6.44	15819056	9415390
5.00×10^{-7}	3.51×10^{-6}	7.02	14852250	10382196
5.00×10^{-7}	3.80×10^{-6}	7.60	14190464	11043982
5.00×10^{-7}	4.08×10^{-6}	8.17	13892458	11341988
5.00×10^{-7}	4.37×10^{-6}	8.74	13272074	11962372
5.00×10^{-7}	4.66×10^{-6}	9.31	13113063	12121383
5.00×10^{-7}	4.94×10^{-6}	9.88	12473677	12760769
5.00×10^{-7}	5.23×10^{-6}	10.5	12052792	13181654
5.00×10^{-7}	5.51×10^{-6}	11.0	11542210	13692236
5.00×10^{-7}	5.79×10^{-6}	11.6	11146696	14087750

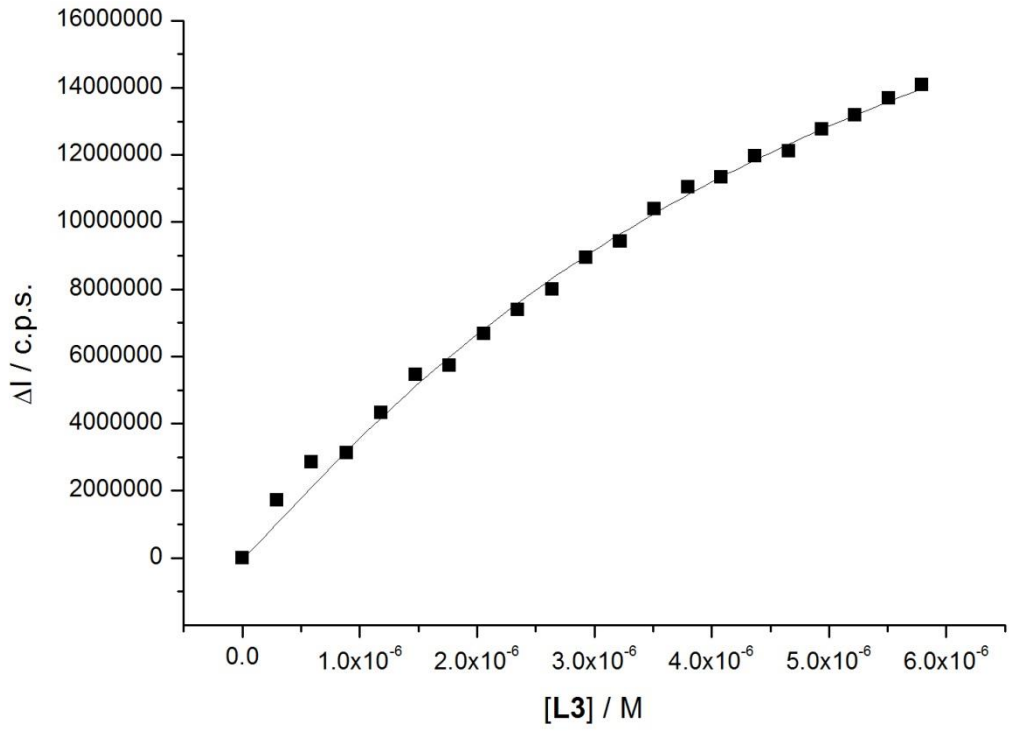

$K_a = 1.76 \times 10^5 \pm 1.24 \times 10^4\ M^{-1}$

$n = 1.0$

Static library **L4** vs. Con A (c.p.s.: counts per second).
100 mM HEPES, pH 7.1, 1 mM $CaCl_2$, 1 mM $MnCl_2$.

[ConA] / M	[L4] / M	[L4]/[ConA]	Fluorescence Intensity / c.p.s.	ΔI / c.p.s.
2.50×10^{-7}	0	0.00	28177595	0
2.50×10^{-7}	1.46×10^{-7}	0.58	25172183	3005412
2.50×10^{-7}	2.91×10^{-7}	1.16	23182137	4995458
2.50×10^{-7}	4.34×10^{-7}	1.73	22161347	6016248
2.50×10^{-7}	5.75×10^{-7}	2.30	20995697	7181898
2.50×10^{-7}	7.14×10^{-7}	2.86	20152325	8025270
2.50×10^{-7}	8.52×10^{-7}	3.41	19447501	8730094
2.50×10^{-7}	9.89×10^{-7}	3.95	18548054	9629541
2.50×10^{-7}	1.12×10^{-6}	4.49	17792521	10385074
2.50×10^{-7}	1.26×10^{-6}	5.03	16771163	11406432
2.50×10^{-7}	1.39×10^{-6}	5.56	16266602	11910993
2.50×10^{-7}	1.52×10^{-6}	6.08	15946274	12231321
2.50×10^{-7}	1.65×10^{-6}	6.59	15239444	12938151
2.50×10^{-7}	1.78×10^{-6}	7.10	14626894	13550701
2.50×10^{-7}	1.90×10^{-6}	7.61	14275403	13902192
2.50×10^{-7}	2.03×10^{-6}	8.11	13768572	14409023
2.50×10^{-7}	2.15×10^{-6}	8.60	13040006	15137589
2.50×10^{-7}	2.27×10^{-6}	9.09	12721860	15455735
2.50×10^{-7}	2.39×10^{-6}	9.57	12406105	15771490
2.50×10^{-7}	2.51×10^{-6}	10.1	12542365	15635230
2.50×10^{-7}	2.63×10^{-6}	10.5	11768778	16408817

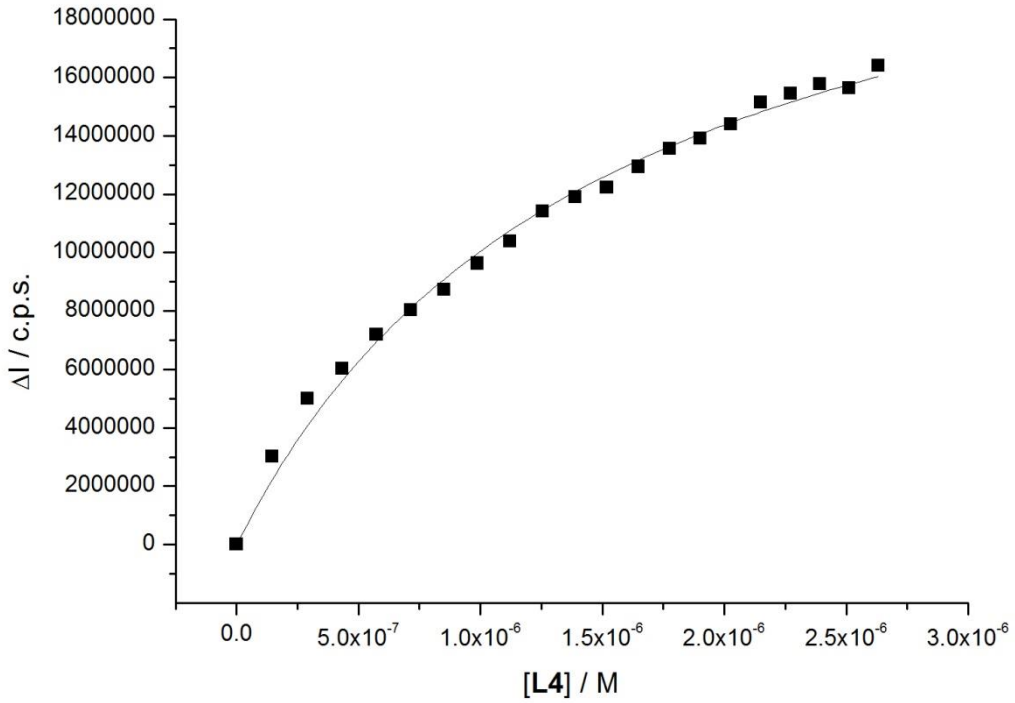

$K_a = 6.62 \times 10^5 \pm 4.65 \times 10^4\ M^{-1}$

$n = 1.0$

Static library **L4** vs. LTB (c.p.s.: counts per second).
100 mM HEPES, pH 7.1, 1 mM $CaCl_2$, 100 mM NaCl.

[LTB] / M	[L4] / M	[L4]/[LTB]	Fluorescence Intensity / c.p.s.	ΔI / c.p.s.
5.00×10^{-7}	0	0.00	22499222	0
5.00×10^{-7}	2.97×10^{-7}	0.59	22018864	480358
5.00×10^{-7}	5.92×10^{-7}	1.18	21166598	1332624
5.00×10^{-7}	8.87×10^{-7}	1.77	20785448	1713774
5.00×10^{-7}	1.18×10^{-6}	2.36	20291807	2207415
5.00×10^{-7}	1.48×10^{-6}	2.95	20004456	2494766
5.00×10^{-7}	1.77×10^{-6}	3.54	19717017	2782205
5.00×10^{-7}	2.06×10^{-6}	4.12	19446339	3052883
5.00×10^{-7}	2.35×10^{-6}	4.70	18941646	3557576
5.00×10^{-7}	2.64×10^{-6}	5.28	18384582	4114640
5.00×10^{-7}	2.93×10^{-6}	5.86	18277050	4222172
5.00×10^{-7}	3.22×10^{-6}	6.44	17968609	4530613
5.00×10^{-7}	3.51×10^{-6}	7.02	17700953	4798269
5.00×10^{-7}	3.80×10^{-6}	7.60	17289307	5209915
5.00×10^{-7}	4.08×10^{-6}	8.17	16894996	5604226
5.00×10^{-7}	4.37×10^{-6}	8.74	16550796	5948426
5.00×10^{-7}	4.66×10^{-6}	9.31	15916641	6582581
5.00×10^{-7}	4.94×10^{-6}	9.88	15619212	6880010
5.00×10^{-7}	5.23×10^{-6}	10.5	15423000	7076222
5.00×10^{-7}	5.51×10^{-6}	11.0	15241631	7257591
5.00×10^{-7}	5.79×10^{-6}	11.6	14835424	7663798

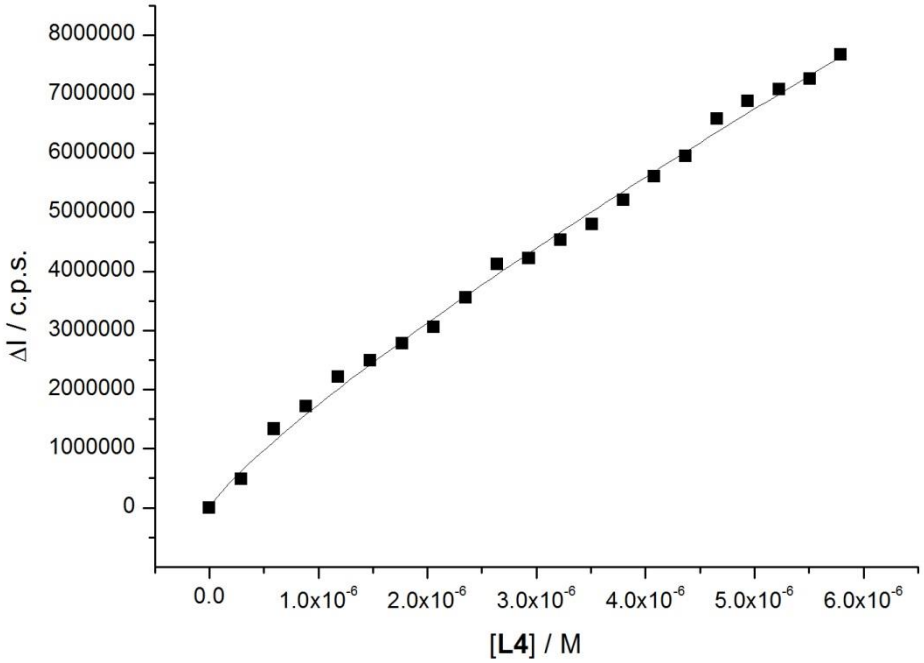

$K_a = 0.625 \pm 4.27 \times 10^4\ M^{-1}$

$n = 1.0$

Static library **L5** vs. Con A (c.p.s.: counts per second).
100 mM HEPES, pH 7.1, 1 mM $CaCl_2$, 1 mM $MnCl_2$.

[ConA] / M	[L5] / M	[L5]/[ConA]	Fluorescence Intensity / c.p.s.	ΔI / c.p.s.
2.50×10^{-7}	0	0.00	32938272	0
2.50×10^{-7}	1.46×10^{-7}	0.58	31484386	1453886
2.50×10^{-7}	2.91×10^{-7}	1.16	29906964	3031308
2.50×10^{-7}	4.34×10^{-7}	1.73	28713769	4224503
2.50×10^{-7}	5.75×10^{-7}	2.30	27697396	5240876
2.50×10^{-7}	7.14×10^{-7}	2.86	26591746	6346526
2.50×10^{-7}	8.52×10^{-7}	3.41	25551507	7386765
2.50×10^{-7}	9.89×10^{-7}	3.95	24543387	8394885
2.50×10^{-7}	1.12×10^{-6}	4.49	23855686	9082586
2.50×10^{-7}	1.39×10^{-6}	5.56	22356097	10582175
2.50×10^{-7}	1.52×10^{-6}	6.08	21750643	11187629
2.50×10^{-7}	1.65×10^{-6}	6.59	21100385	11837887
2.50×10^{-7}	1.78×10^{-6}	7.10	20443336	12494936
2.50×10^{-7}	1.90×10^{-6}	7.61	19947746	12990526
2.50×10^{-7}	2.03×10^{-6}	8.11	19217792	13720480
2.50×10^{-7}	2.15×10^{-6}	8.60	18941431	13996841
2.50×10^{-7}	2.27×10^{-6}	9.09	18483481	14454791
2.50×10^{-7}	2.39×10^{-6}	9.57	18122559	14815713
2.50×10^{-7}	2.51×10^{-6}	10.1	17518840	15419432
2.50×10^{-7}	2.63×10^{-6}	10.5	17097473	15840799

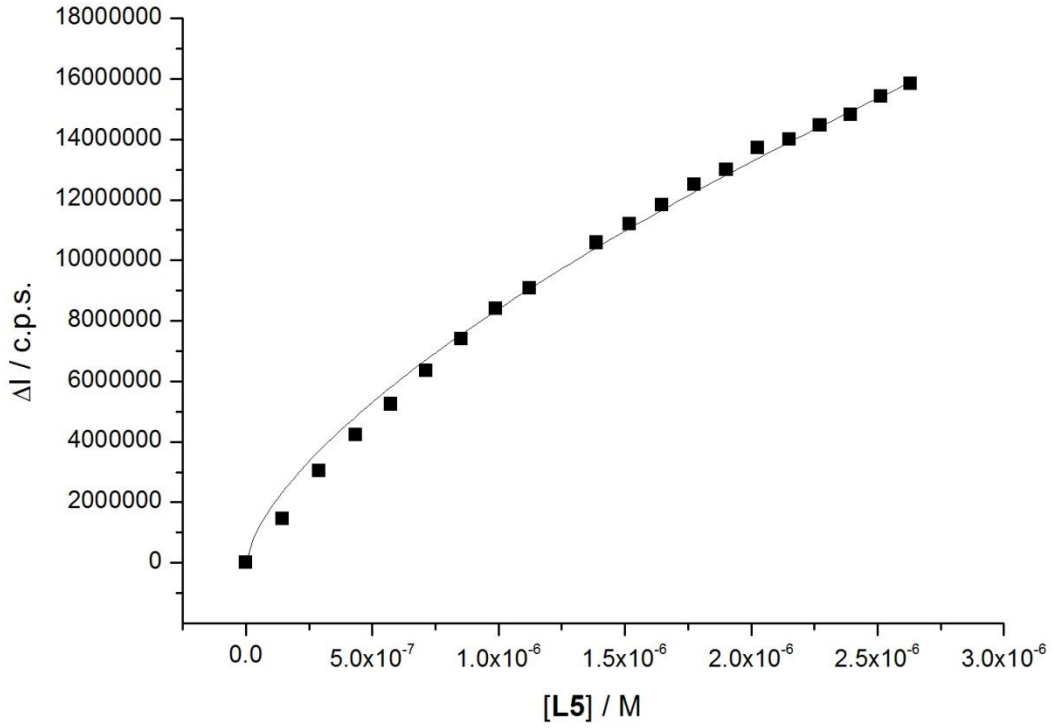

$K_a = 0.181 \pm 5.53 \times 10^3\ M^{-1}$

$n = 0.7$

Static library **L5** vs. LTB (c.p.s.: counts per second).
100 mM HEPES, pH 7.1, 1 mM $CaCl_2$, 100 mM NaCl.

[LTB] / M	[L5] / M	[L5]/[LTB]	Fluorescence Intensity / c.p.s.	ΔI / c.p.s.
5.00×10^{-7}	0	0.00	22173180	0
5.00×10^{-7}	2.97×10^{-7}	0.59	21559760	613420
5.00×10^{-7}	5.92×10^{-7}	1.18	20991129	1182051
5.00×10^{-7}	8.87×10^{-7}	1.77	20004150	2169030
5.00×10^{-7}	1.18×10^{-6}	2.36	19488917	2684263
5.00×10^{-7}	1.48×10^{-6}	2.95	18382626	3790554
5.00×10^{-7}	1.77×10^{-6}	3.54	17472041	4701139
5.00×10^{-7}	2.06×10^{-6}	4.12	16437427	5735753
5.00×10^{-7}	2.35×10^{-6}	4.70	16222599	5950581
5.00×10^{-7}	2.64×10^{-6}	5.28	15778687	6394493
5.00×10^{-7}	2.93×10^{-6}	5.86	15089178	7084002
5.00×10^{-7}	3.22×10^{-6}	6.44	14521280	7651900
5.00×10^{-7}	3.51×10^{-6}	7.02	14274805	7898375
5.00×10^{-7}	3.80×10^{-6}	7.60	13822607	8350573
5.00×10^{-7}	4.08×10^{-6}	8.17	13293536	8879644
5.00×10^{-7}	4.37×10^{-6}	8.74	12823964	9349216
5.00×10^{-7}	4.66×10^{-6}	9.31	12534525	9638655
5.00×10^{-7}	4.94×10^{-6}	9.88	12087849	10085331
5.00×10^{-7}	5.23×10^{-6}	10.5	11538792	10634388
5.00×10^{-7}	5.51×10^{-6}	11.0	11375055	10798125
5.00×10^{-7}	5.79×10^{-6}	11.6	10980085	11193095

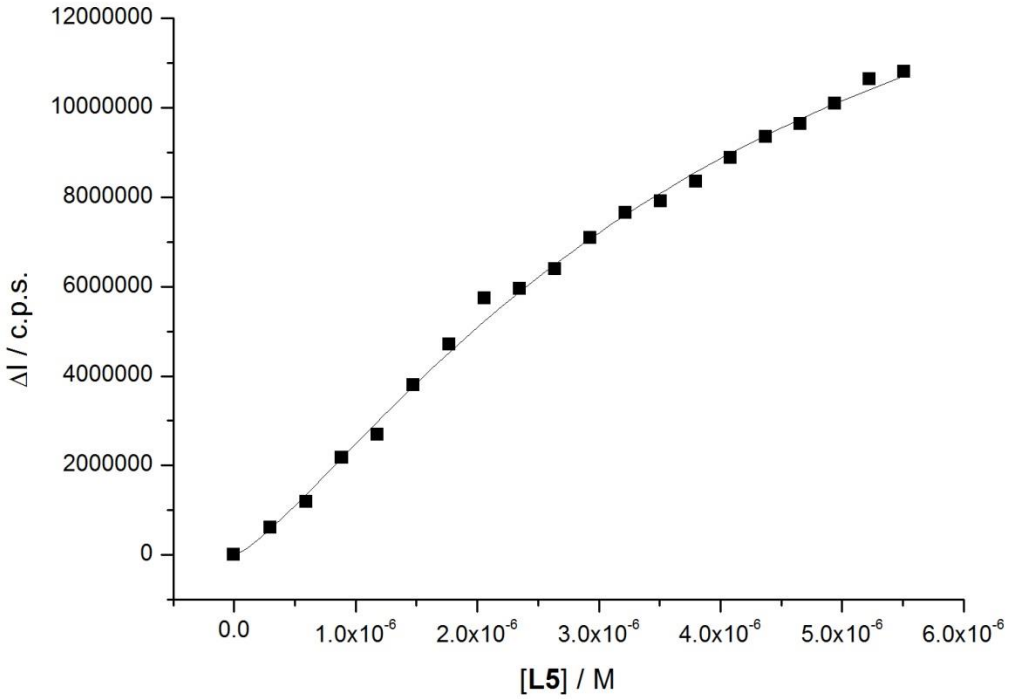

$K_a = 2.45 \times 10^5 \pm 9.83 \times 10^3\ M^{-1}$

$n = 0.7$

Polymer mixture **L6** vs. Con A (c.p.s.: counts per second).
100 mM HEPES, pH 7.1, 1 mM $CaCl_2$, 1 mM $MnCl_2$.

[ConA] / M	[L6] / M	[L6]/[ConA]	Fluorescence Intensity / c.p.s.	ΔI / c.p.s.
2.50×10^{-7}	0	0.00	33537753	0
2.50×10^{-7}	2.78×10^{-8}	0.11	30068554	3469199
2.50×10^{-7}	5.52×10^{-8}	0.22	26241458	7296295
2.50×10^{-7}	8.24×10^{-8}	0.33	24390126	9147627
2.50×10^{-7}	1.09×10^{-7}	0.44	22168268	11369485
2.50×10^{-7}	1.36×10^{-7}	0.54	20890562	12647191
2.50×10^{-7}	1.62×10^{-7}	0.65	20194065	13343688
2.50×10^{-7}	1.88×10^{-7}	0.75	19487524	14050229
2.50×10^{-7}	2.13×10^{-7}	0.85	18623845	14913908
2.50×10^{-7}	2.39×10^{-7}	0.96	18044334	15493419
2.50×10^{-7}	2.64×10^{-7}	1.06	17402147	16135606
2.50×10^{-7}	2.89×10^{-7}	1.15	16841244	16696509
2.50×10^{-7}	3.13×10^{-7}	1.25	16420559	17117194
2.50×10^{-7}	3.37×10^{-7}	1.35	15787595	17750158
2.50×10^{-7}	3.61×10^{-7}	1.45	15282265	18255488
2.50×10^{-7}	3.85×10^{-7}	1.54	14778900	18758853
2.50×10^{-7}	4.09×10^{-7}	1.63	14239588	19298165
2.50×10^{-7}	4.32×10^{-7}	1.73	13881632	19656121
2.50×10^{-7}	4.55×10^{-7}	1.82	13408219	20129534
2.50×10^{-7}	4.78×10^{-7}	1.91	13045367	20492386
2.50×10^{-7}	5.00×10^{-7}	2.00	12651944	20885809

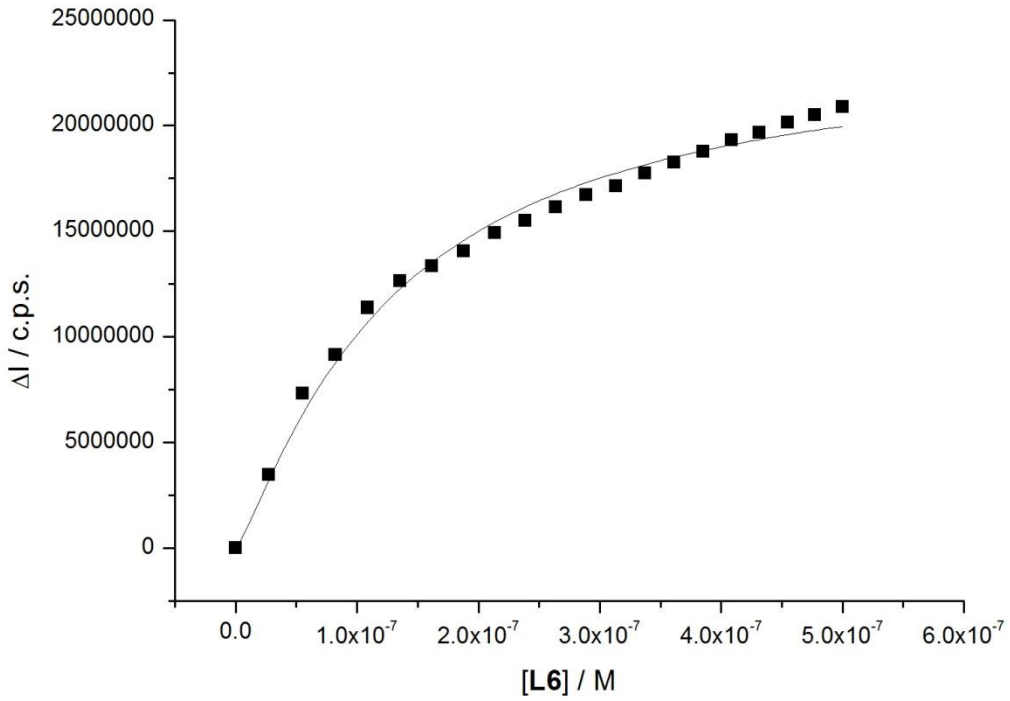

$K_a = 7.69 \times 10^6 \pm 4.63 \times 10^5\ M^{-1}$

$n = 0.8$

Polymer mixture **L7** vs. LTB (c.p.s.: counts per second).
100 mM HEPES, pH 7.1, 1 mM $CaCl_2$, 100 mM NaCl.

[LTB] / M	[L7] / M	[L7]/[LTB]	Fluorescence Intensity / c.p.s.	ΔI / c.p.s.
5.00×10^{-7}	0	0.00	22376250	0
5.00×10^{-7}	6.16×10^{-8}	0.12	20887323	1488927
5.00×10^{-7}	1.23×10^{-7}	0.25	20107991	2268259
5.00×10^{-7}	1.84×10^{-7}	0.37	19549935	2826315
5.00×10^{-7}	2.45×10^{-7}	0.49	19170234	3206016
5.00×10^{-7}	3.67×10^{-7}	0.73	18801540	3574710
5.00×10^{-7}	4.28×10^{-7}	0.86	18478697	3897553
5.00×10^{-7}	4.88×10^{-7}	0.98	18083211	4293039
5.00×10^{-7}	5.49×10^{-7}	1.10	17770624	4605626
5.00×10^{-7}	6.09×10^{-7}	1.22	17412119	4964131
5.00×10^{-7}	6.69×10^{-7}	1.34	17198652	5177598
5.00×10^{-7}	7.29×10^{-7}	1.46	16750315	5625935
5.00×10^{-7}	7.89×10^{-7}	1.58	16661624	5714626
5.00×10^{-7}	8.48×10^{-7}	1.70	16269541	6106709
5.00×10^{-7}	9.08×10^{-7}	1.82	16184774	6191476
5.00×10^{-7}	9.67×10^{-7}	1.93	15863954	6512296
5.00×10^{-7}	1.03×10^{-6}	2.05	15579532	6796718
5.00×10^{-7}	1.09×10^{-6}	2.17	15443595	6932655
5.00×10^{-7}	1.14×10^{-6}	2.29	15341979	7034271
5.00×10^{-7}	1.20×10^{-6}	2.41	15202089	7174161

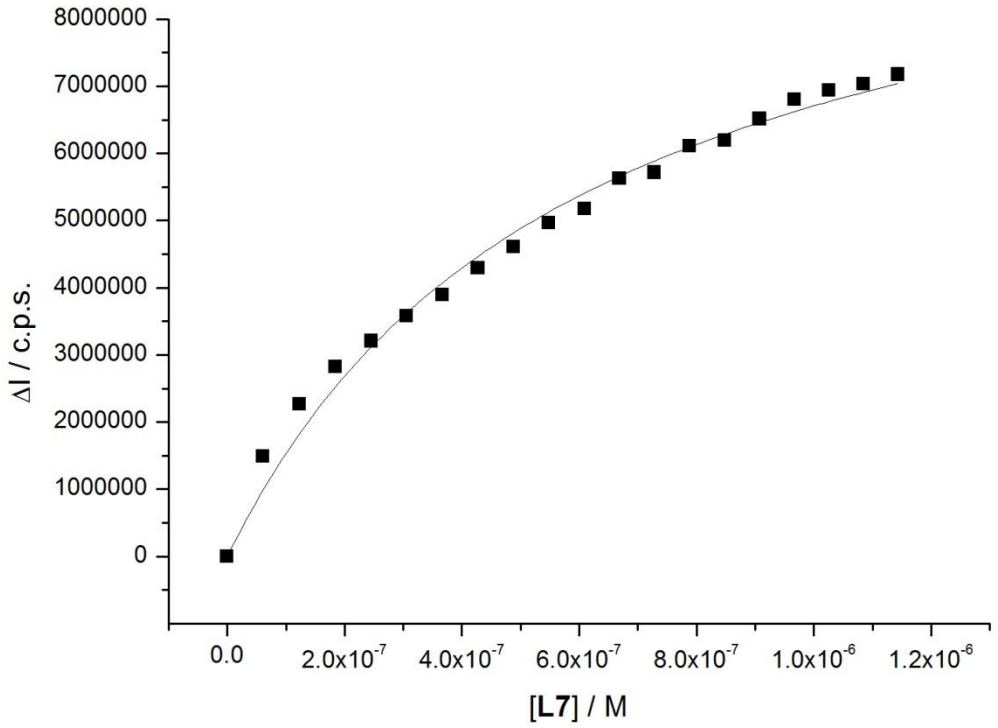

$K_a = 6.11 \times 10^6 \pm 9.38 \times 10^5\ M^{-1}$

$n = 1.0$